Chapter 1 Introduction

1-1 History of GaN LEDs

WIDE BANDGAP light-emitting diodes (LEDs) that are III-Nitride, ranging from ultraviolet to the short-wavelength part of the visible spectrum have been intensely developed in the past ten years [1-2]. GaN-based shot-wavelength devices, such as blue light-emitting diodes (LEDs) and laser diodes (LDs), are required for a number of applications, including solid-state lighting, full-color electroluminescent displays, laser printers, read-write laser sources for high-density information storage on magnetic and optical media, and sources for short-distance optical communications. The solid-state lighting is the most high-profile and desired application of the GaN-based materials due to the high luminance efficiency, reliability and durability of the semiconductor light-emitting devices [3]. In 1972, J. I. Pankove et al. fabricated the first blue LED using III-nitrides materials with a metal-i-n structure [4]. Since then, related researches went on continually. However, the device performance was limited by the poorly conducting p-type GaN. Until in the late 1980s, I. Aksaski and H. Amano et al. [5-6] developed the low-temperature buffer layer and Low-Energy Electron Beam Interaction (LEEBI) techniques to obtain conductive p-type GaN, the first GaN blue LED constructed of a real p-n junction, which greatly improved the device performance. In 1992, S. Nakamura et al. [7] achieved conductive p-type GaN with high temperature thermal annealing in nitrogen ambient and high-quality InGaN films for the first time which emitted a strong band-to-band emission from green to ultraviolet (UV) by changing the In content of InGaN using MOCVD system. The full-color semiconductor lighting has become a reality with these great progresses of techniques.

1-2 Flip Chip Technology

Flip chip technology has been developed from the IBM corporation to provide connections between bonding pads of the chips and the metallization on the substrates since 1960. It is first proposed technique called the Controlled Collapse Chip Connection (C4) to displace wire bonding, increased IO density, and decrease cost [8]. The so-called C4 process starts with depositing under bump metallurgy (UBM) on the bonding pads of chips to supply good adhesion between the bonding pads and the bumps. UBM usually consists of three layers: adhesion and/or barrier layer, wetting layer, and oxidation barrier layer. After that, solder bumps are formed on the UBM and reflow to become solder ball. The next step is to put down the top surface metallurgy (TSM) on the substrate. The chips are aligned and joined the substrate. Subsequently, it is developed many methods of connection between bonding pads of the chips and the metallization on the substrates, such as Solder Bump, Tape-Automated Bonding (TAB), Conductive Adhesives, Anisotropic Conductive Adhesives, Wire Bonding, Metal Bump, Polymer Bump, and Composite Bump.

The definition of flip chip technology is a chip mounted on the substrate with various interconnects materials and methods. Figure 1-1 shows various flip chip interconnection such as wire interconnects, fluxless solder bumps, tape-automated bonding, isotropic and anisotropic conductive adhesives, metal bumps, compliant bumps, and pressure contacts. With the development of flip chip technology, it is applied to light emitting diodes due to the advantages of electrical and thermal dissipation performance. Figure 1-2 shows the structure of conventional GaN-based LED. Sapphire material is the common substrate to grow GaN film, but it is an insulator and poor thermal material. Therefore, n- and p- pads must be the same side and lead to bonding pads baffle light output to decrease light extraction efficiency. Figure 1-3 shows the structure of flip chip GaN-based LED. It has high extraction efficiency compared to that of conventional LEDs due to the lower refraction index contrast between sapphire and air. This leads critical angle of light output to become larger and let total internal reflection reduce. Furthermore, n- and p- pads of flip chip LEDs don't baffle light output and it could add a high reflective mirror on the sub-mount to direct downward light to sapphire substrate. Therefore, flip chip technique can provide 1.5~1.7 times of light output power enhancement compared to that of the conventional GaN-based LEDs [9]. Finally, heat can be conducted to a high thermal conductivity sub-mount by bonding metal to lead better thermal dissipation. It is an important advantage for high power LEDs applications.

1-3 Epilayer-transfer Technology

Epilayer-transfer technology including wafer bonding [10-13] and substrate detaching are widely used in achieving high brightness AlGaInP-based LEDs [14-18]. By this method, the epi-layer is transferred to a better thermal and electrical conductivity substrate to improve the light extraction efficiency and drooping characteristics of LED devices. III-nitride semiconductor is promising materials for opto-electronic devices in the ultraviolet to blue/green spectrum. Due to lack of lattice match substrate, the majority of III-nitride devices are grown hetero-epitaxially onto sapphire (Al2O3) substrate, providing a hexagonal template for the growth of wurtzite GaN. However, the poor electrical conductivity and low thermal conductivity of the sapphire substrates constrain the characteristics of the electronic devices. The epilayer-transfer technology with the conjunction of wafer bonding and laser lift-off techniques may be used as a direct approach for eliminating the sapphire growth substrate and for integrating GaN with more thermally and electrically conductive substrate materials. The drooping characteristics of the electronic devices can be achieved by transferring the GaN epilayer onto other substrates to improve the electrical conductivity and the heat dissipation capacities. Beginning with the work of Kelly et al., [19] and Wang et al. [20] have now demonstrated that GaN films grown on a substrate can subsequently be separated from the substrate by a laser illumination process. In laser lift-off techniques [19-24], a pulsed laser beam with a photon energy is transparent for the sapphire, yet it will be absorbed by the interfacial GaN, increasing the temperature at the interface, inducing the decomposition of the interfacial GaN into gaseous nitrogen and gallium droplets as shown in Fig.1-4. The films can then be separated by either re-melting the metal and sliding the film away or etching the metal away with HCl. This process is termed laser-assisted film debonding here and has considerable potential for fabricating devices when used in conjunction with wafer bonding techniques.

1-4 Monte Carlo ray-tracing

TracePro is a comprehensive, versatile software tool for modeling the propagation of light in imaging and non-imaging opto-mechanical systems, as shown in Fig. 1-5. TracePro is a Monte Carlo ray tracing program that accounts for flux or light power in your optical system, as well as the irradiance or the distribution of light.

In Monte Carlo raytracing, scattering and diffraction are treated as random processes. Instead of propagating a distribution of light, discrete samples of the distribution, or rays, are propagated with BSDFs (Bidirectional Scattering Distribution Functions) used as probability distributions for determining ray directions. Monte Carlo ray tracing has several advantages over finite element methods. Below list is the characteristic of this software.

- Geometry can be procedural
- No tessellation is necessary
- It is not necessary to precompute a representation for the solution
- Geometry can be duplicated using instancing
- Any type of BRDF can be handled
- Specular reflections (on any shape) are easy
- Memory consumption is low
- The accuracy is controlled at the pixel/image level

By using TracePro, we set up a model of our optical system within the program including optical and non-optical surfaces, and trace rays through the model. We can set up a model importing from a lens design program like OSLO, from a CAD program via SAT, STP, or IGS files, or by creating the solid geometry directly in TracePro. The model includes not only the geometric data specifying the surfaces and optical material data, but also the radiometric properties of the surfaces, i.e., the absorptance, reflectance, transmittance, and scattering coefficients. Rays propagate through the model with portions of the flux of each ray allocated for absorption, specular reflection and transmission, and scattering. This forms a “tree” of rays. The flux of a ray is reduced at each ray-surface interaction, with its flux being reduced in value each time. This process continues until the flux of the ray falls below a threshold. We can run TracePro ray-traces in Analysis Mode and view the incident illuminance (or irradiance) on any surface in the model.

1-5 Organization of this dissertation

This dissertation provides the flip-chip and epilayer-transferred types of III-nitride device. It covers their fabrication, electronic, and optical properties. This dissertation is classified into two subjects. The first subject is concerned with FC-LEDs with micro-pillar array surface structure, FC-LEDs with geometric sapphire shaping structure, and FC-LEDs with triple light scattering layer, including the process, electric and light output performance of flip-chip type GaN-based LED were investigated in the chapter 2, 3, and 4. In the following, the epilayer-transferred type LEDs with modified surface structures were demonstrated including roughened mesh surface and photonic crystal surface structures. The process, electric and light output performance of the sidewalls nano-roughened LEDs are also investigated in the chapter 5 and 6. Finally, a conclusion is presented.

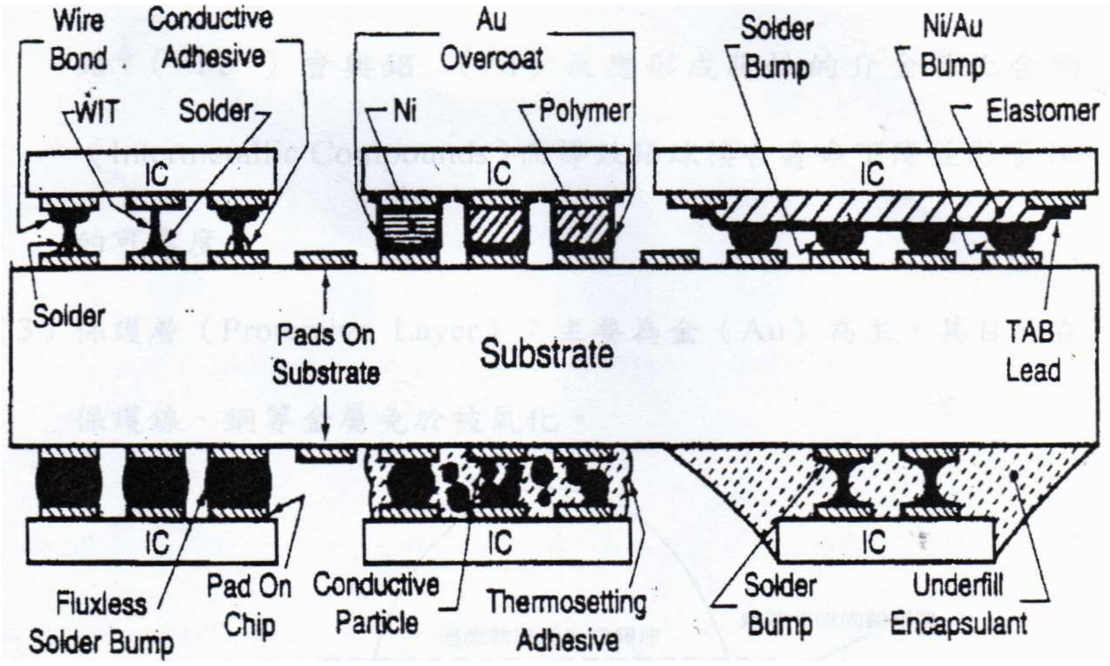

Figure 1-1 Various flip chip technologies.

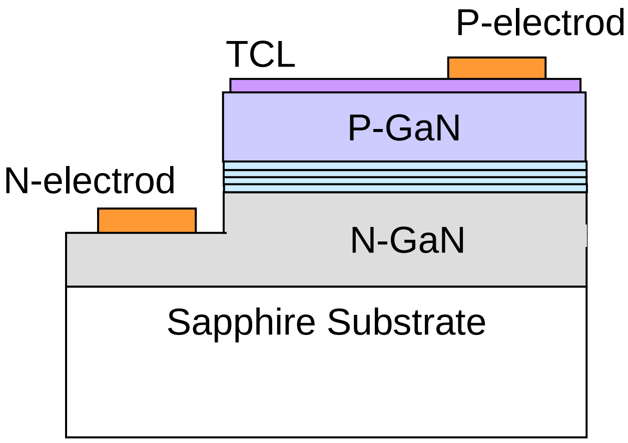

Figure 1-2 Structure of conventional GaN-based LED.

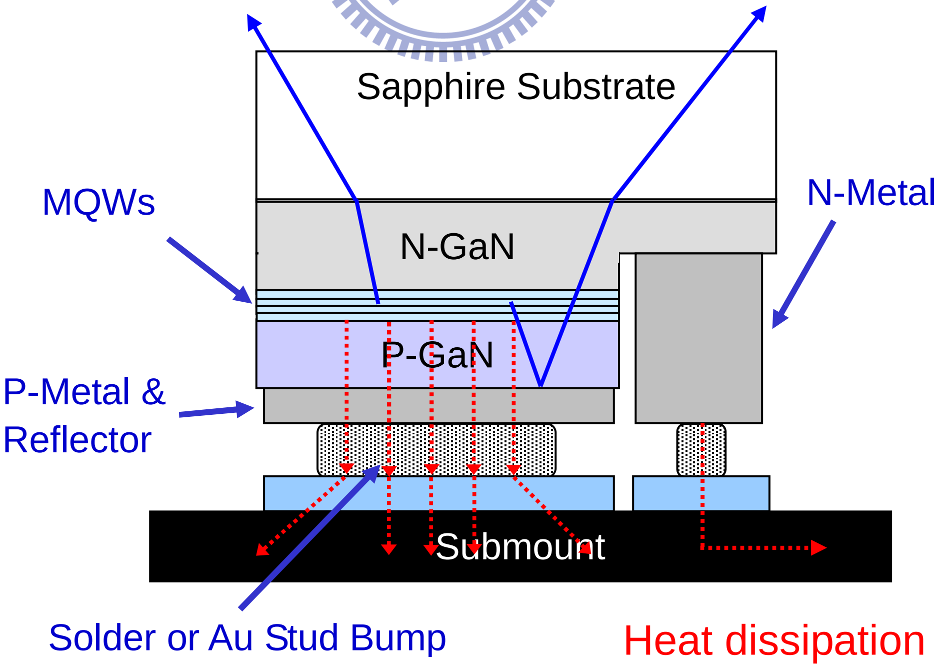

Figure 1-3 Structure of Flip chip GaN-based LED.

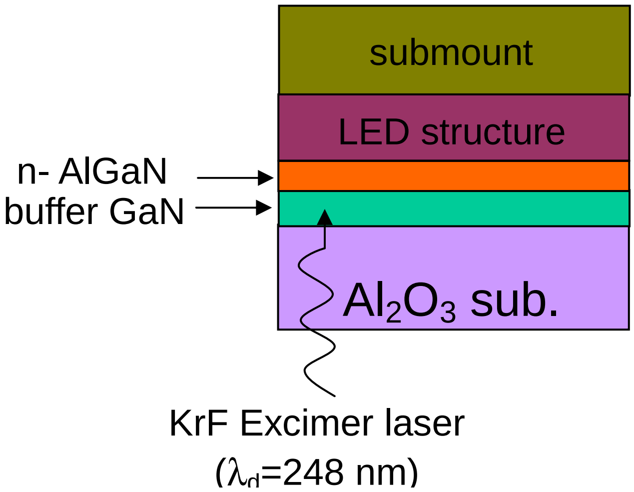

Figure 1-4 Schematic drawing of laser lift-off process.

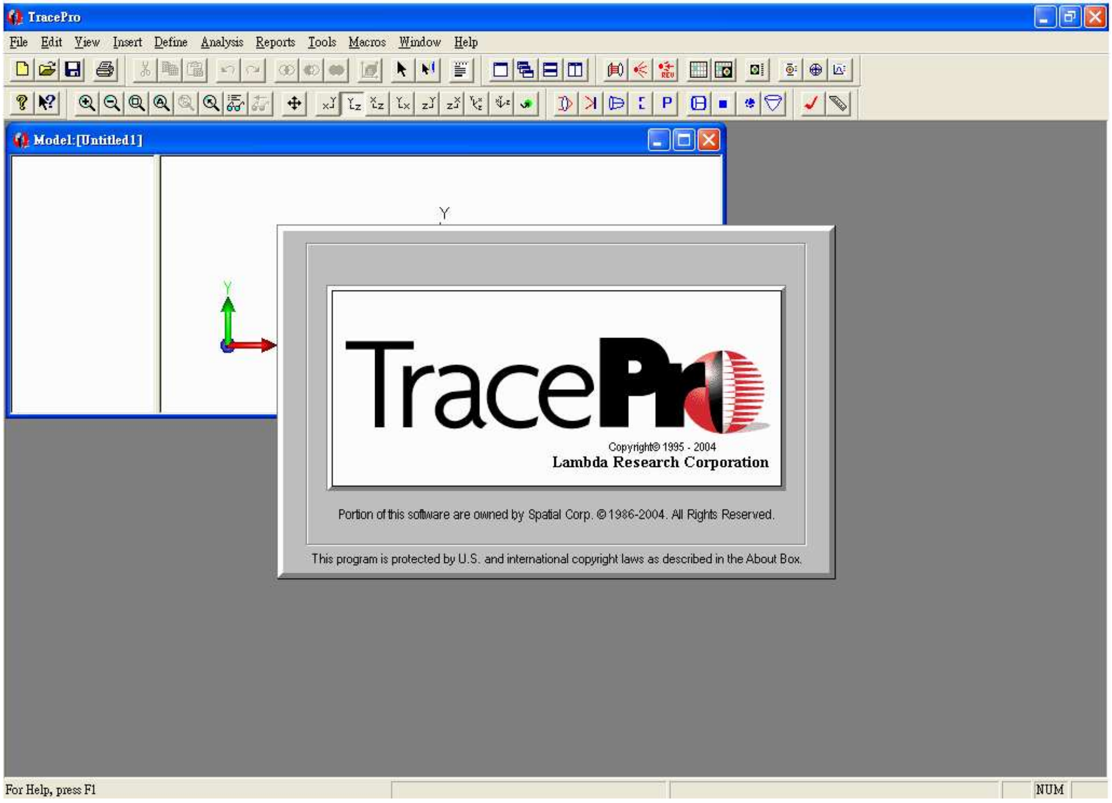

Copyright© 1995 - 2004
Lambda Research Corporation

Portion of this software are owned by Spatial Corp. ©1986-2004. All Rights Reserved.

This program is protected by U.S. and international copyright laws as described in the About Box.

For Help, press F1

Figure 1-5 Picture of TracePro software.

Chapter 2

Flip-Chip Light-Emitting-Diodes with Textured Micro Pillar Arrays (MPAFC-LEDs)

2-1 Progress in flip-chip light-emitting diodes

WIDE BANDGAP light-emitting diodes (LEDs) that are III-Nitride, ranging from ultraviolet to the short-wavelength part of the visible spectrum have been intensely developed in the past ten years. Recently, as the brightness of GaN-based LEDs has increased, applications such as traffic signals, backlight for cell phone, and LCD-TV have become possible. However, as for the replacement of conventional fluorescent lighting source with solid-state lighting, it still needs a great effort for improving the light extraction efficiency as well as internal quantum efficiency of LEDs. The conventional LEDs are inherently inefficient because photons are generated through a spontaneous emission process and emitted in all directions. A large fraction of light emitted downward toward the substrate does not contribute to useable light output. In addition, there is an inherent problem associated with conventional nitride LEDs, i.e., the poor thermal conductivity of the sapphire substrate. It has been shown that the flip-chip techniques are an effective way to further enhance light extraction and heat dissipation [25]. Therefore, the FC-LEDs were always used in high current and high power operation to alleviate the thermal budget problem. The FC-LEDs configuration has high extraction efficiency compared to conventional LEDs due to the thicker light extraction windows layer and lower refraction index contrast between sapphire substrate (n=1.76) and air (n=1). This leads critical angle of light output to become larger and let total internal reflection reduce. Furthermore, metal contact including n- and p- metal of FC-LEDs wouldn’t baffle light output and can be served as a reflective mirror to reflect the light and extract through transparent sapphire substrate [26-28]. However, FC-LEDs still have total internal reflection effect between the sapphire substrate and air, reducing the extraction efficiency of transparent windows layer. The surface roughness technique is an approach for light output enhancement has been proved due to the scattering of photons from the textured semiconductor surface and the probability of photons escaping from semiconductor to can be increased [29-31]. In this work, the combinations of conductive omni-directional reflectors (ODR) and micro pillar-array sapphire surface were developed. The conductive ODR [32] was not only served as an ohmic contact layer but also high reflective mirror. The use of highly reflective omnidirectional reflectors allows radiated light with any incident angle to be reflected to the top surface of the device [33-34]. The formation of micro pillar arrays on the bottom side of sapphire surface can be a better way to improve the probability of photons escape through the textured sapphire surface. The comparisons of FC-LEDs performance versus different micro pillar depth and shape will be discussed.

2-2 Fabrication of MPAFC-LEDs

The GaN LED structure with dominant wavelength at 460 nm used in this study is grown by metal-organic chemical vapor deposition (MOCVD) on c-plane sapphire substrates. The LED structure consists of a 2-μm-thick undoped GaN layer, a 2-μm-thick highly conductive n-type GaN layer, a 0.2-μm-thick InGaN/GaN MQW, a 0.2-μm-thick p-type GaN layer and n InGaN/GaN short period super-lattice (SPS) tunneling contact layers for indium-tin-oxide (ITO).

Figure 2-1 shows the fabrication steps of flip-chip GaN LEDs with micro-pillar-arrays. Top-emitting LEDs with a size of 1000 μm × 1000 μm are fabricated using standard photolithography and BCl_3/Cl_2 inductively coupled plasma (ICP) etching for current isolation purposes. The p-GaN and active layers are partially etched by an ICP etcher to expose an n-GaN layer for electrode formation. An indium-tin-oxide of 250 nm is deposited on p-GaN layer as the transparent conductive layer. The samples are then annealed at 500℃ for 10 minutes in air. The Cr/Pt/Au (50 nm/50 nm/2500 nm) metals are deposited for the p-and n-contact pads. After completing the conventional face-up LED structure, the sapphire is ground to let sapphire thickness become 100 μm. The Ni metal of 500 nm is deposited onto the bottom side of sapphire substrate as the dry etching mask layer. The sample is then subjected to the ICP process using Cl_2/BCl_3 (10 sccm/30 sccm) plasma with an ICP power of 850 W and RF power of 400 W to form the micro pillar arrays for light extraction purpose. The ICP etching rate for the sapphire is approximately 800 Å/min. The processed LED wafer is subjected to the laser scribed and broken into 1000 μm × 1000 μm chips.

As for the silicon sub-mount preparation, the Ti/Al (500 Å /2000 Å) metals are deposited onto the silicon sub-mount as a mirror. Secondly, the SiO_2 film of 800 Å is deposited onto it as a passivation. The Au metal of 2 μm is deposited for n and p bonding pad. The silicon sub-mount is subjected to stud bump process. Fig. 2-2 (a) and (b) show the top view and side view images of the silicon sub-mount before flip-chip bonding. Finally, the chips are flip-chip bonded on silicon sub-mount using Panasonic ultra sonic flip chip bonder for electrical and optical measurement as shown in Fig. 2-3.

2-3 Characteristics of MPAFC-LEDs

The surface morphology of a FC-LED with micro pillar-array sapphire surface is examined by scanning electron microscope as shown in Fig. 2-4.The periodic distance for pillar-array is about 5.5 μm with the depth of the pillar between ~1.1 μm and 3.2 μm . Furthermore, the bevel angle of pillar is changed from 8° to 35° with increasing dry etching time. In attempt to verify the effect of micro pillar array surface on light extraction efficiency, the various depths and bevel angle of pillar is formed for further comparison. Fig. 2-4 (a)-(b) show the rather smooth top surface and side wall and the inset is the cross view of one micro pillar. With the increase of the dry etching time, the surface of micro pillar becomes rougher and the bigger bevel angle is obtained as shown in Fig. 2-4 (c). Even the pineapple like textured pillar surface is obtained as shown in Fig. 2-4 (d). The results may be ascribed to the uniformity of Ni hard mask, which results in partial over etching and the uneven pillar surface.

The LED chips are packaged into TO can without epoxy resin for the subsequent measurement. The light-current-voltage (L-I-V) characteristics are measured using a high current measure unit (KEITHLEY 240). The light output power of the flip-chip LEDs are measured using an integrated sphere with a calibrated power meter. The corresponding I-V characteristics of flat surface FC-LEDs and micro-pillar-array FC-LEDs (MPAFC-LEDs) are also measured respectively as shown in Fig. 2-5. It is found that the I-V curve of MPAFC-LEDs present a normal p-n diode behavior with a forward voltage (@ 350 mA) of 3.4 V, indicating that there is no heating and charging damages for the fabrication process of micro-pillar-array during ICP etching process.

The light output power-current characteristics of the flat FC-LEDs and MPAFC-LEDs are shown in Fig. 2-6. We clearly observed that the output powers of the MPAFC-LEDs are larger than those of the flat FC-LEDs. At an injection current of 350 mA, it is found that the MQW emission peaks of those devices are located at about 460nm, and the light output powers of the flat FC-LEDs, 1.1 μm, 1.8 μm, 2.7 μm and 3.2 μm depth of the MPAFC-LEDs are about 151, 165, 179, 227 and 252mW, respectively. Figure 2-7 shows the light extraction efficiency enhancement of MPAFC-LEDs with various depth of pillar is 10%~68% at 350 mA current injection compared to a conventional flat surface FC-LED. It is indicated that the textured sapphire surface reduces the total internal reflection and improves the probability of photons escaping from semiconductor to air. Furthermore, with the increase of pillar depth (1.1 μm~3.2 μm) and bevel angle (8°- 35°), the light output power of 3.2 μm MPAFC-LED [Fig. 2-4 (d)] is increased by 55% compared to the 1.1 μm MPAFC-LED [Fig. 2-4 (a)] under 350mA current injection. These results can be attributed to the increase of the effective surface areas by increasing the depth and bevel angle of micro disk.

Figure 2-8 (a) and (b) shows the images of conventional flat surface FC-LED and MPAFC-LED under 350 mA current injection. Intensity distributions are also shown. The EL intensities observed from the MPAFC-LED clearly exceeded those from the conventional flat FC-LED under the same current injection, especially on the FC-LED top surface. The improved light extraction efficiency can be further supported by the beam view analysis results.

Obviously, the results indicate that the sapphire substrate with micro-pillar-array surface reduces the internal light reflection and increases the light extraction efficiency. The probability of light escaping from the sapphire to air is increased due to the increase of escape cone by micro-pillar-array structure [35]. Such an enhancement can be attributed to the top surface roughness and the fact which photons are more likely to be emitted from the surface-roughed device, resulting in an increase of the light output power of the MPAFC-LED.

2-4 Monte-Carlo ray-tracing calculations

In order to investigate the fundamental of enhancement of light output with different etching time of MPAFC-LEDs, we used the commercial ray-tracing software employing the Monte-Carlo algorithm to obtain trajectory of ray-tracing, enhancement efficiency and spatial intensity distributions of radiometric and photometric data.

The simulated structure and properties of FC-LEDs are shown in Fig. 2-9 and table 2-1, respectively. Table 2-1 (a) shows the material variable of the models, and table 2-1 (b) shows the surface variable of the models. The wavelength and temperature in this simulation are 460 nm and 300 K, respectively. Figure 2-9 (a) shows the structure of the simulated models, and Fig. 2-9 (b) shows the models in the TracePro software. The epitaxial layer is not clear in the Fig. 2-9 (b). Figure 2-9 (c) is a sketch of the pattern on the backside surface of the sapphire substrate. The circles in the Fig. 2-9 (c) represent micro-pillar-array in these models. The distance of the center of the micro-pillar-array is about 5.5 μm and the simulated models which are similar to the geometric pattern of micro pillar structure as shown in Fig. 2-4 (a)~(d) are designed.

The solid model is built up with combing the simple solid objects and each semiconductor layers adjoin to the others. Light rays are generated in the active layer with a uniform random distribution. Monochromatic radiation with the peak wavelength of the measured spectral emission (460 nm) is used in the simulation.

Figure 2-10 (a) and (b) shows the irradiance maps of conventional flat FC-LEDs and 3.2 μm MPAFC-LEDs, respectively. The intensity of 3.2 μm MPAFC-LEDs clearly exceeds that of conventional flat FC-LEDs conforming to Fig. 2-8 (a) and (b).

The output power versus different depth of micro-pillar-array simulating with TracePro software can be obtained from the irradiance maps. Therefore, the enhancement efficiency can be calculated and it is found that the efficiency is increased by larger heights of micro-pillar-array as shown in Fig. 2-11. The simulated results are similar to experiment performance except 3.2 um point because the simulated model doesn’t consider the further enhancement due to nano roughness of micro-pillar-array sidewalls. Consequently, the improved light extraction efficiency can be further supported by the simulation data as shown in Fig. 2-11.

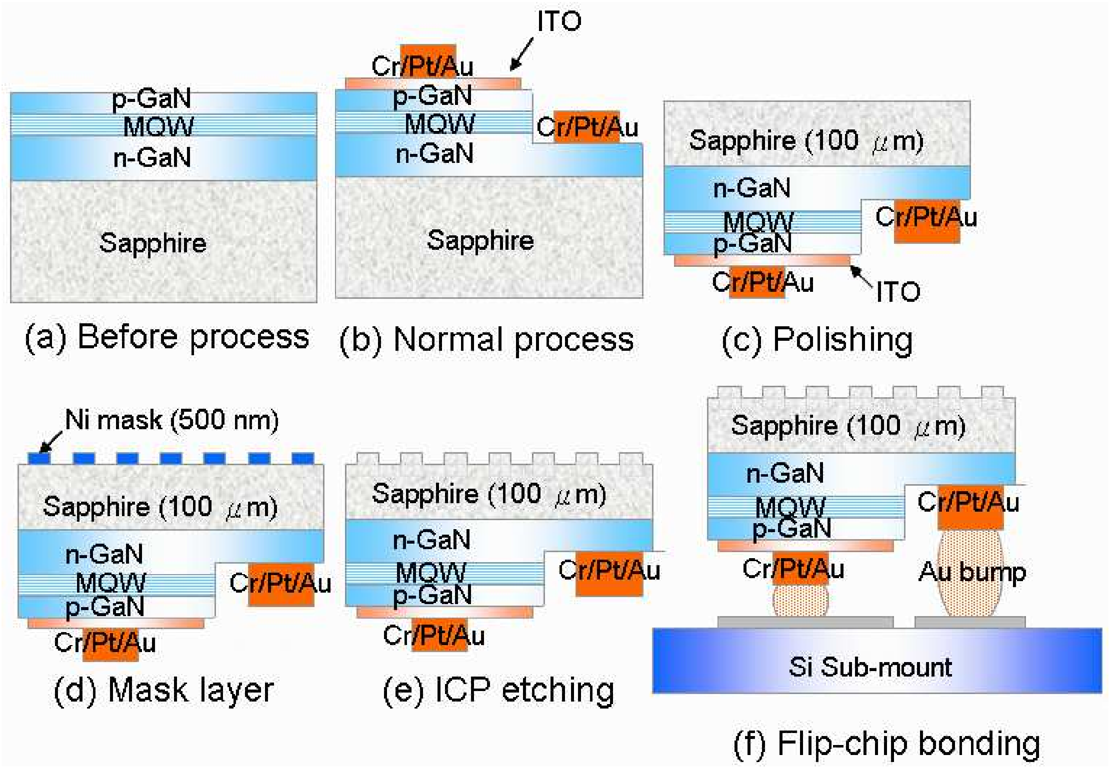

Figure 2-1 Schematic drawings of fabrication steps of GaN LEDs with micro-pillar-arrays.

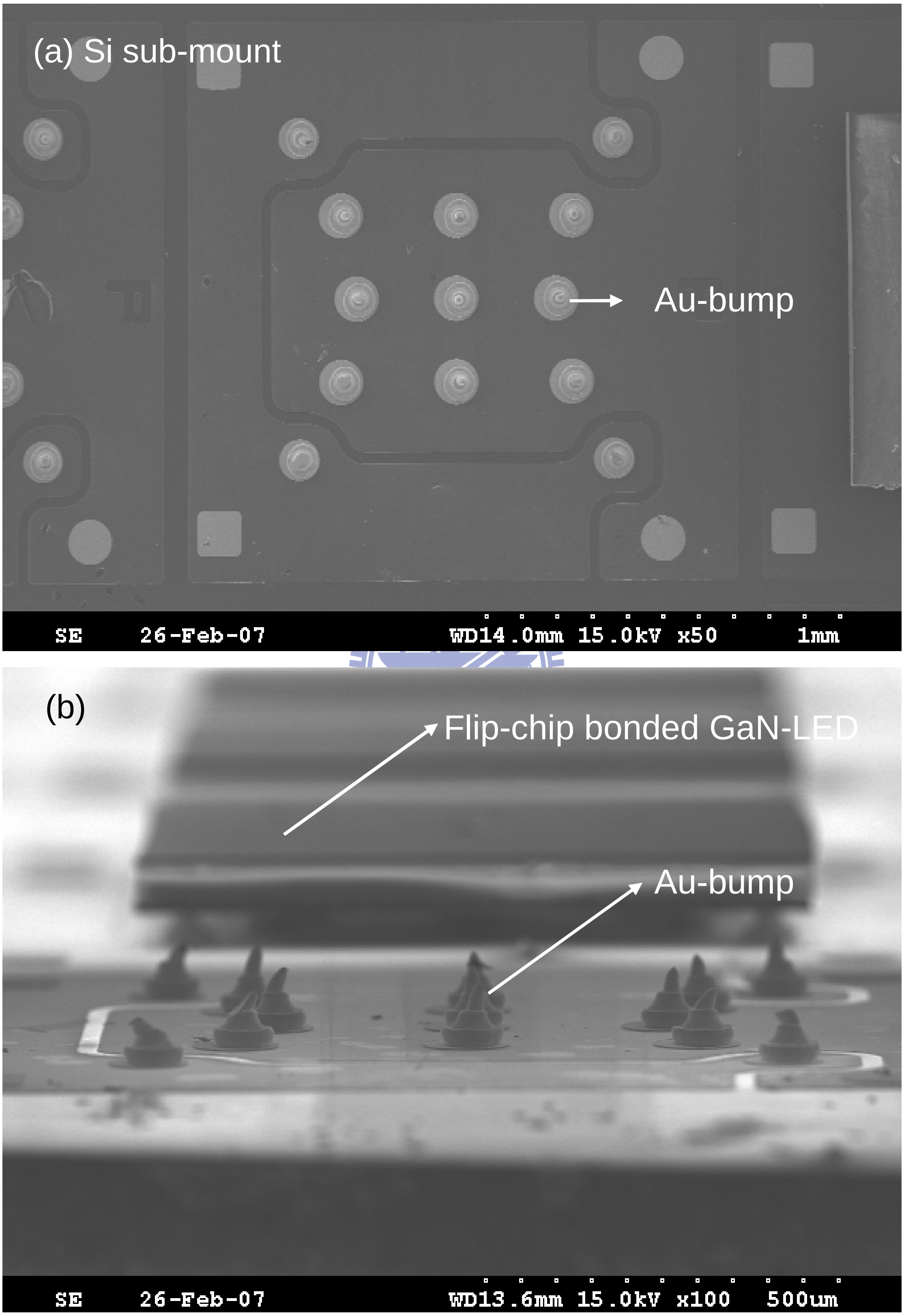

Figure 2-2 Scanning electron micrographs (SEM) images of Si sub-mount before flip chip bonding. (a) Top view and (b) Side view.

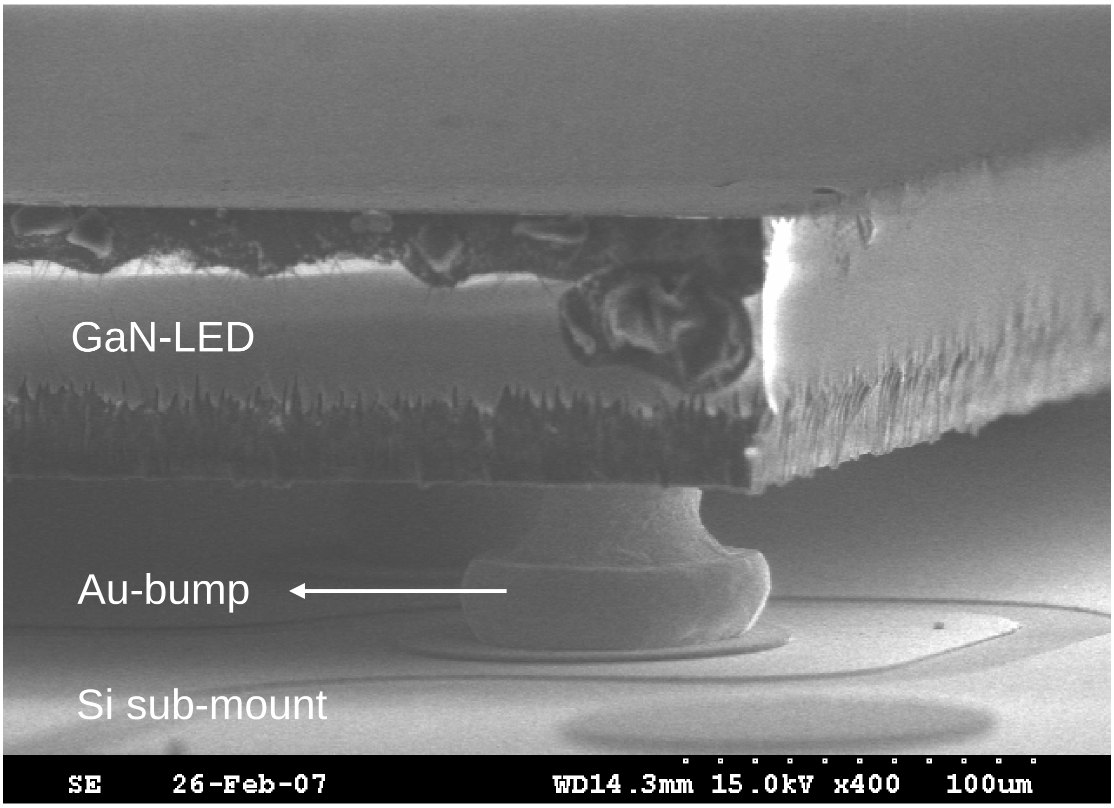

Figure 2-3 SEM image of a chip bonding on the Si sub-mount.

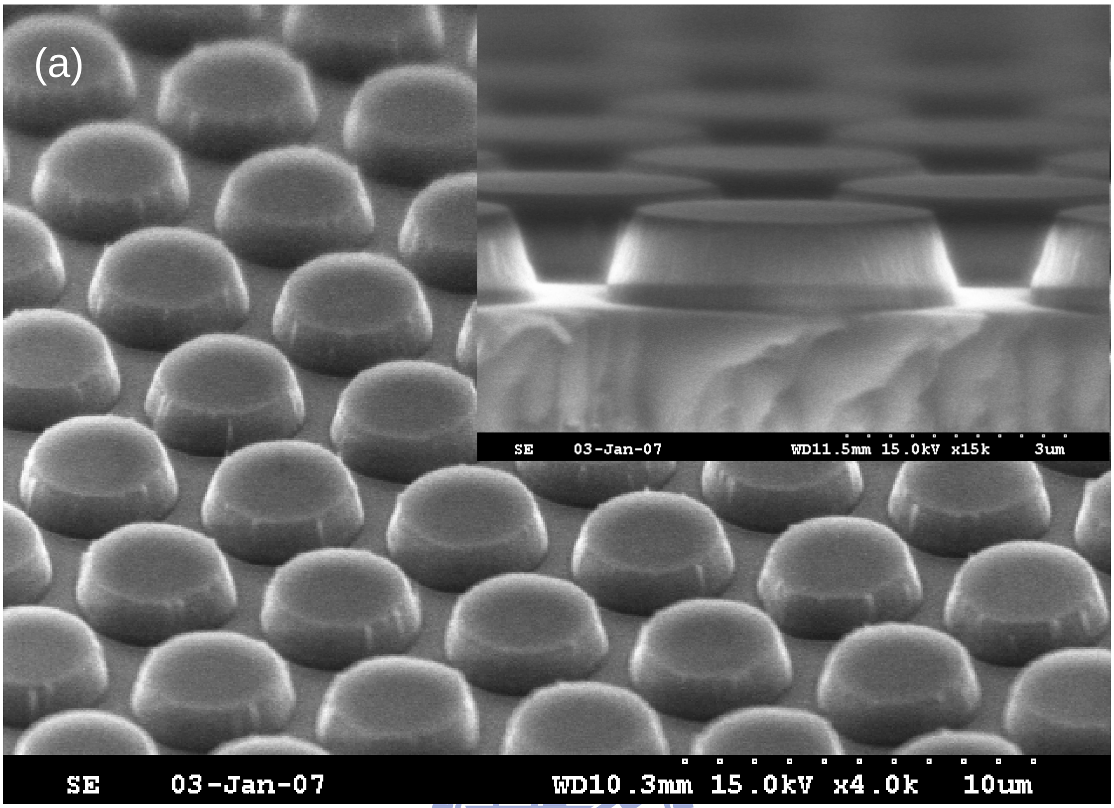
(a)
SE 03-Jan-07 WD11.5mm 15.0kV x15k 3um
SE 03-Jan-07 WD10.3mm 15.0kV x4.0k 10um

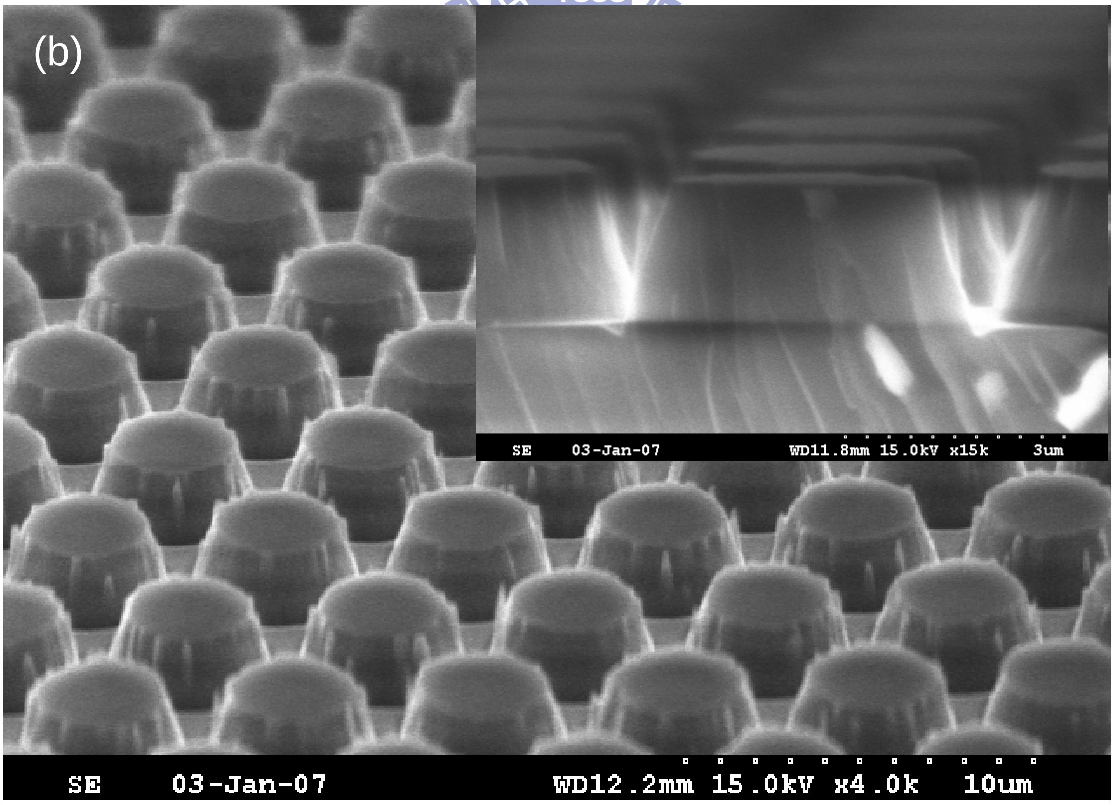
(b)
SE 03-Jan-07 WD11.8mm 15.0kV x15k 3um
SE 03-Jan-07 WD12.2mm 15.0kV x4.0k 10um

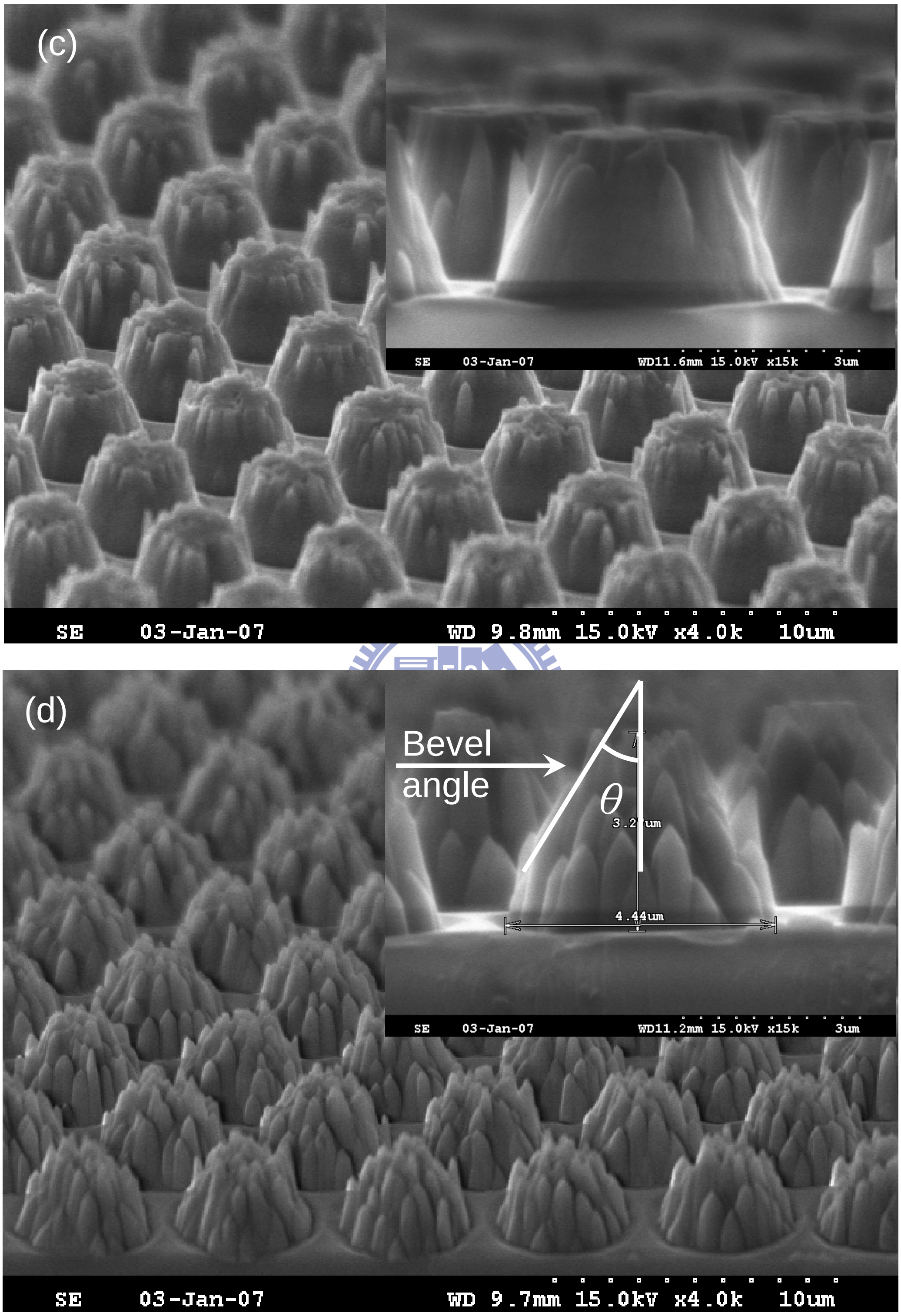

Figure 2-4 SEM images of micro-pillar-array surface of sapphire backside with various depth and bevel angle. (a) 1.1 μm MPA, (b) 1.8 μm MPA, (c) 2.7 μm MPA, and (d) 3.2μm MPA.

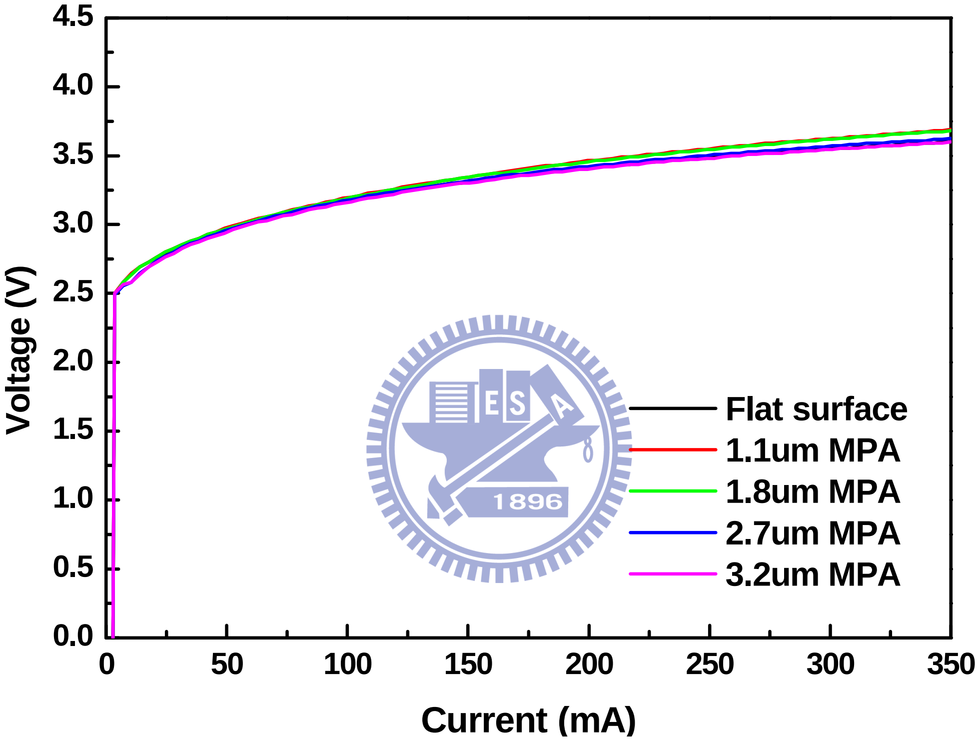

Figure 2-5 The current-voltage (I-V) characteristics of flat surface FC-LEDs and MPAFC-LEDs.

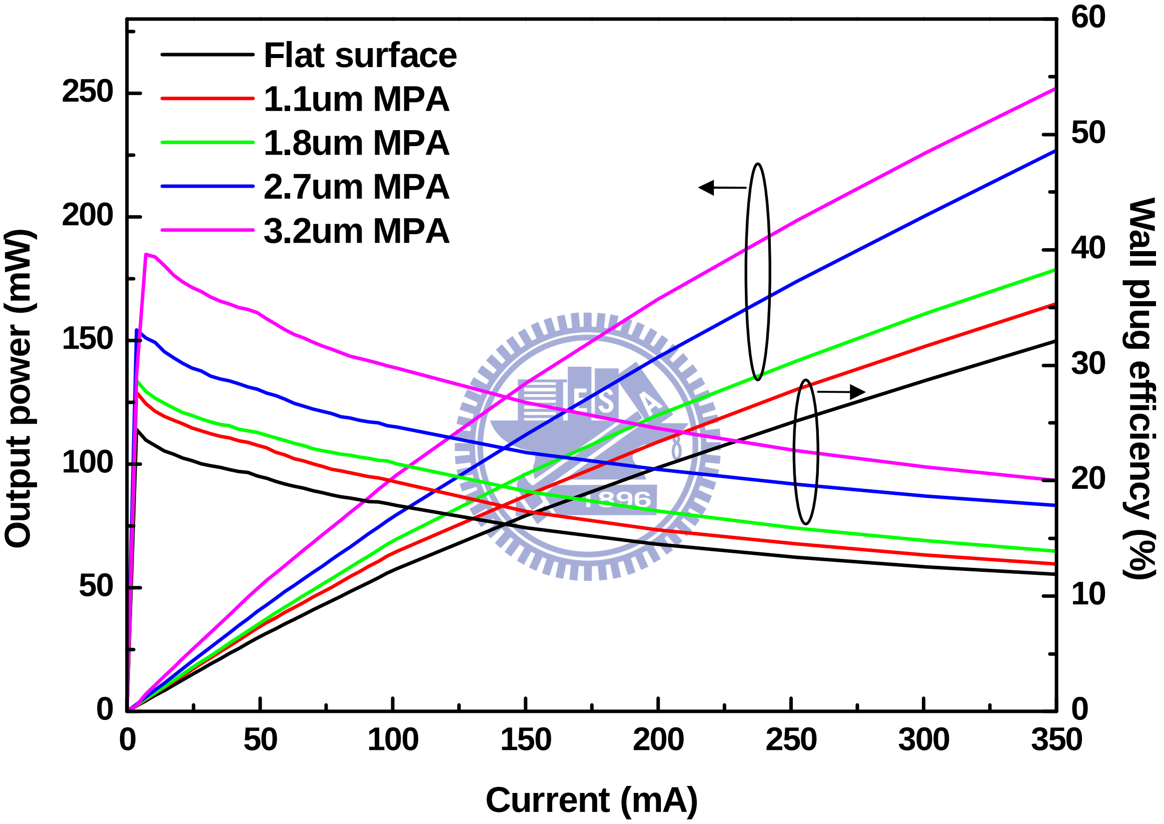

Figure 2-6 The light output power-current (L-I) curves of flat surface FC-LEDs and MPAFC-LEDs.

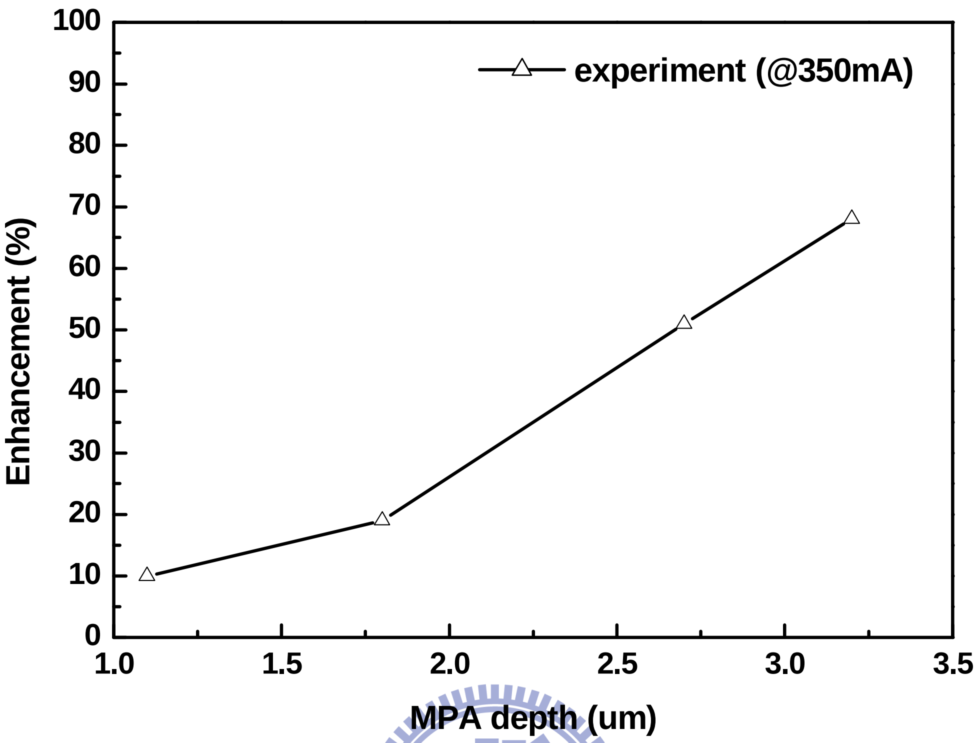

Figure 2-7 Light extraction enhancement of experimental results versus different depth of MPA.

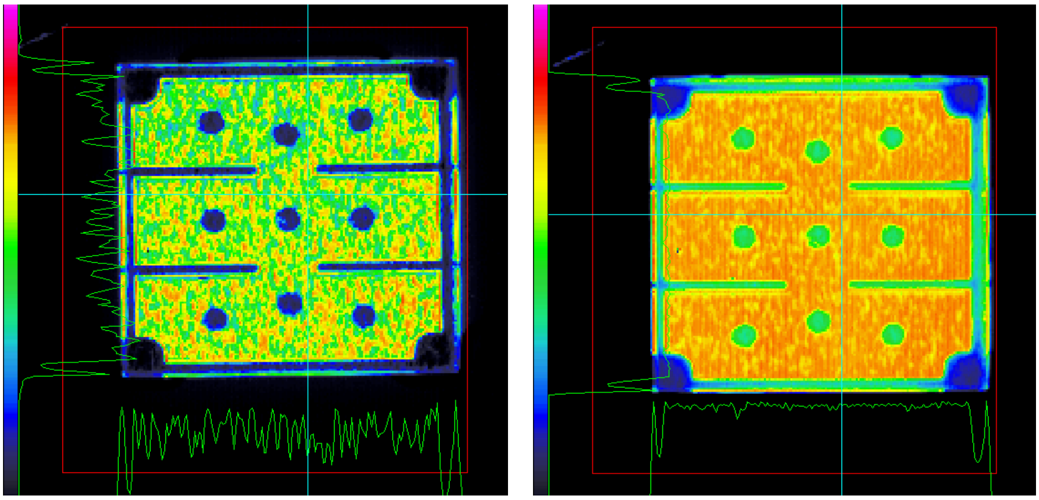

(a) (b)

Figure 2-8 Photons of (a) conventional flat surface FC-LED and (b) micro pillar-array FC-LED at a dc injection current of 350 mA.

(a)

	thickness	index
sapphire	100 μm	1.7
n-GaN	4 μm	2.45
MQW	0.2 μm	2.65
p-GaN	0.2 μm	2.45
ITO	0.2 μm	2

(b)

	reflectance	transmission	absorptance
Al mirror	90%	0%	10%
p-pad	50%	0%	50%
n-pad	50%	0%	50%

Table 2-1 (a) shows the material variable of the models and (b) shows the surface variable of the models.

(a)

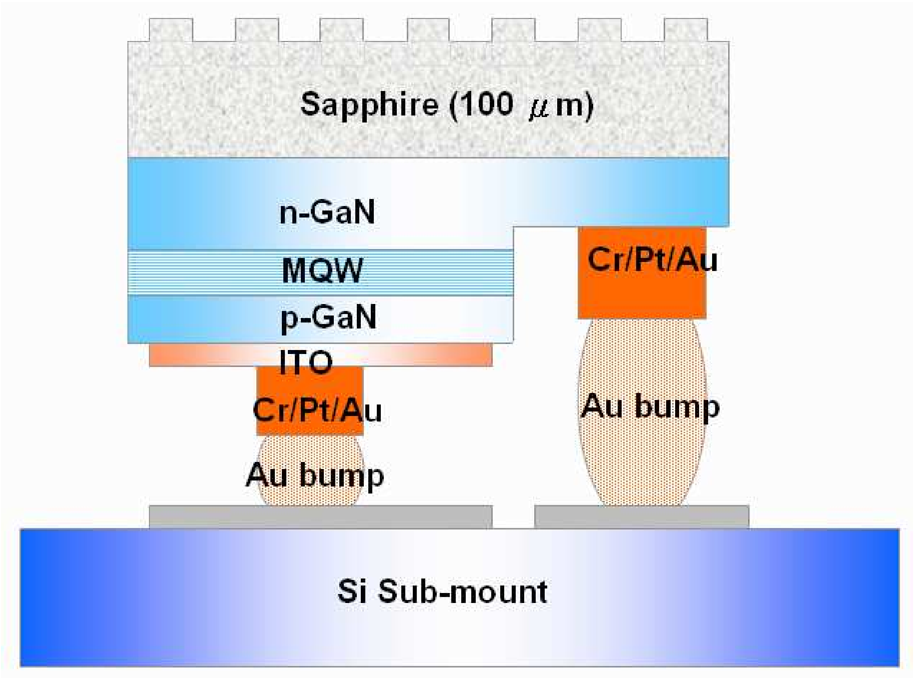
Sapphire (100 μm)
n-GaN
MQW
p-GaN
ITO
Cr/Pt/Au
Au bump
Cr/Pt/Au
Au bump
Si Sub-mount

(b)

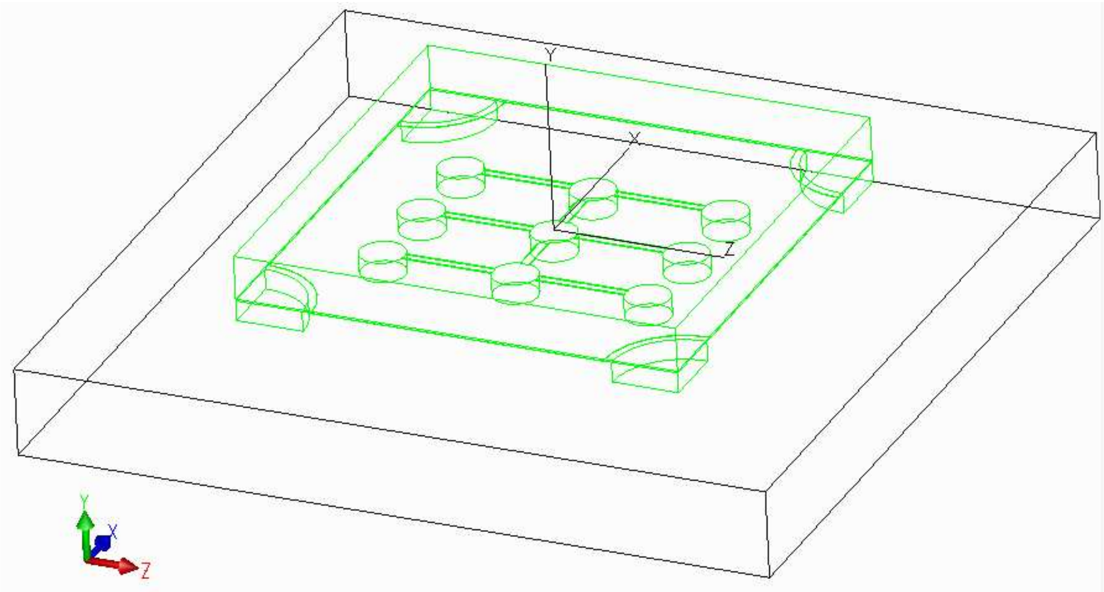
Y
X
Z
Y
X
Z

(c)

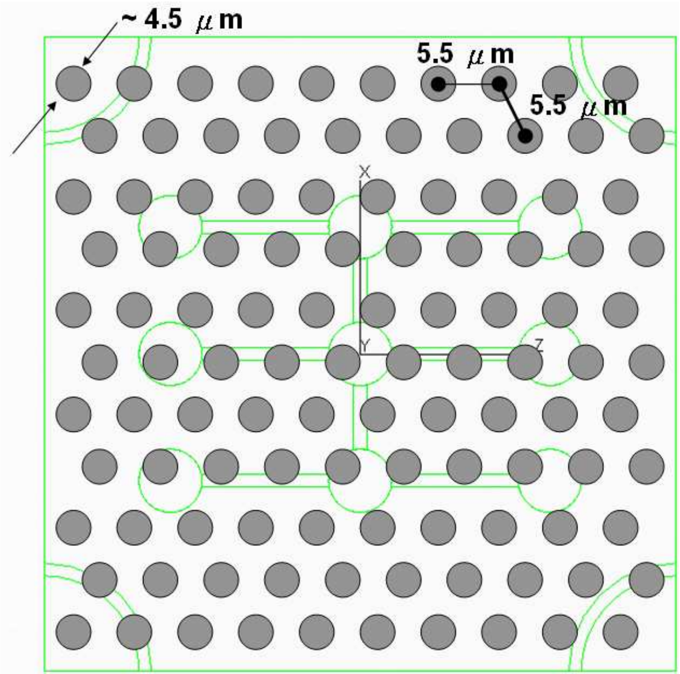

Figure 2-9 (a) shows the structure of the simulated models, (b) shows the models in the TracePro software, and (c) is a sketch of the pattern on the backside surface of the sapphire substrate.

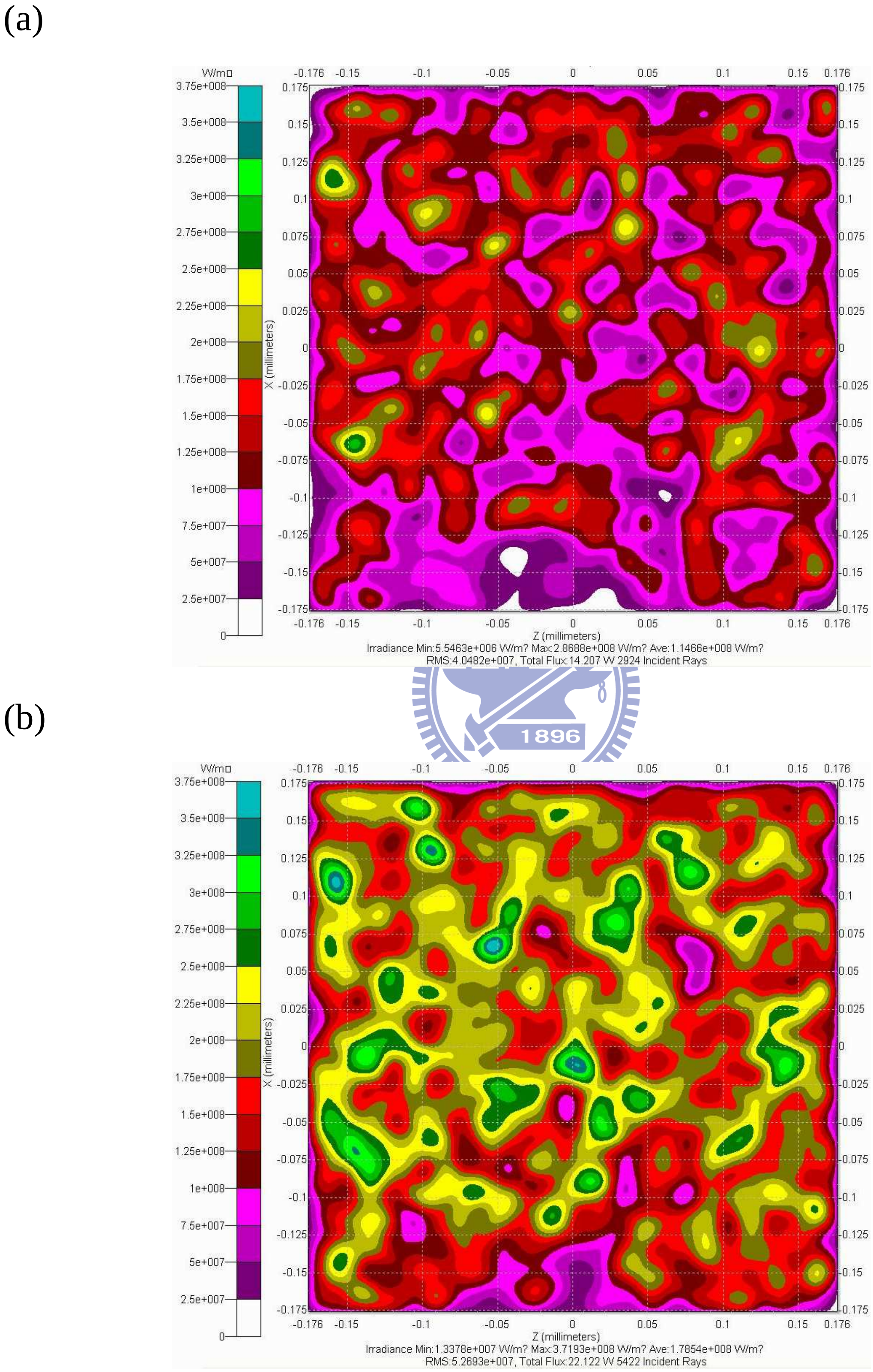

Figure 2-10 The simulation results by Monte-Carlo ray-tracing. (a) and (b) show the irradiance maps of conventional flat FC-LEDs and 3.2 μm MPAFC-LEDs, respectively.

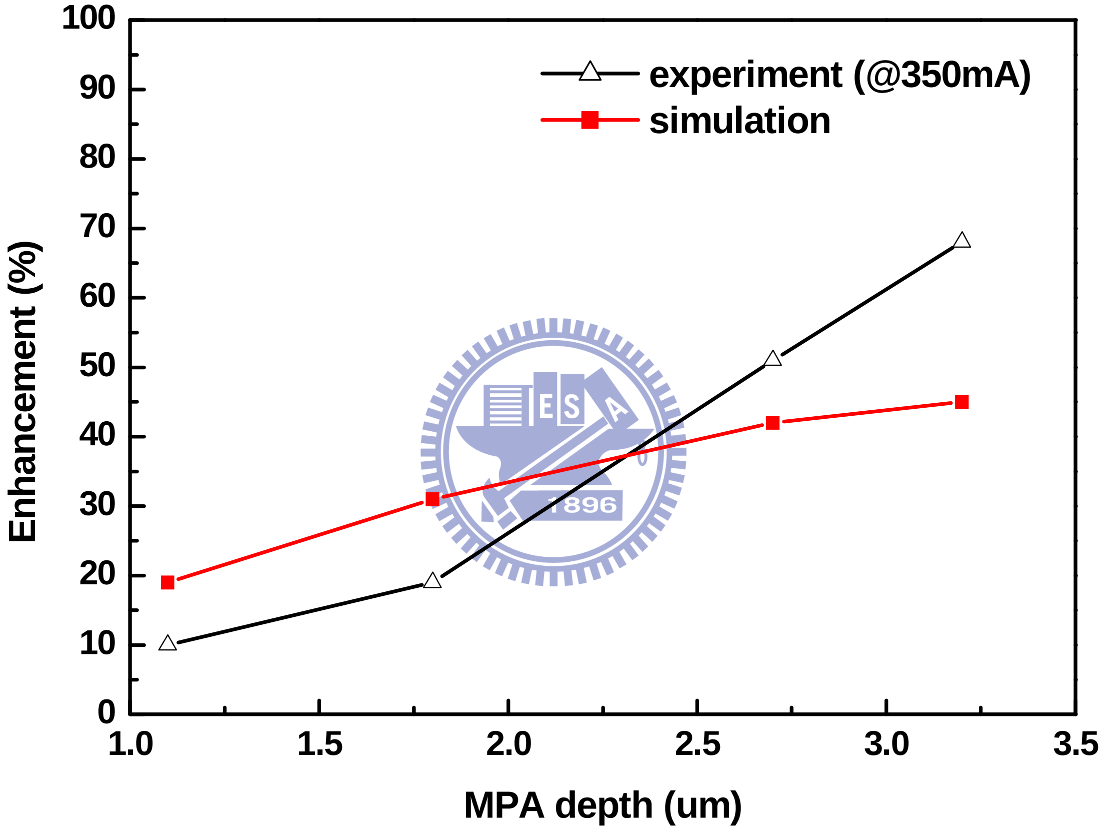

Figure 2-11 Light extraction enhancement comparison of experimental and simulation results versus different depth of MDA.

Chapter 3

Flip-Chip Light-Emitting-Diodes with Geometric Sapphire Shaping Structure (SSFC-LEDs)

3-1 Progress of geometric LED shaping structure

Previously, there has been intensive research into the improvement of light extraction efficiency and the enhancement of brightness in the LEDs. The geometric chip structure effect on the light extraction efficiency enhancement has been discussed in many papers [36–39]. Krames et al reported the extraction efficiency enhancement from truncated-inverted-pyramid AlGaInP-based LEDs [36]. Eisert et al reported the experimental and simulated results for enhancing light extraction efficiency from the GaN-based LEDs chip with the undercut SiC substrate [37]. Chang et al reported 10% output power enhancement from the InGaN–GaNmultiple quantum-well (MQW) LEDs by the introduction of thewavelike textured sidewalls [38]. Kao et al reported light-output enhancement in a nitride-based light-emitting diode with 22◦ undercut sidewalls [39]. All these methods have one thing in common, which is that photons generated within the LEDs can experience multiple opportunities to find the escape cone. As a result, the light extraction efficiency and the LED output intensity could both be enhanced significantly. It is said that a simple method to fabricate oblique sidewall will be beneficial to raise the brightness of the nitride-based LEDs. In this work, the nitride-based FC-LEDs with a geometric sapphire shaping structure were developed. The formation of oblique sapphire sidewalls on the bottom side of the sapphire surface can be a better way to improve the probability of photons escaping through the oblique sidewalls. The electrical and optical properties of the sapphire-shaped FC-LEDs (SSFC-LEDs) are reported.

3-2 Fabrication of SSFC-LEDs

The GaN LED structure with dominant wavelength at 460nm used in this study is grown by metal-organic chemical vapor deposition (MOCVD) on c-plane sapphire substrates. The LED structure consists of a 2-μm-thick undoped GaN layer, a 2-μm-thick highly conductive n-type GaN layer, a 0.2-μm-thick InGaN/GaN MQW, a 0.2-μm-thick p-type GaN layer and n InGaN/GaN short period super-lattice (SPS) tunneling contact layers for indium-tin-oxide (ITO).

Figure 3-1 shows the fabrication steps of flip-chip GaN LEDs with geometric sapphire shaping structure (GaN SSFC-LEDs). First, the SiO_2 film with size of 1000 μm × 1000 μm is deposited onto the backside of sapphire substrate by plasma enhance chemical vapor deposition and defined using standard photolithography to serve as the wet etching hard mask. Avoiding damaging the epitaxial layer, the SiO_2 film is also deposited on the epitaxial layer as the sheathing. The sapphire substrate is then immersed into a H_2SO_4:H_3PO_4 (3:1) solution at an etching temperature of 330 ℃ for 70 minutes. The sapphire wet etching rate is about 1.4 μm/minute in this sturdy and can be related to the H_3PO_4 composition and the etching temperature. After finishing the sapphire shaping process, top-emitting LEDs with a size of 1000 μm × 1000 μm are fabricated using standard photolithography process which are aligned with the backside sapphire shaping pattern and are partially etched using an inductively coupled plasma etcher to expose an n-GaN layer for electrode formation. A indium tin oxide (250nm) is deposited on p-GaN layer as the transparent conductive layer. The samples are then annealed at 500 °C for 10 minutes in air. The Cr/Pt/Au (50 nm/50 nm/2500 nm) metals are deposited for the p- and n-contact pads. After conventional LEDs processes, the processed LED wafer is subjected to the laser scribed and broken into 1000 μm × 1000 μm chips.

As for the silicon sub-mount preparation, the Ti/Al (500 Å /2000 Å) metals are deposited onto the silicon sub-mount as a mirror. Secondly, the SiO_2 film of 800 Å is deposited onto it as a passivation. The Au metal of 2 μm is deposited for n and p bonding pad. The silicon sub-mount is subjected to stud bump process. Finally, the LED chips with oblique sapphire shaping sidewall are flip-chip bonded on silicon sub-mount using Panasonic ultra sonic flip chip bonder for electrical and optical measurement. Figure 3-2 shows the schematic drawing of the GaN SSFC-LEDs and a sketch indicating light may be extracted from the oblique sapphire sidewall.

3-3 Characteristics of SSFC-LEDs

Figure 3-3 shows the scanning electron micrographs (SEM) images of sapphire shaping structure (a) top and (b) cross-sectional views. In this study, the sapphire is etched for 70 minutes via the etching rate about 1.4 μm/minute and etching depth is about 100 μm as shown in figure 3-3 (b). The crystallography facets are (1-102), (1-106) and (11-25) plane against the (0001) c-axis and their angles against the (0001) c-axis are 60°, 30° and 50° respectively, as shown in figure 3-4 (a)-(c). Furthermore, the etching structures are all V-grooves. The V-sharp structure can be used to form a cleaving line to break the thick (~450 μm) sapphire substrate. The SEM images of CFC-LEDs and SSFC-LEDs are shown in Fig. 3-5. The sapphire shaping area and greatly thick windows layer are obviously observed on the SSFC-LED structure compared with the CFC-LED. The oblique sapphire geometry improves light extraction by reducing totally internally reflected (TIR) photons from the sidewall interfaces, allowing them to escape through the oblique sidewall. In addition, thicker sapphire windows layer offers significant advantages over conventional thin sapphire window layer structure by facilitating light emission from the edges of the chip. These two processes provide the SSFC-LED device with a significant reduction in photon path length for extraction compared to a conventional chip. Such benefits are shown in the photomicrographs figure 3-6 (a) CFC-LED and (b) SSFC-LED. Note that light appears to radiate evenly from the thicker windows layer and oblique sidewall of the SSFC-LED (b) as compared with that of CFC-LED (a), indicating that light extraction efficiency can be improved due to the oblique sapphire geometry and thicker window layer.

The LED chips are packaged into TO can without epoxy resin for the subsequent measurement. The corresponding I-V characteristics of SSFC-LEDs and CFC-LEDs are measured respectively as shown in Fig. 3-7. It is found that the I-V curve of SSFC-LEDs exhibits a normal p-n diode behavior with a forward voltage (@350mA) of 3.5 V, indicating that high temperature sapphire wet etching process dose not appear to adversely affect I-V characteristics of these devices.

Figure 3-8 shows the light output power and wall plug efficiency as a function of injection current for λ_p~460 nm devices of SSFC-LEDs and CFC-LEDs. It is clearly observed that the light output powers of the SSFC-LEDs are larger than those of the CFC-LEDs. Under 350 mA current injections, it is found that the enhancement of light output powers of the SSFC-LEDs and CFC-LEDs can be significantly raised from 150 mW to 234 mW and the wall plug efficiency can be increased from 12.26% to 18.98%. We note that bare SSFC-LEDs (without encapsulating an epoxy lens) exhibits 55% light extraction efficiency enhancement under 350 current injection compared to the CFC-LEDs. It is indicated that the geometric sapphire sidewall reduces the total internal reflection and improves the probability of photons escaping from semiconductor to air. Furthermore, thicker sapphire window layer offers significant advantages over conventional thin sapphire window layer structure by facilitating light emission from the edges of the chip.

Figure 3-9 shows normalized far-field patterns of the SSFC-LED and CFC-LED under 20 mA current injection, respectively. For detail comparison, the normalized far-field patterns via two directions ((1-106)-plane to (1-102)-plane, X-axis; (11-25)-plane to (11-25)-plane, Y-axis) are measured. It can be observed that the electroluminescence (EL) intensities of SSFC-LEDs is concentrated on the near vertical direction (i.e. about between 70° and 110°). In contrast, EL intensities observed from the SSFC-LED are concentrated on the near horizontal direction (i.e. smaller than 60° or larger than 120°) compared to those of the CFC-LED. Figure 3-10 shows the normalized three-dimensional far-field patterns of

SSFC-LEDs and CFC-LEDs, which verifying that the oblique sidewall can vary far-field patterns and lead to larger 50% viewing angles. Such an enhancement could be attributed to the oblique sidewall and thicker window layer that photons can have a larger probability to be emitted from the device in the near horizontal directions.

3-3 Monte-Carlo ray-tracing calculations

In order to investigate the fundamental of enhancement of light output with different etching time of sapphire shaping FC-LEDs. we used the commercial ray-tracing software employing the Monte-Carlo algorithm to obtain trajectory of ray-tracing, enhancement efficiency and spatial intensity distributions of radiometric and photometric data.

The shape and size of the solid model for the ray-tracing calculation is determined and exactly the same as the SEM images and microscopic measurements of the geometry of SSFC-LEDs as shown in figure 3-11.

The solid model is built up with combing the simple solid objects and each semiconductor layers adjoin to the others. Light rays are generated in the active layer with a uniform random distribution. Monochromatic radiation with the peak wavelength of the measured spectral emission (460 nm) is used in the simulation. Figure 3-12 (a) and (b) shows the candela maps of CFC-LEDs and 100 μm SSFC-LEDs, respectively. The intensity of 100 μm SSFC-LEDs obviously exceeds that of CFC-LEDs and the intensity distribution is the same as normalized far-field patterns of CFC-LEDs and 100 μm SSFC-LEDs. Therefore, the improved light extraction efficiency can be further supported by the simulation result and the increase of light output power of SSFC-LEDs can be verified by ray-tracing situations as shown in figure 3-13 because oblique sidewall can reduce photon path length and absorption to lead to enhance light output power.

The output power versus different etching depth of SSFC-LEDs simulating with TracePro software can be obtained from the irradiance maps. Therefore, the enhancement efficiency can be calculated and it is found that the extraction efficiency is increased by larger etching depth of SSFC-LEDs as shown in figure 3-14. The simulated result of 100 μm SSFC-LEDs is similar to experiment performance of 55% and enhancement efficiency gradually converges. According to simulation data, we will employ longer etching time to enhance extraction efficiency of FC-LEDs further in the future.

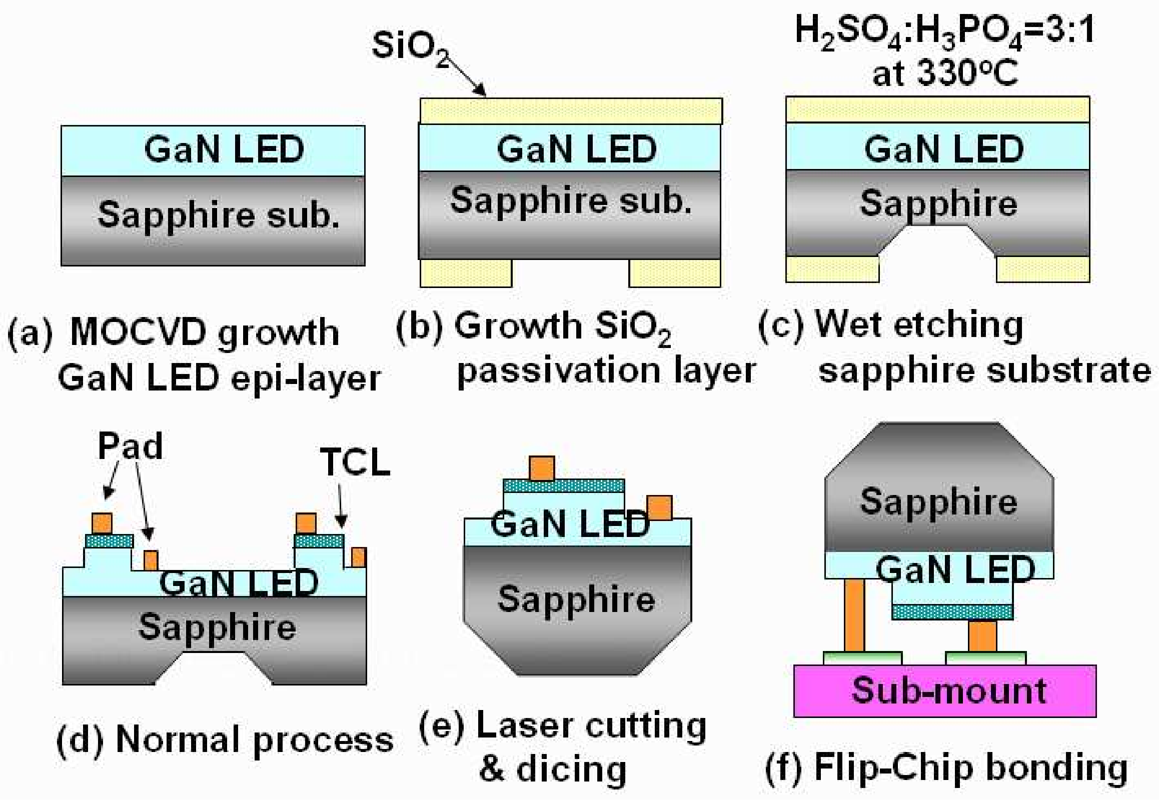

Figure 3-1 Schematic of fabrication steps of sapphire shaping FC-LEDs.

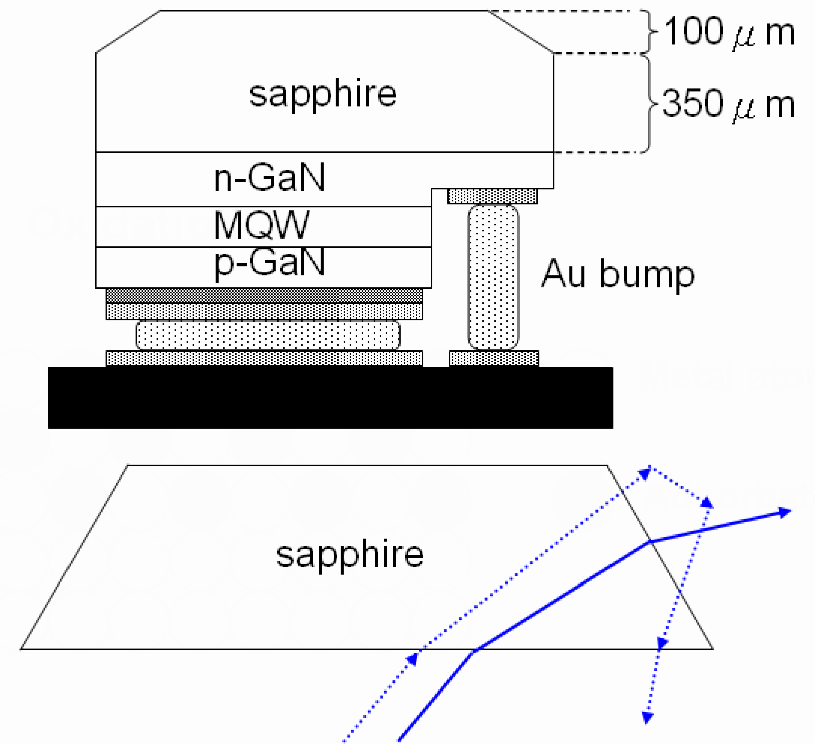

Figure 3-2 Schematic drawing of the GaN SSFC-LEDs, illustrating the means by which light may be extracted from the oblique sapphire sidewall.

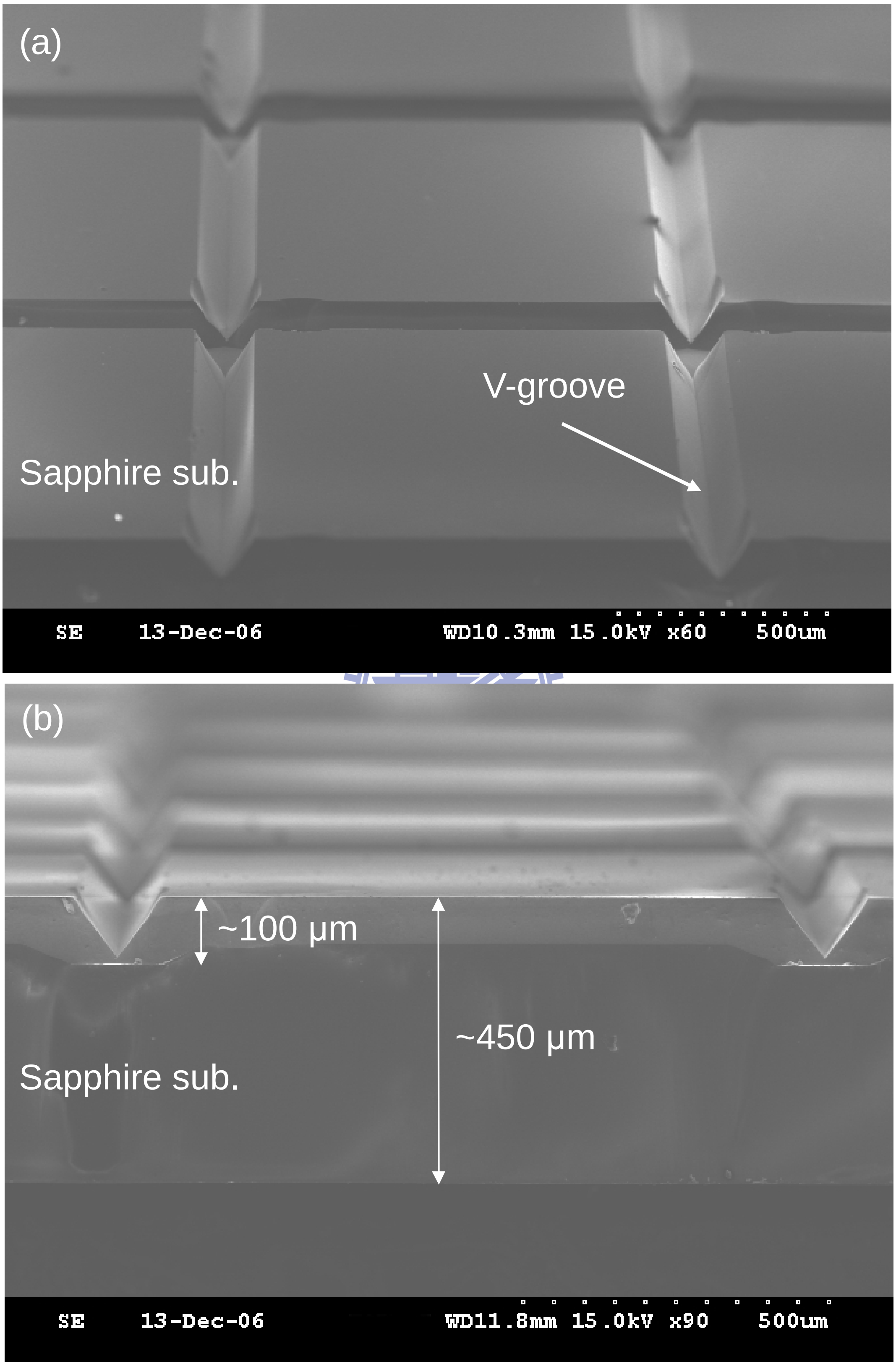

Figure 3-3 SEM images of sapphire shaping structure (a) top and (b) cross-sectional views.

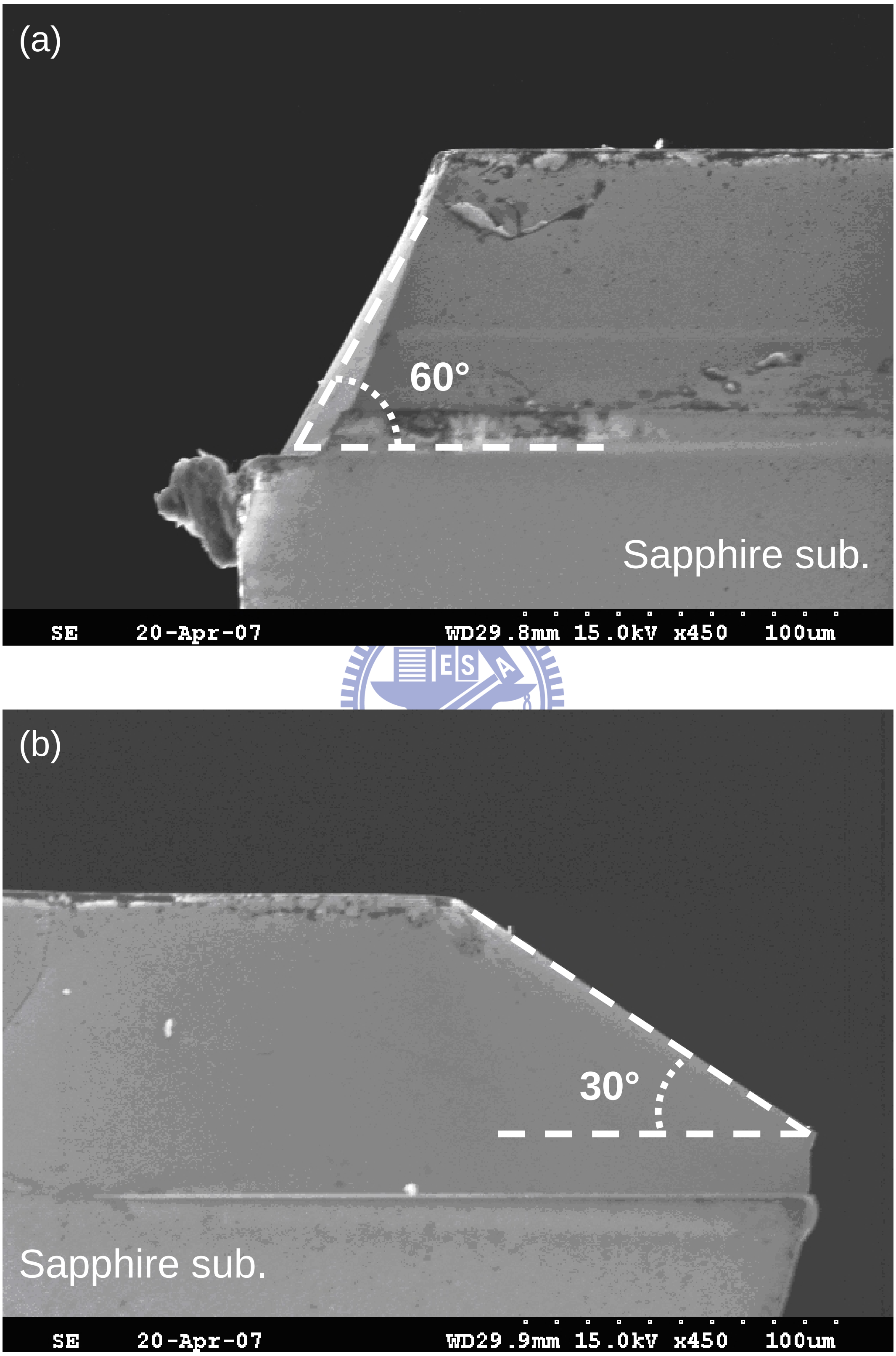
(a)
60°
Sapphire sub.
SE 20-Apr-07 WD29.8mm 15.0kV x450 100um
(b)
30°
Sapphire sub.
SE 20-Apr-07 WD29.9mm 15.0kV x450 100um

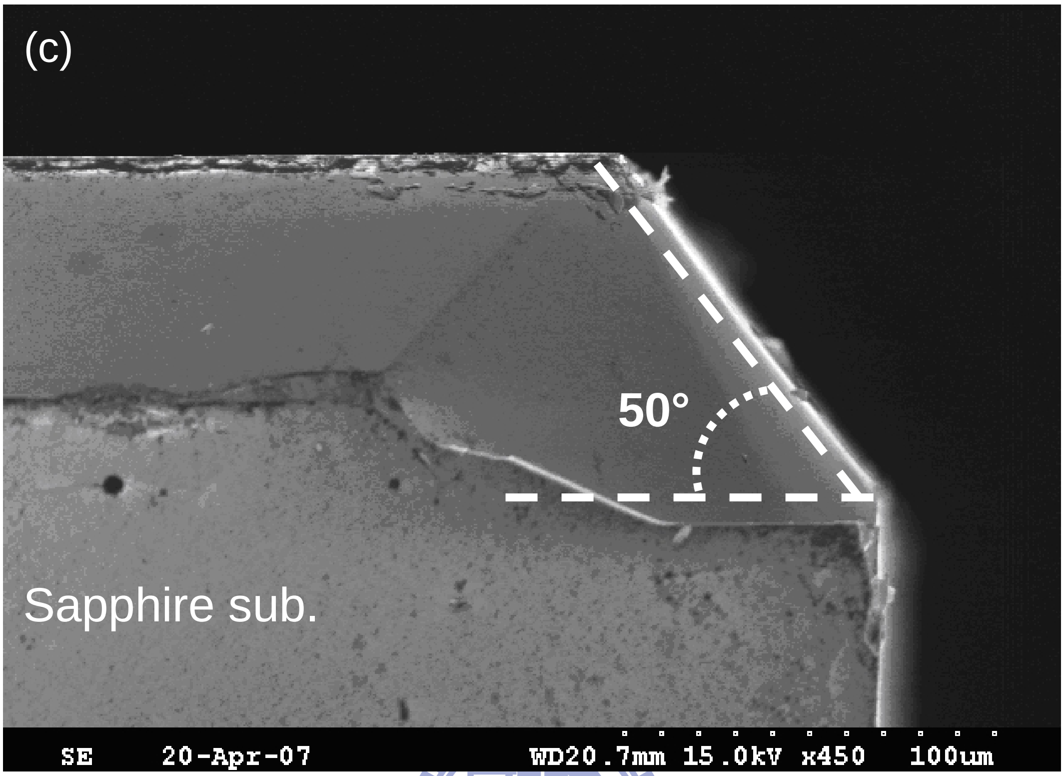

Figure 3-4 SEM images of the crystallography facets of (a) R-plane (60°), (b) A-plane (30°), and (c) M-plane (50°) against (0001) c-axis, respectively.

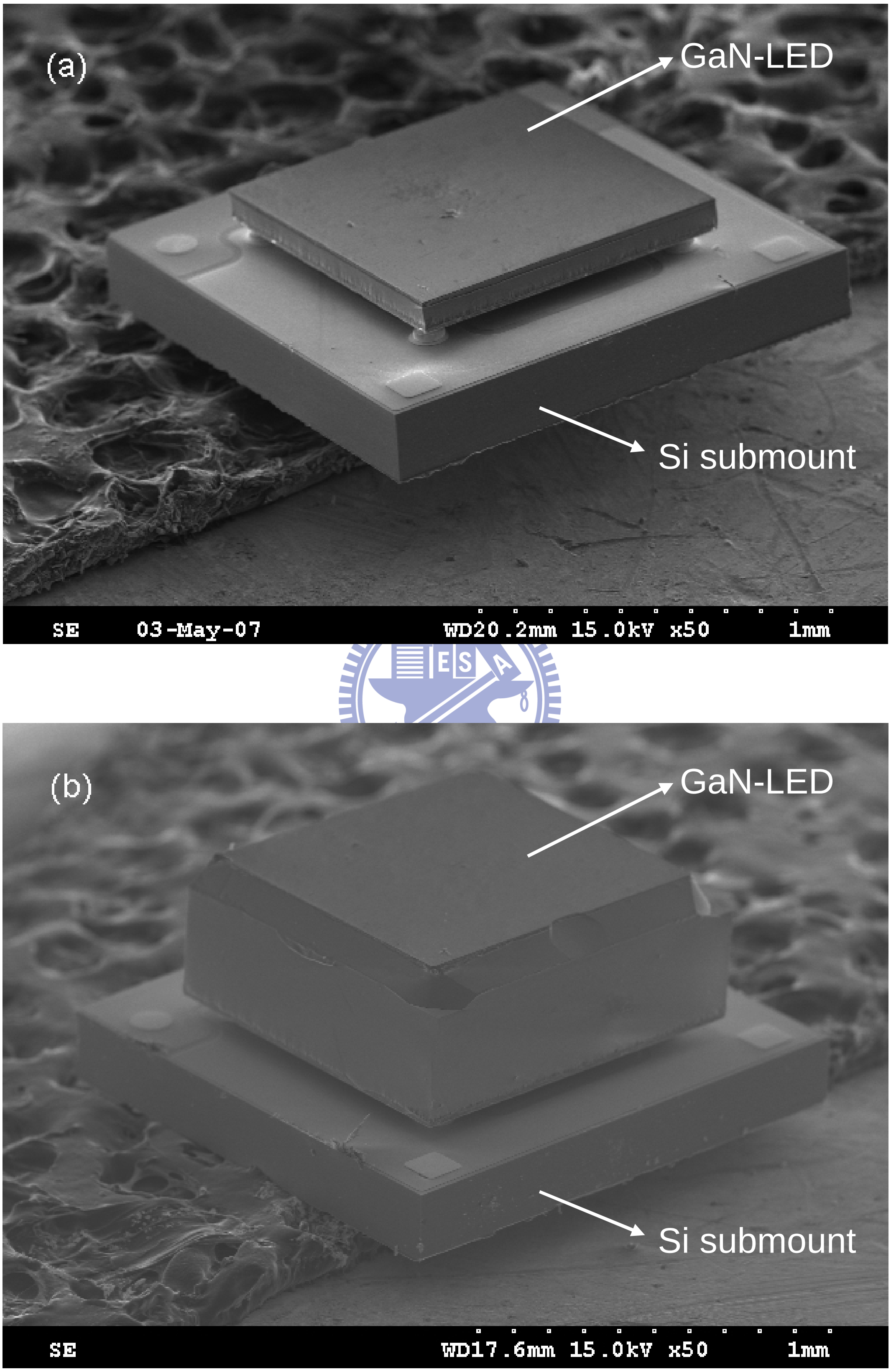

Figure 3-5 SEM images of (a) CFC-LED and (b) SSFC-LED devices.

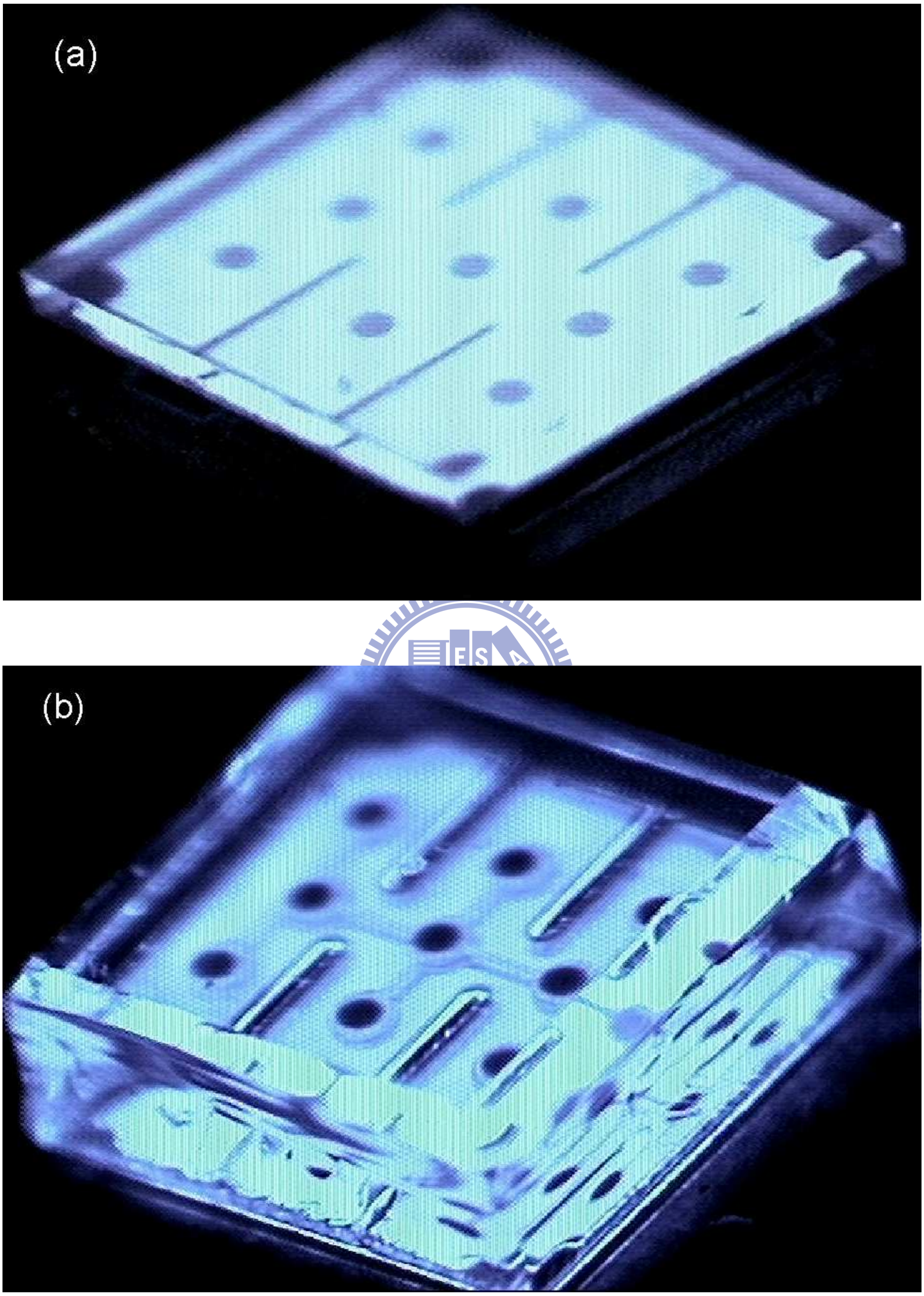

Figure 3-6 Photomicrographs of (a) CFC-LED and (b) SSFC-LED chips (40X40 mil) operating at 20 mA (dc) with an emission wavelength of λ_p~460 nm.

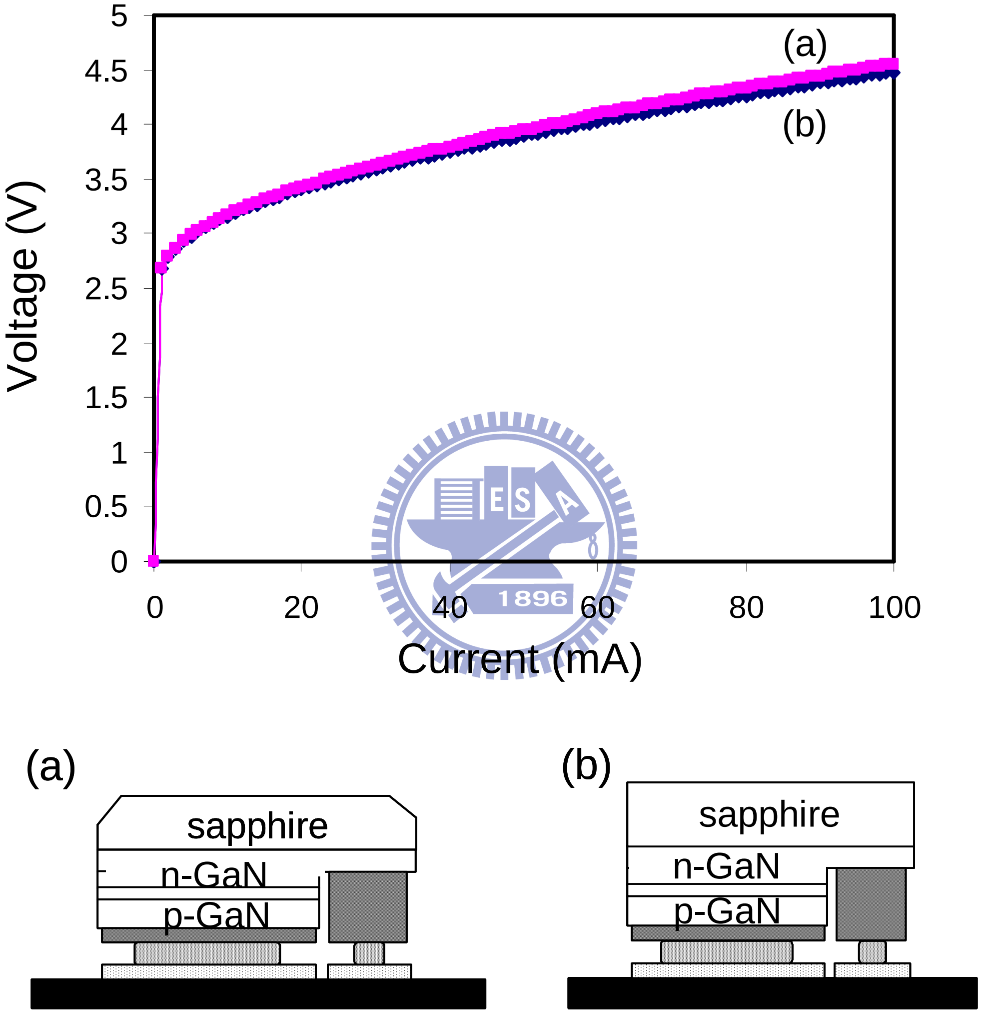

Figure 3-7 The corresponding current-voltage (I-V) characteristics of SSFC-LEDs and CFC-LEDs.

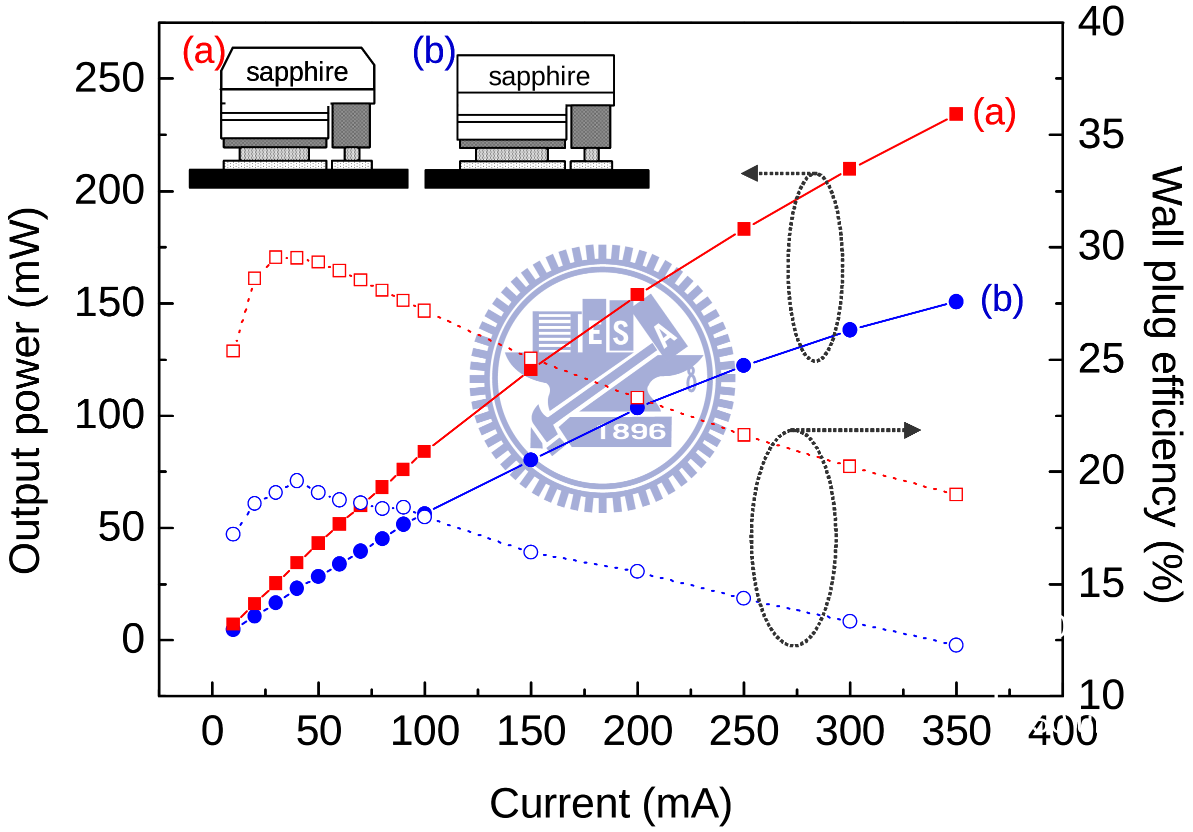

Figure 3-8 The light output power and wall plug efficiency as a function of injection current for λ_p~460 nm devices of SSFC-LEDs and CFC-LEDs.

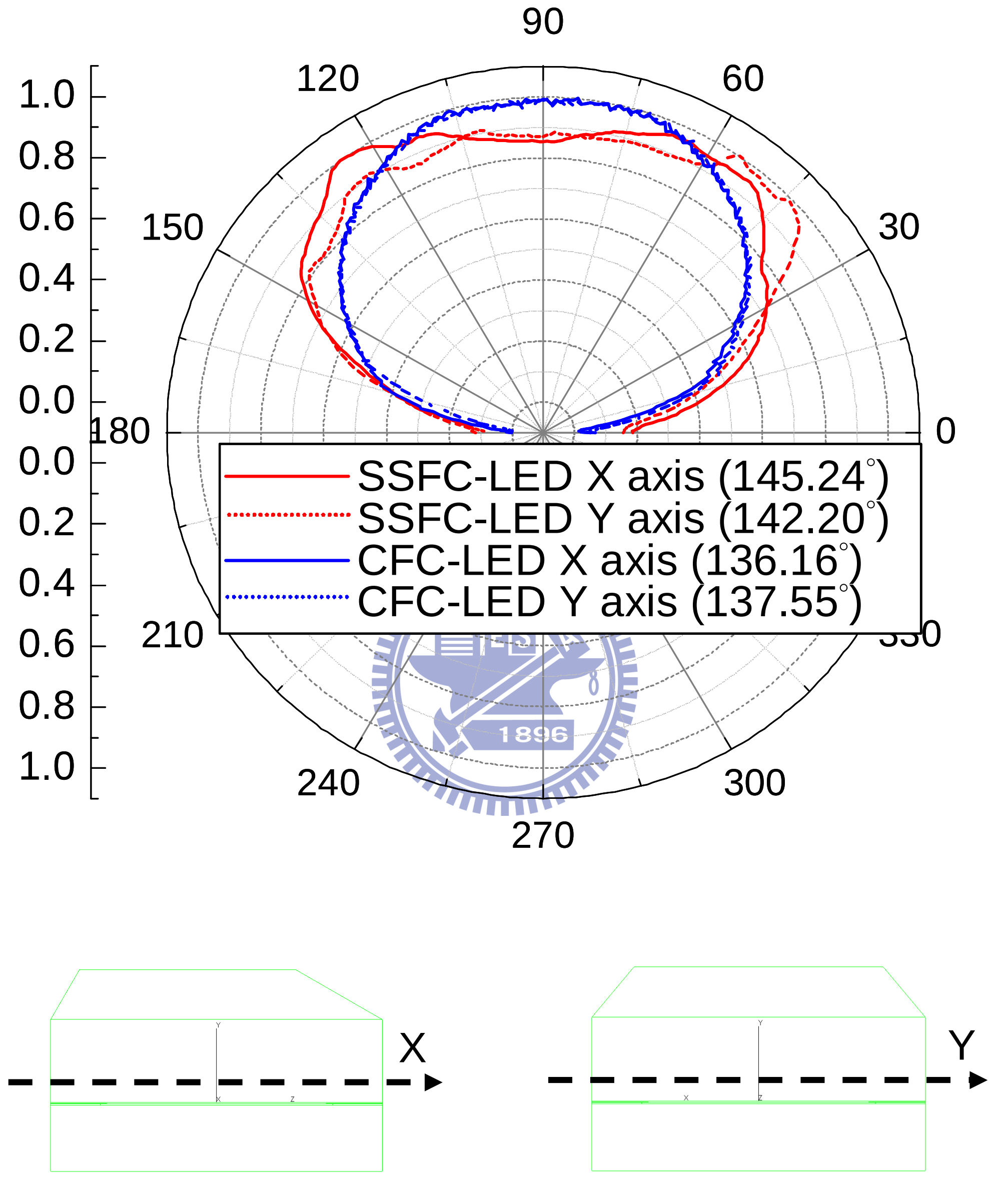

Figure 3-9 The normalized far-field patterns of the SSFC-LED and CFC-LED versus two directions ((1-106)-plane to (1-102)-plane, X-axis; (11-25)-plane to (11-25)-plane, Y-axis), respectively.

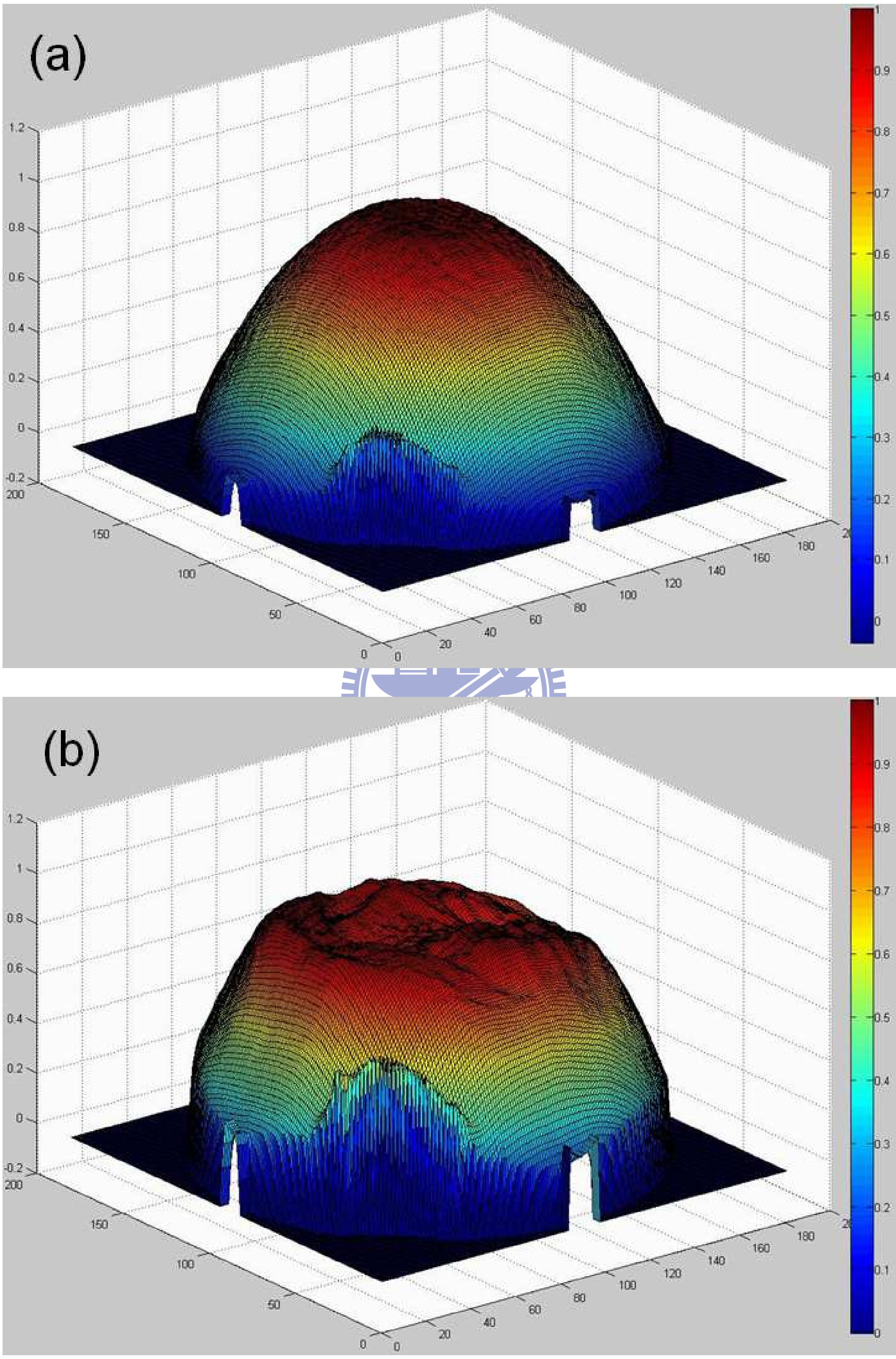

Figure 3-10 The normalized three-dimensional far-field patterns of (a) CFC-LEDs and (b) SSFC-LEDs.

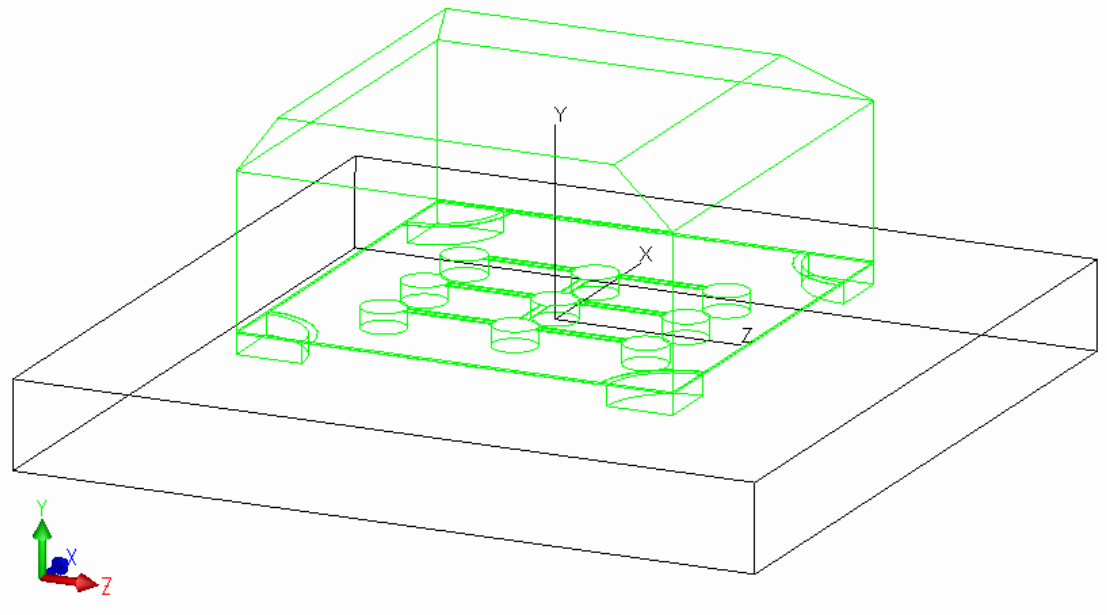

Figure 3-11 The structure of the siumalted model in TracePro software.

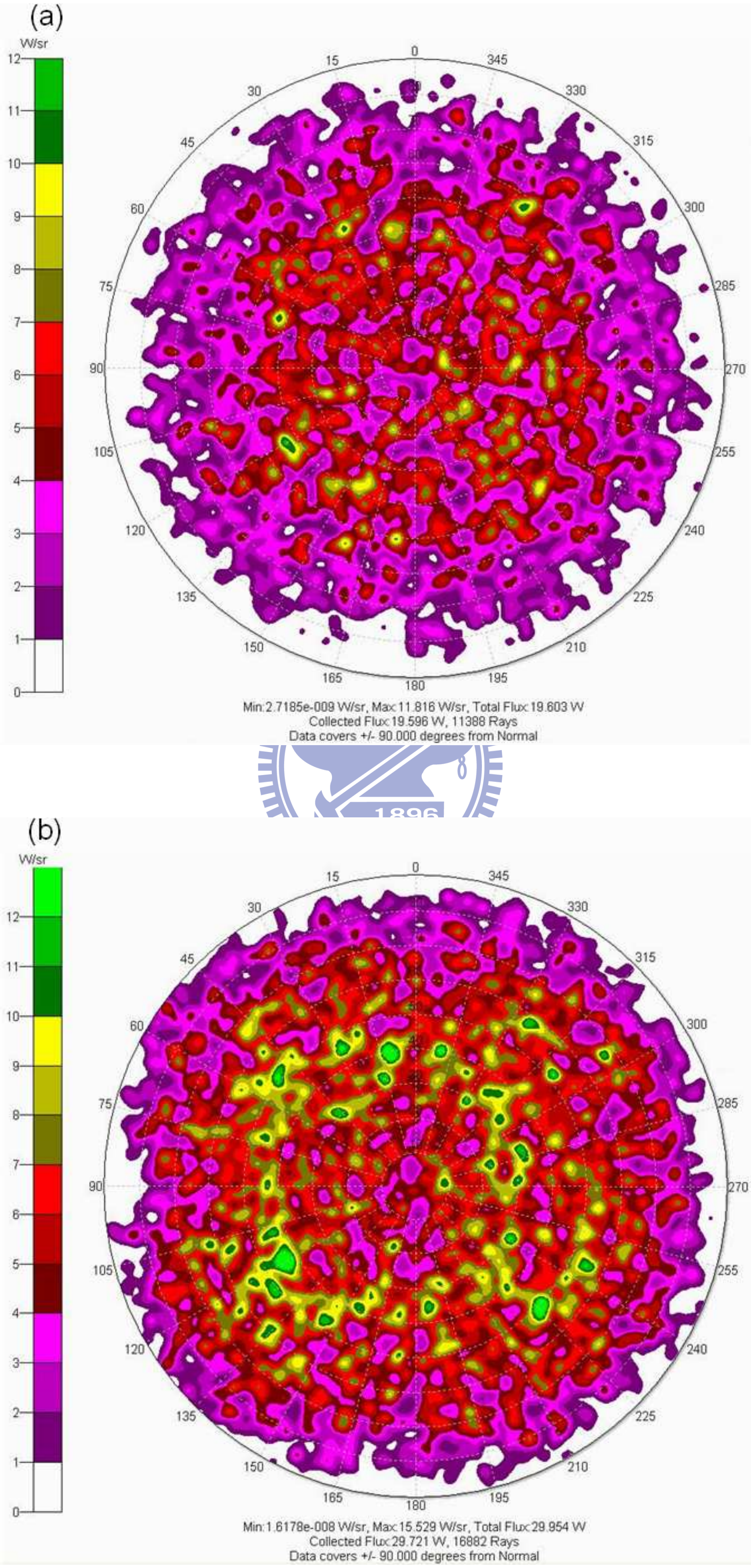

Figure 3-12 The candela maps of (a) CFC-LEDs and (b) 100 μm SSFC-LEDs.

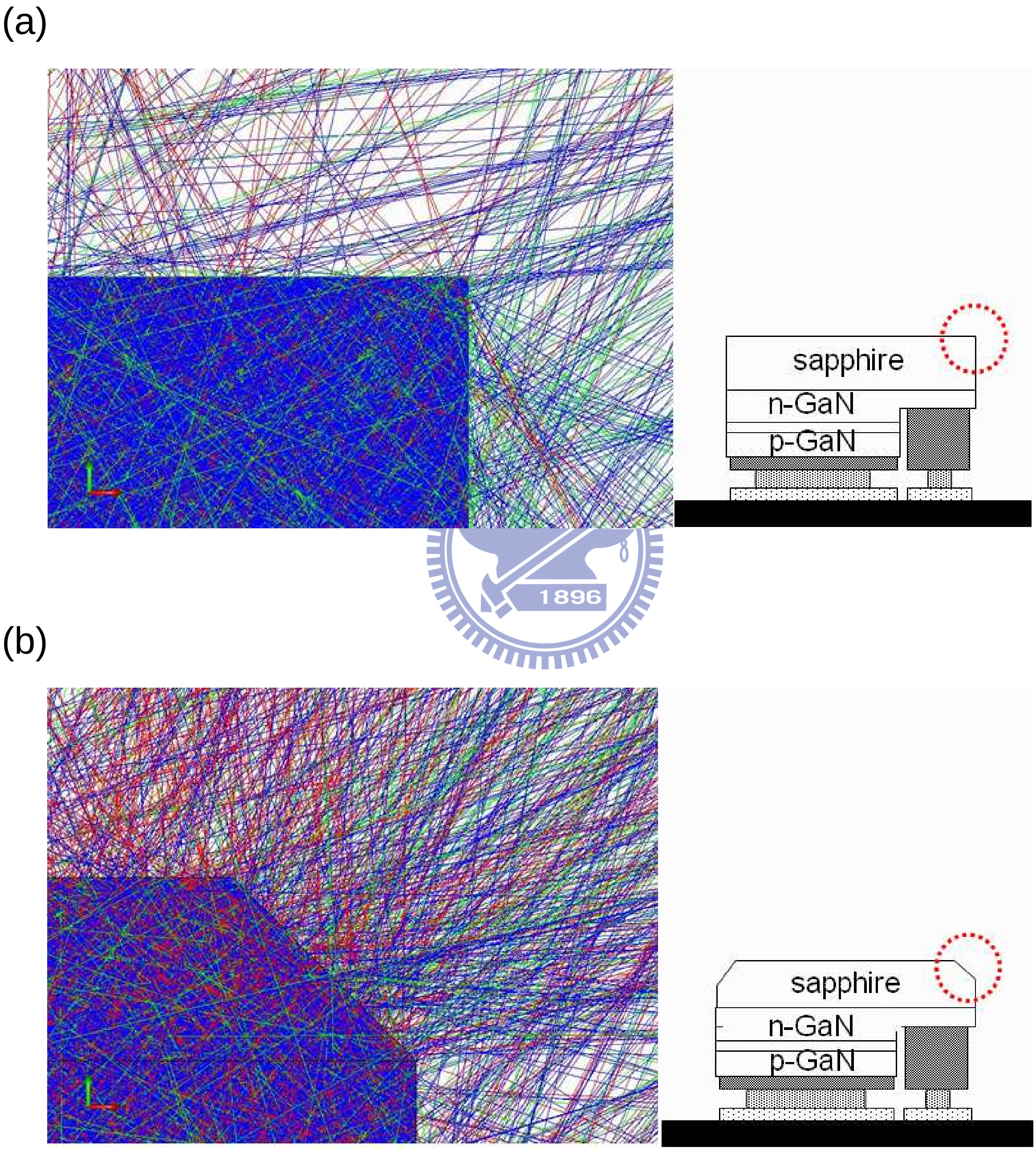

Figure 3-13 The ray-tracing images of oblique sidewall of (a) CFC-LEDs and (b) SSFC-LEDs.

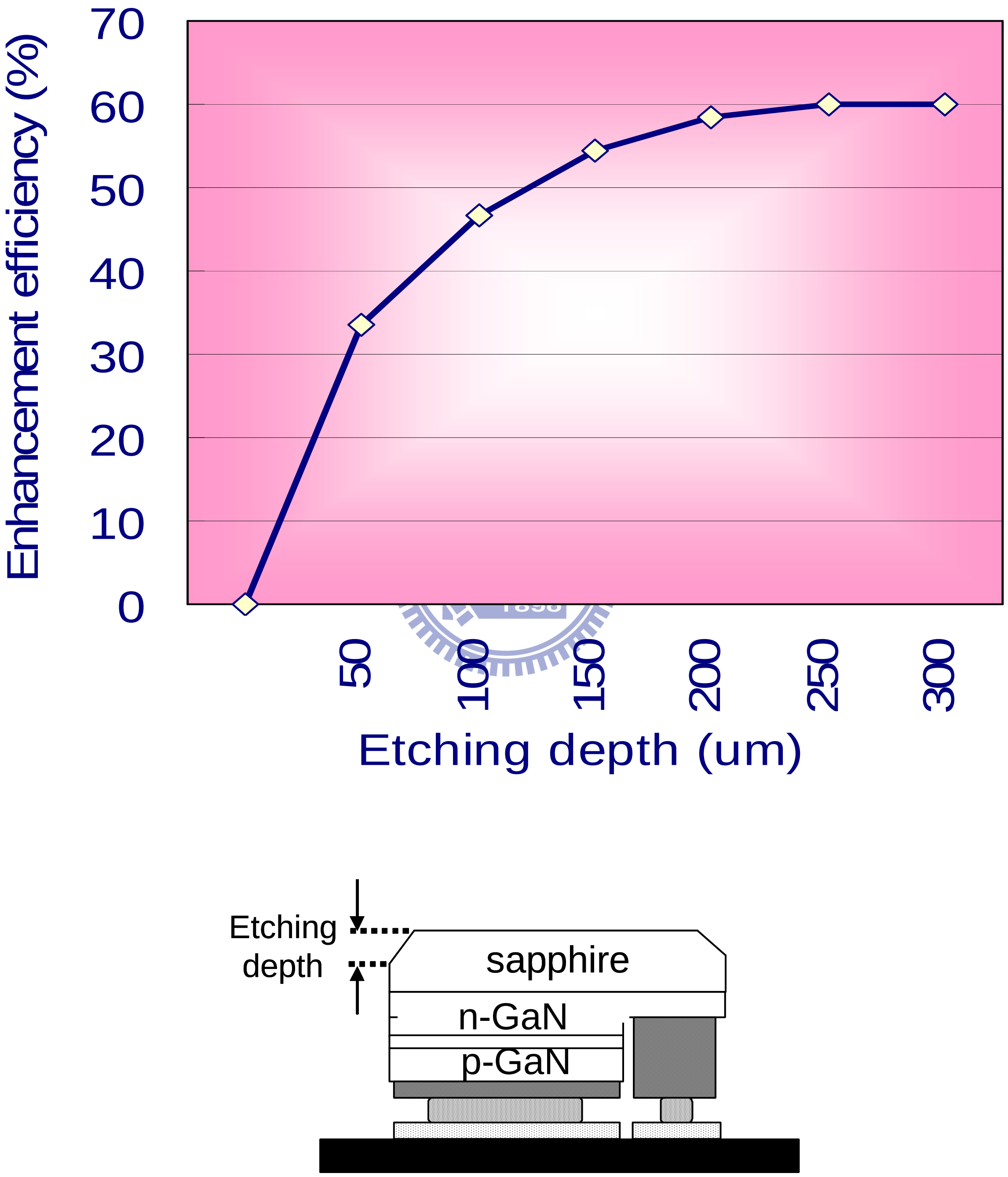

Figure 3-14 The calculated enhancement of the light extraction efficiency with the increasing of etching depth of SSFC-LEDs.

Chapter 4

Flip-Chip Light-Emitting Diodes with Triple Light Scattering Layers

4-1 Fabrication of FC-LEDs with triple light scattering layers

Figure 4-1 shows the schematic drawings of fabrication steps of FC-LEDs with triple light scattering layers. The GaN LED wafers used in this study were grown by MOCVD onto c-face (0001) 2 in. diameter PSS. Fabrication of PSS was illustrated as follows: the Ni films with bump-array patterns of 3 μm diameter and 3 μm spacing were deposited onto the sapphire substrate by e-beam evaporator and defined by standard photolithography to serve as the dry-etching hard mask. The sapphire substrate was then dry etched using an inductively coupled plasma (ICP) etcher with an etching depth of 1 μm. In this study, GaN-LED structure comprised a 1.5 μm-thick undoped GaN layer, a 2.5-μm-thick highly conductive n-type GaN layer, a 0.2-μm-thick InGaN/GaN MQW, a 0.2-μm-thick p-type GaN layer and InGaN/GaN short period super-lattice (SPS) tunneling contact layers for indium-tin-oxide (ITO) ohmic contact. Top-emitting LEDs with a size of 1000 μm × 1000 μm were fabricated using standard photolithography and ICP etcher for current isolation purpose. The p-GaN and active layers were partially etched by an ICP etcher to expose an n-GaN layer for electrode formation. An ITO film (250 nm) was deposited on p-GaN layer as the transparent conductive layer. The samples were then annealed at 500 °C for 10 min in air. The Cr/Pt/Au (50 nm/50 nm/2500 nm) metals were deposited for the p- and n-contact pads. After completing the conventional face-up LED structure, the Ni (500nm) metal with bump-array patterns of 3 μm diameter and 3 μm spacing was deposited onto the bottom side of sapphire substrate as the hard mask. The sample was then subjected to the ICP process using Cl2/BCl3 (10 sccm/30 sccm) plasma with an ICP power of 850 W and RF power of 400 W to form the micro-pillar arrays surface for light extraction purpose. The processed LED wafer was then subjected to the laser scribe and broken into 1000 × 1000 μm2 chips. Finally, the LED chips were flip-chip bonded on SiO2/Al (80nm/200 nm) coated silicon sub-mount using Panasonic ultra sonic flip chip bonder for electrical and optical measurement. A schematic drawing of the GaN FC-LED with triple light scattering layers including top pineapple like pillar arrays surface layer, interface pattern sapphire layer, and bottom naturally textured p-GaN layer was shown in Fig. 4-2.

4-2 Characteristics of FC-LEDs with triple light scattering layers

The surface morphologies of triple light scattering layers were examined by scanning electron micrographs. Fig. 4-3 shows the top sapphire surface with 5.5 μm periodic distance and 3.2 μm depth of pillar-arrays structure. Such a pineapple like pillar surface could be ascribed to the non-uniform Ni hard mask and various etching rate in the center and rim areas of etch pillar which result in partial over etching and the uneven pillar surface. Fig. 4-4 shows the patterned sapphire substrate after epi-growth. In this study, the patterns with 3 μm diameter, 3 μm spacing, and 1 μm etching depth were form on the sapphire substrate for epi-growth. According to the figure, the PSS can be buried completely by GaN epitaxial layer without appearance of void. Figures 4-5(a)-(c) show the SEM images of naturally textured p-GaN surface. The pyramid structures were observed after the Mg-treatment. One can see as the Mg-treatment time increased, the density of the nano-pyramids was increased obviously since the nuclei sites will be increased as the Mg-treatment time increased.

In this study, four types of FC-LEDs were fabricated for comparison: conventional FC-LEDs, FC-LEDs with bottom side naturally textured p-GaN surface [LED-I], FC-LEDs with bottom side naturally textured p-GaN surface and interface pattern sapphire substrate layer [LED-II], and FC-LEDs with triple light scattering layers [LED-III]. The corresponding current-voltage (I-V) and output power-current (L-I) characteristics of these four types FC-LEDs were shown in Fig. 4-6. It was found that the I-V curves were almost identical for these devices. The forward voltage (@ 350 mA) was all about 3.55 V for these four devices. The similarity of electrical property indicates that the implementing of triple light scattering layers would not result in any degradation in the electrical properties of nitride-based FC-LEDs. According to the L-I curves, it could be seen that output power of LED-I, -II, and -III were all larger than that of conventional FC-LEDs. By adopting the naturally textured p-GaN layer, the TIR effect can be reduced and the light escape probability can be increased at the GaN-air interface resulting in the higher output power of LED-I. Furthermore, the output power can be further enhanced by epi-growth on PSS. The interface pattern sapphire substrate not only reduces the dislocation but increases the light scattering from GaN to sapphire substrate [40-42]. Finally, by a combination of epi-growth naturally textured surface, epi-growth on PSS, and micro-pillar array sapphire surface techniques, it is found that the light output power of LED-III could be significantly raised from 119 mW to 191 mW under 350 mA current injections compared to that of conventional FC-LEDs. This result can be attributed to the implemented of triple light scattering layers. The internal quantum efficiency and external quantum efficiency could be improved by epi-growth on the PSS. Beside, top pineapple like textured sapphire surface and bottom naturally textured p-GaN surface can efficiently reduce the totally internal reflection effect and enhance the light extraction from sapphire to air and GaN to air, respectively. The LED-III offer a significant advantage over conventional FC-LEDs by facilitating light emission from the top pineapple-like pillar array surface and bottom naturally textured p-GaN surface. By these arts, it notes that the bare FC-ELDs with triple light scattering layers (without an epoxy lens encapsulated) present 60 % output power enhancement at 350 mA current injection compared to that of conventional FC-LEDs. To further investigate the influence of triple light scattering layers on light-output performance of an LED chip, intensity distribution measurements were performed on LED-III and conventional FC-LEDs. Fig. 4-6 shows the photos of the devices under 20 mA current injections. Each light output intensity distributions were also shown in the same figure. It was obviously observed that the EL intensities of LED-III were clearly exceeded those of conventional FC-LED under the same injection current at the top surface area. Such an enhancement could be attributed to the adopting of triple light scattering layers that photos could have a larger probability to emitted from the device and, thus, achieve even brighter LEDs.

In summary, the FC-LEDs with triple light scattering layers were investigated. The formation of FC-LEDs structure increased the light output power up to 60 %. The novel FC-LEDs structure could not only reduce the TIR effect but efficiently facilitate light emission from the top pineapple-like pillar arrays surface and bottom naturally textured p-GaN surface.

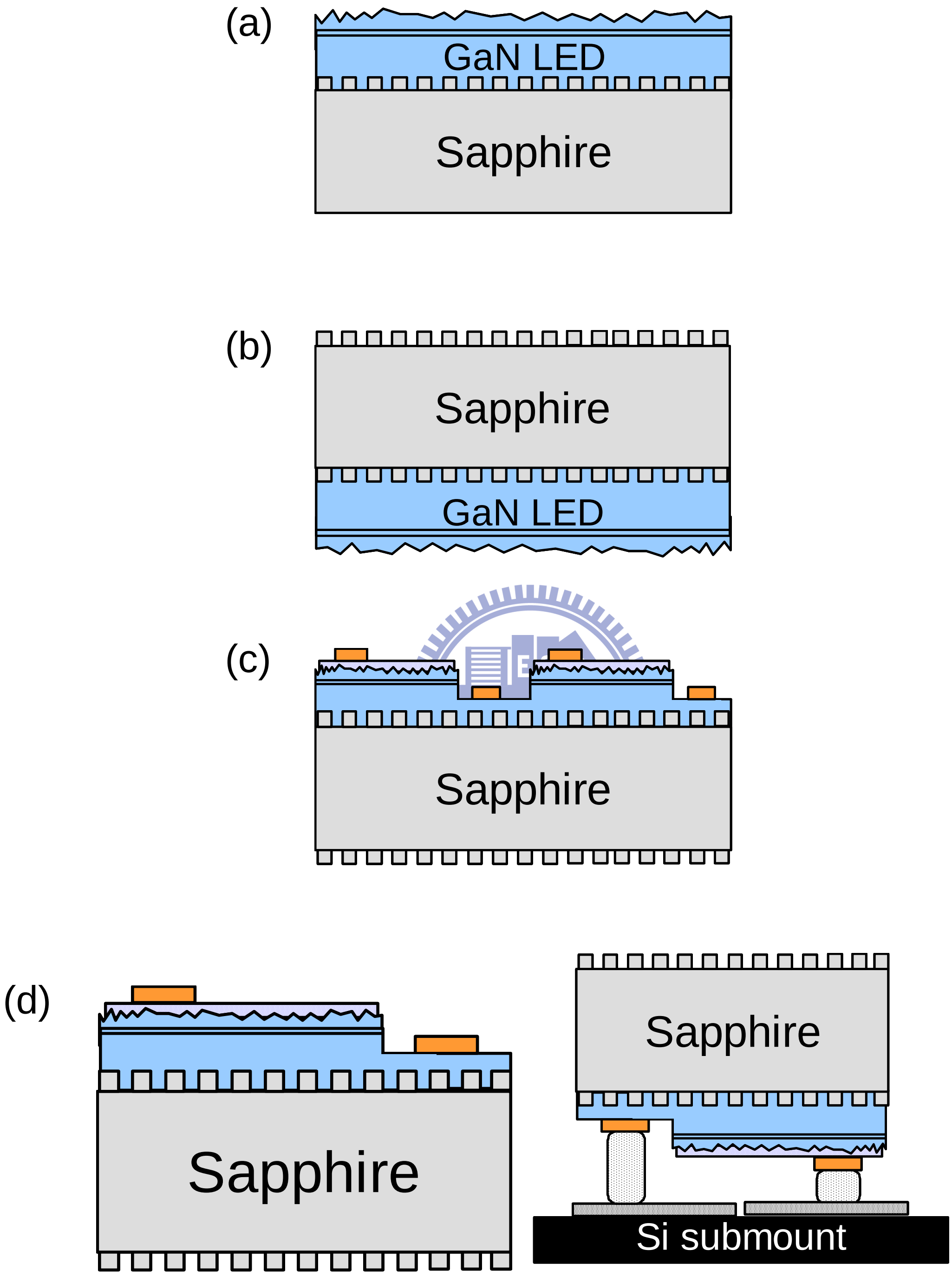

Figure 4-1 Schematic drawings of fabrication steps of FC-LEDs with triple light scattering layers: (a) Epi-growth on pattern sapphire substrate with naturally surface roughness, (b) back-side pattern formation, (c) standard chip process, and (d) chip separation and flip-chip bonding.

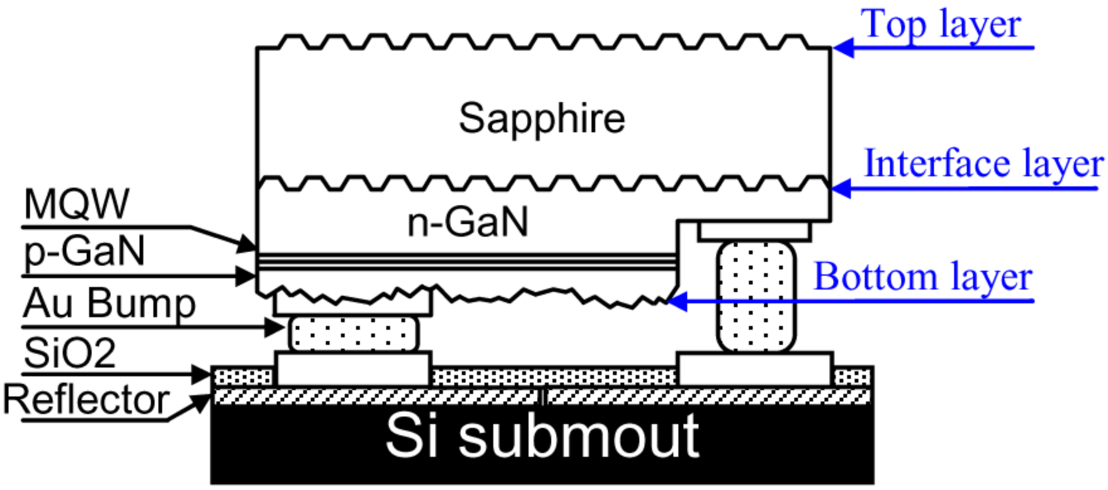

Fig. 4-2 Schematic drawing of the FC-LEDs with triple-light scattering layers

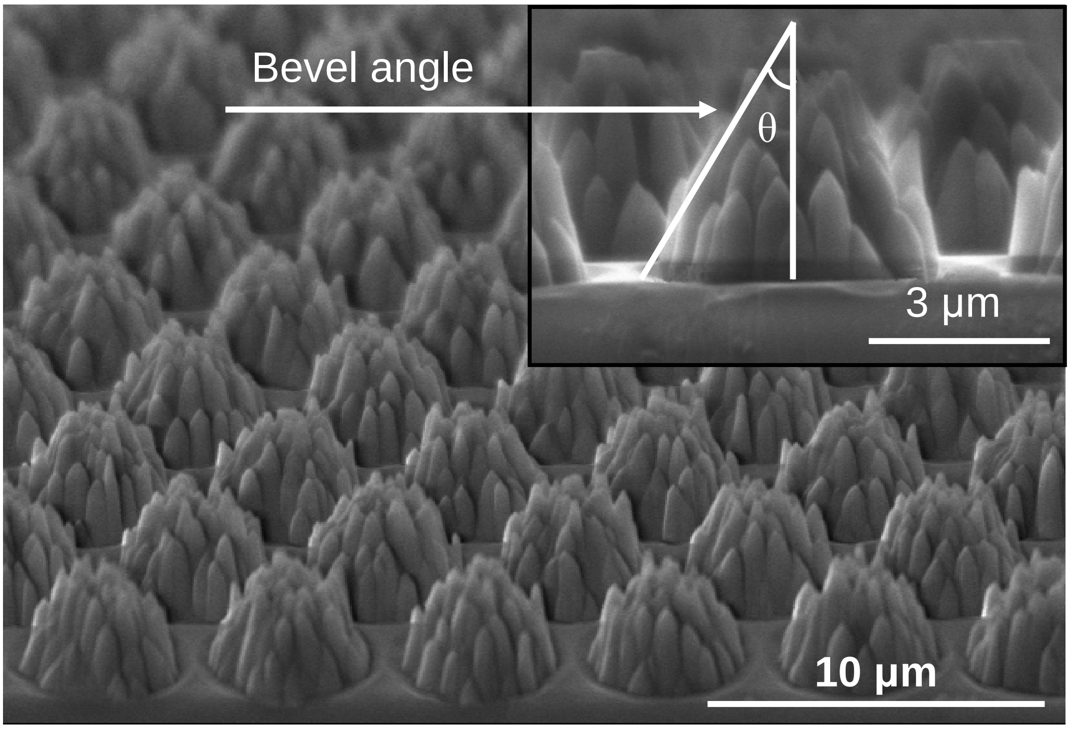

Figure 4-3 Scanning electron microscope of top surface sapphire textured layer

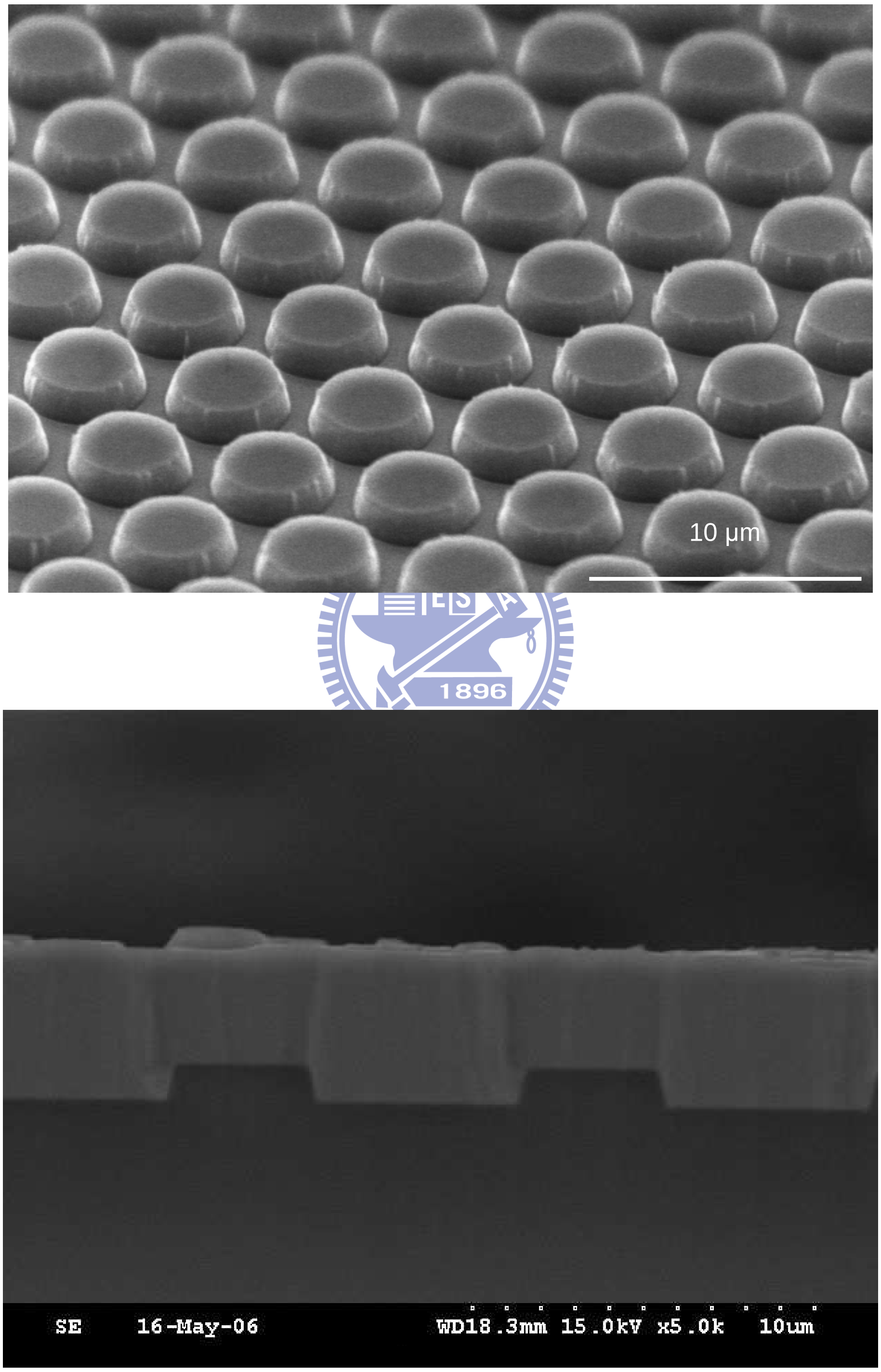

(a)

(b)

Figure 4-4 SEM images of surface morphology of (a) pattern sapphire substrate and (b) Epi-growth on pattern sapphire substrate.

(a)

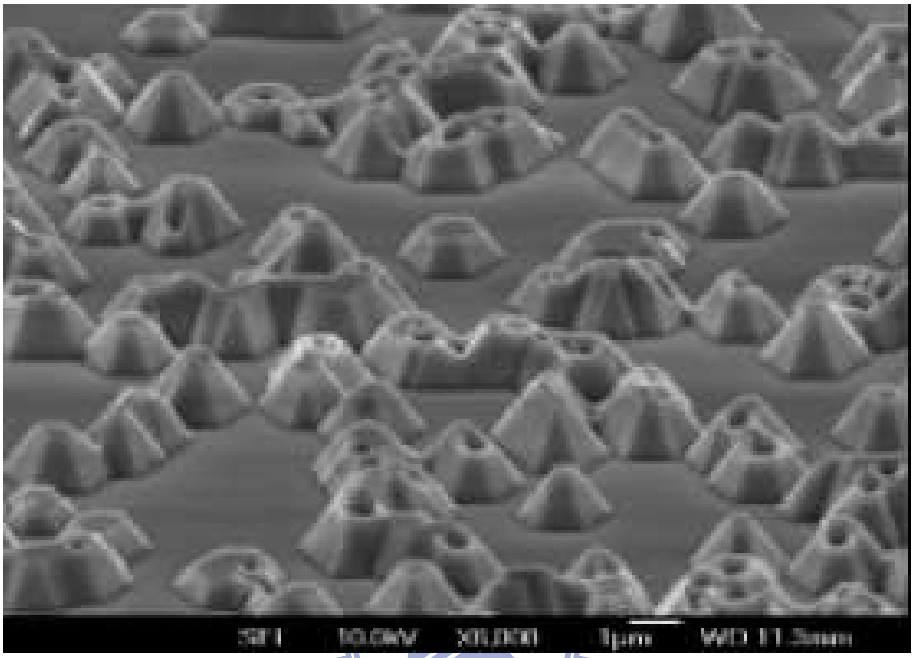

(b)

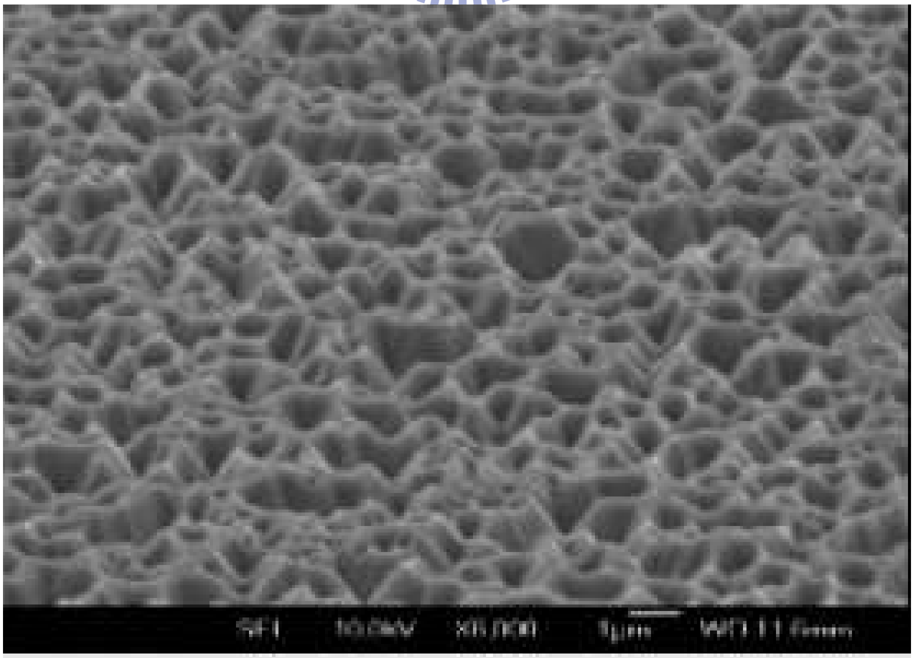

(c)

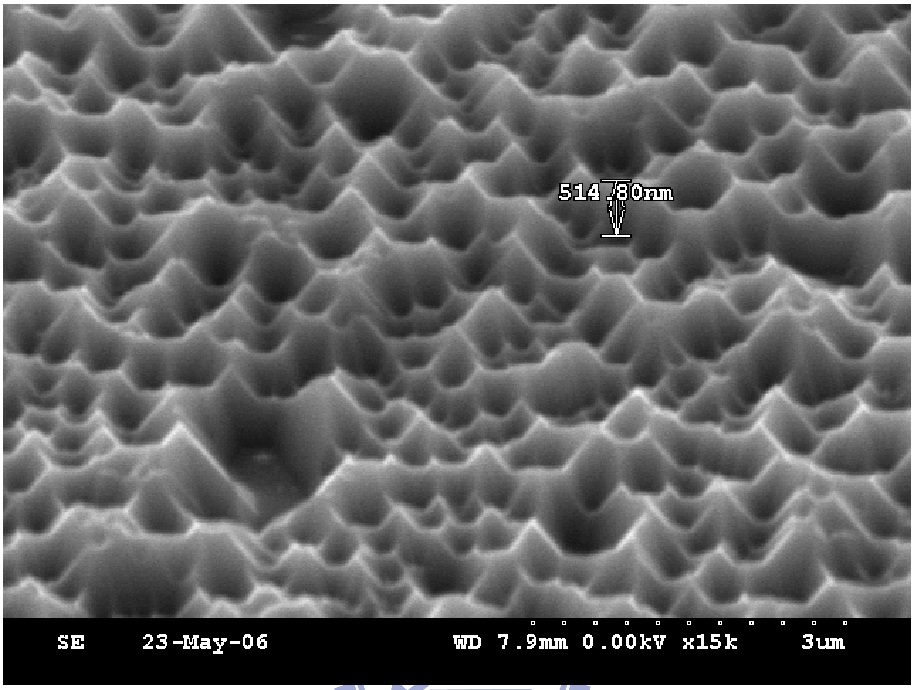

Figure 4-5 Naturally textured P-GaN layer with different Mg-treatment

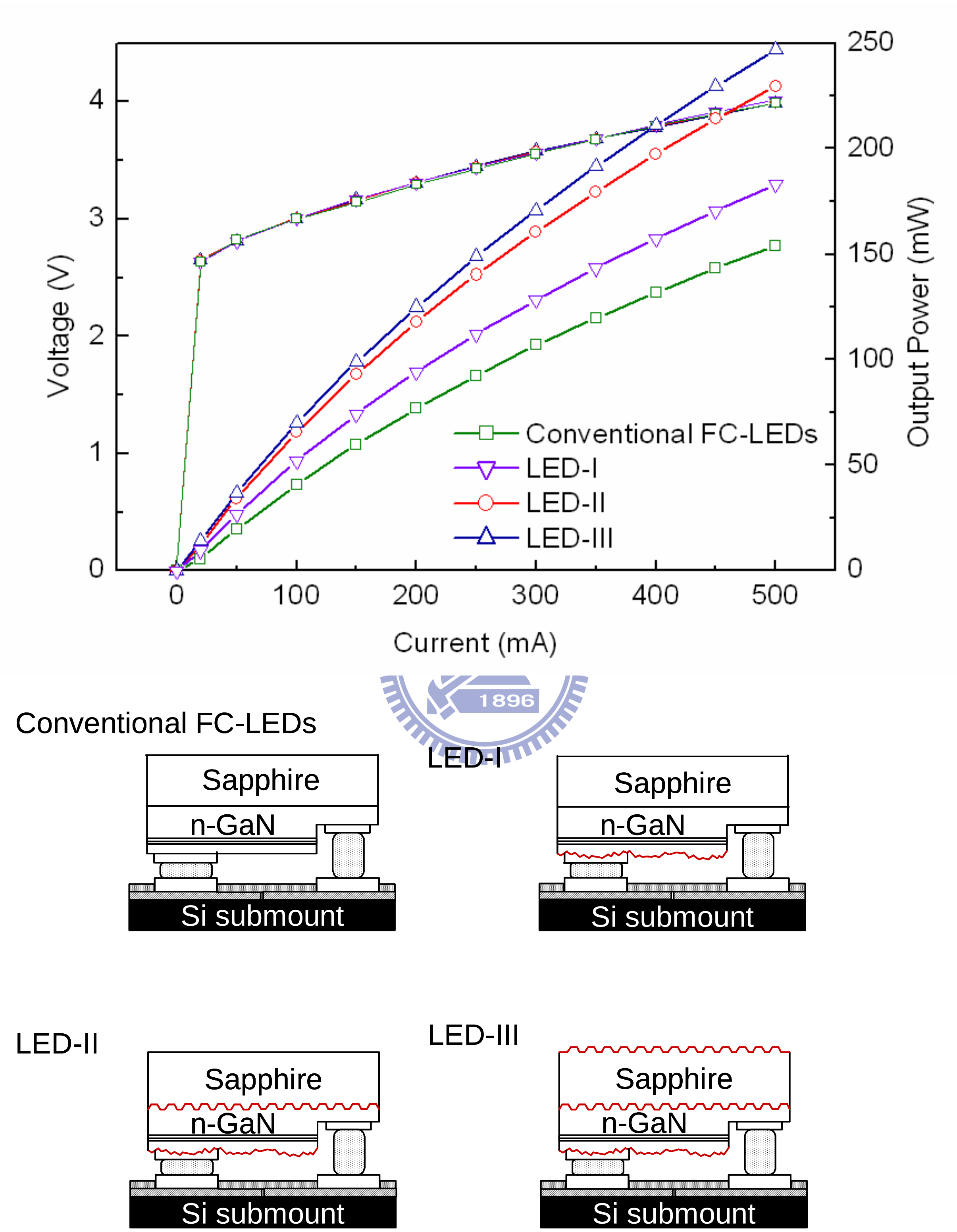

Figure 4-6 The corresponding current-voltage (I-V) and intensity-current (L-I) characteristics of the four types FC-LEDs

Chapter 5

Luminance Enhancement of Vertical Injection Light-Emitting Diodes by Surface Modification

5-1 Progress in vertical-injection near-ultraviolet light-emitting diodes

Recently, tremendous progress has been achieved in GaN-based blue, green and ultraviolet (UV) light emitting diodes (LEDs). High brightness GaN-based blue and green LEDs have already been extensively used in outdoor displays, traffic lights ,LCD backlight and exterior automotive lighting, etc. and show a greater potential to replace incandescent bulbs and fluorescent lamps. UV emitters are of interest for fluorescence based chemical sensing, flame detection, optical storage and a pumping source for exciting phosphor applications [43]. These nitride-based LEDs are also potentially useful for solid state lighting. Although the blue/green LEDs are commercially available, it is still difficult to manufacture high-power UV LEDs. It can be ascribed to the sensitivity to dislocation and the total internal reflection effect which influence the total external quantum efficiency [44-47]. Nowadays, laser lift-off (LLO) LEDs was demonstrated to be one of high potential light-emitting devices to achieve high brightness operation due to its excellent thermal dissipation [48]. In addition, surface roughness technique seems to have high probability to provide large enhancement due to random scattering from the roughened surface [49-50]. Therefore, how to further reduce the dislocation density and improve the light extraction efficiency are important issues for fabricating high-performance UV LEDs. In this letter, the pattern sapphire substrate (PSS), wafer bonding, LLO, and chemical wet etching surface treatment processes were implemented to fabricate the roughened mesh-surface NUV-VLEDs for further enhancement of NUV-VLEDs. Both internal quantum efficiency and external quantum efficiency can be improved by the combination of crystal growth on PSS and VLEDs structure techniques. The electrical and optical properties of the roughened mesh-surface VLEDs will be reported.

5-2 Fabrication of vertical-injection near-ultraviolet light-emitting diodes with a roughened mesh-surface

The NUV-LED wafers used in this study were grown by low-pressure metal organic chemical vapor deposition onto c-face (0001) 2 in. diameter patterned and conventional sapphire substrates at the same growth run. Fabrication of PSSs was illustrated as follows: The Ni film with bump-array patterns of 3 μm diameter and 3 μm spacing was deposited onto the sapphire substrate by e-beam evaporator and defined by standard photolithography to serve as the dry etching mask. The sapphire substrate was then dry etched using an inductively coupled plasma (ICP) etcher with an etching depth of 1 μm. Fig. 5-1(a) shows the top and cross- sectional side views scanning electron microscope (SEM) images of the pattern sapphire substrate. In this report, the NUV-LED structure comprised a 40-nm-thick GaN nucleation layer, a 2.0 um-thick undoped GaN layer, a 2.5 um-thick Si-doped n-type GaN cladding layer, an unintentionally doped active region of 405-nm emitting wavelength with five periods of InGaN–GaN multiple quantum wells, a 0.2 μm -thick Mg-doped p-type GaN cladding layer and a Si-doped n-InGaN-GaN short period superlattice (SPS) structure. Fig. 5-1(b) shows a cross-sectional SEM micrograph of a GaN-based LED grown on a PSS. According to Fig. 5-1(b), the PSS can be buried completely by a GaN epitaxial layer without appearance of void. By performing a detail comparison, both types of NUV-LED wafers with and without PSS were subjected to the VLEDs processes. Fig. 2 shows the diagrams of fabrication process for VLEDs. The fabrication process of VLEDs on Si began with the deposition of highly reflective ohmic contact layer Ni/Ag/Pt and Cr/Au bonding layer on p-GaN. Both types of samples were then bonded onto a Cr/Au-coated p-type conducting Si substrate at 350 ℃ for 1 hr to form the structure of sapphire (with and without PSS)/GaN LED/NiAgPt/CrAu-AuCr/Si [Fig. 5-2 (a)]. The wafer bonded samples were then subjected to the LLO process to form the u-GaN (with and without mesh-surface)/n-GaN/MQW/p-GaN structure on Si [Fig. 5-2 (b)]. A KrF excimer laser at wavelength of 248 nm with a pulse width of 25 ns was used to remove the sapphire substrate. The incident laser with a beam size of 1.0 mm × 1.0 mm was incident from the polished backside of the sapphire substrate onto the sapphire/GaN interface to decompose GaN into Ga and N. After the sapphire substrate removing, the sapphire-removed samples were dipped into HCl solution to remove the residual Ga on the u-GaN. The details of the LLO process can be described in. Then the u-GaN was etched away to expose the n-GaN layer by an ICP etcher. Then, a square mesa of 750 µm x 750 µm was created by ICP for current isolation purpose. In order to further increase the light extraction efficiency of VLEDs, the top n-GaN surfaces surface treated through a chemical etching using 40 % KOH by weight dissolved in ethylene- glycol solution at 120 ℃ for 120 sec [51]. Finally, a Cr/Pt/Au electrode was deposited as the n-type contact and the VLEDs with and without mesh-surface was obtained [Fig. 5-2 (c)]. The surface morphology of VLEDs was examined by SEM as shown in fig. 3. It is obviously observed that the mesh-surface was naturally formed due to the epi-growth on PSS. According to Fig. 5-3(b), the hole-array mesh-surface of 3 µm diameter, 3 µm spacing and 1 µm depth shows a complementary structure from the PSS and was nearly crack-free. It indicates that the epi-layer was not adversely affected to device structure during LLO process. Shown in fig. 5-3 (c) is a SEM image of the mesh-surface after KOH chemical etching at 120 ℃ for 120 sec.

5-3 Characteristics of vertical-injection near-ultraviolet light-emitting diodes with a roughened mesh-surface

Notice that our roughened mesh-surface shows hexagonal cone-like features. Such a roughening surface can improve the escape probability of photons for luminance enhancement of VLEDs. Figure 4 shows the room-temperature electroluminescence (EL) spectra of the flat-surface and mesh-surface VLEDs under 20 mA current injection. The EL peak positions of both the LEDs were located at 405 nm. The EL intensity of the mesh-surface LED is higher than that of the flat-surface one. This significant enhancement in EL intensity could be attributed to the increase of the extraction efficiency by scattering the emission light from the mesh-surface [52]. Additionally, it is believed that the improvement in the internal quantum efficiency (IQE) of the PSS LED could also contribute to the higher EL intensity of mesh-surface VLED. Current-voltage (I-V) and intensity-current (L-I) characteristics of four types VLEDs: conventional flat-surface VLEDs with [LED I] and without [LED II] chemical etching, mesh-surface VLEDs with [LED III] and without [LED IV] chemical etching were shown in fig. 5-5. It was found that the I-V curves were almost identical and similarity (~3.5 V @ 350 mA) for these devices indicating that the fabrication processes would not result in any degradation in the electrical properties of nitride-based LEDs. According to the corresponding L-I characteristics, four types of VLEDs showed linear characteristics up to 500 mA which indicating a good thermal dissipation management for the VLEDs structure design. It is clearly observed that the light output power of the LED-III was higher than those of LED I. This result could be attributed to the increase of total external quantum efficiency by scattering the emission light from the mesh-surface and dislocation reduction of epi-growth on PSS. Furthermore, it is found that the light output power of meshed and flat surface VLEDs could be significantly raised from 100 mW [LED-III] to 130 mW [LED-IV] and 75 mW [LED-I] to 110 mW [LED-II] under 350 mA current injection respectively after chemical wet etching surface roughening process. We note that bare LED-IV (without an epoxy lens encapsulated) exhibit about 20% output power enhancement compared to that of LED-II. Such an enhancement can be ascribed to the increase of surface emission area which improves the probability of photons escaping from semiconductor to air and the reduction of dislocation which increases the internal quantum efficiency by adopting the PSS. These two processes provide the roughened mesh-surface VLEDs with a significant further enhancement in output power compared to the conventional VLEDs.

In summary, the NUC-VLEDs with rough meshed-surface structure were investigated. The formation rough meshed-surface structure improves not only the surface emission area but the escape probability of photons due to the angular randomization of photos insides the LED structure. In addition, the IQE can be increase by adopting the PSS process. By this novel device design, the output power can be further enhanced up to 20 %.

5-4 Progress in ultraviolet LEDs

UV-LEDs are of interest as a light source for exciting phosphors, medical equipment, air cleaners, and environmental sensors. In particular, most of the phosphors for white fluorescent lamps have a high conversion efficiency of less than 370 nm in the UV spectral region. Therefore, it is important to develop high-efficiency UV-LEDs that emit less than 370 nm light in order to fabricate high luminous white LEDs by coupling UV-LEDs and phosphors for solid-state lighting applications. Although the blue/green LEDs are commercially available, it is still difficult to manufacture high brightness UV-LEDs due to poor quantum efficiency. Several works focusing on efficient current injection by introducing current blocking layers [53], highly efficient radiative carrier recombination by introducing a high-quality bulk GaN substrate [54], the emission enhancement of LEDs by the introduction of an AlInGaN quaternary active layer [55], and the improvement in quality of LEDs by utilizing the AlGaN epitaxial lateral overgrowth technique [56] have attempted to improve device performance. However, light extraction efficiency is also limited due to the self-absorption effect of the GaN layer. The self-absorption of UV lights in the bulk GaN substrate, thick GaN buffer/contact layer under the active layer, or the p-type GaN contact layer result in the lower external quantum efficiency. Therefore, GaN-free structure design is a key issue for enhancing the light extraction of UV-LEDs [57]. Recently, state-of-the art vertical injection GaN-based LEDs were demonstrated to be high-potential light emitting devices capable of achieving high brightness operation due to their excellent thermal dissipation.8,9 In addition, the surface roughness technique seems to have great potential to provide large enhancement due to random scattering from the roughened surface. Zhou et al.reported 2.5 times light extraction gain for deep UV-LEDs by utilizing laser lift-off (LLO) and surface roughening to enhance the extraction efficiency of near- and deep-UV vertical LEDs. However, the self-absorption effect of GaN requires further investigation. In this article we report the fabrication and characteristics of GaN-free vertical injection UV-LEDs. We mainly investigated the self-absorption effect of GaN layers on the light-output power of vertical-injection LEDs VLEDs┐. Furthermore, an additional chemical wet etching process was implemented to fabricate the roughened surface of UV-LEDs for further light extraction enhancement. The electrical and optical properties of the UV-VLEDs are reported.

5-5 Fabrication of vertical-injection ultraviolet light-emitting diodes with the GaN-free and surface roughness structures

The UV-LED wafers used in this paper were grown by low pressure metal organic chemical vapor deposition onto c-face 0001 in. diam sapphire substrates. The LED structure comprised a 40 nm thick GaN nucleation layer, a 1 umm thick undoped GaN layer, a 2-m thick Si-doped n-type Al0.05Ga0.95N cladding layer, an unintentionally doped active region of 365 nm emitting wavelength with five periods of In0.01Ga0.99N/Al0.1Ga0.9N multiple quantum wells, a 20 nm thick Mg-doped p-type Al0.2Ga0.8N cladding layer, and a 0.15 └m thick Mg-doped p-type Al0.05Ga0.95N contact layer. The fabrication process of VLEDs on Si began with the deposition of a highly reflective ohmic contact stack Ni 1 nm/Ag 200 nm, a Pt 100 nm diffusion barrier, and bonding metal stack Ti 500 nm/Pt 50 nm/Au 1000 nm┐ on the p-side of the LED wafer. The metal-coated wafer was then flipped and bonded onto a

Ti 50 nm┐/AuSn 2000 nm-coated p-type conducting Si wafer at 300°C for 30 min. The wafer-bonded sample was then subjected to the LLO process. A KrF excimer laser at wavelength of 248 nm with a pulse width of 25 ns was used to remove the sapphire substrate. The incident laser flux was set to a value of about 0.6 J/cm2. The incident laser was incident from the polished back side of the sapphire substrate onto the sapphire/GaN interface to decompose GaN into Ga and N. Then the u-GaN was etched away to expose the n-AlGaN contact layer by an inductively coupled plasma ICP etcher to form a GaN-free structure, and another ICP etch is used to define the square mesa of 750 x 750 um for current isolation purposes. Following the n-contact deposition and annealing processes, the processed sample was immersed in 45 wt % KOH dissolved in ethylene-glycol solution at 110°C for 180 s to form the rough surface for light extraction proposes. Finally, the GaN-free UV-VLEDs with roughened surface were obtained. For detailed comparison, the conventional p-side up UV-LED was also fabricated using the same lot of UV-LED wafers.

5-6 Characteristics of vertical-injection ultraviolet light-emitting diodes with the GaN-free and surface roughness structures

Shown in Fig. 5-6 are the schematic drawings of the conventional UV-LED and surface-roughened GaN-free UV-VLED. In order to perform the lower threading dislocation density of UV-LEDs, the AlGaN-based UV-LEDs were grown on the GaN template in this study as described above. The inserted scanning electron microscope micrograph was the surface morphology of UV-VLEDs after

the chemical wet etching process for further luminance enhancement of UV-VLEDs. Figure 5-7 shows the room-temperature electroluminescence_EL_ spectra of the GaN-free UV-LEDs under 20 mA current injections. A sharp single-peak emission, where the peak wavelength and the full-width at half maximum were 365 and 8 nm, was observed. The inset shows a photomicrograph of the UV-VLED with the designed GaN-free and roughened surface structures at a driving current of 20 mA. The emission light was distributed uniformly over 750 x 750 um size due to the vertical structure device design as shown in this figure. The surface of the VLED was also examined by atomic force microscopy (AFM), as shown in Fig. 5-8. The sapphire removed sample shows a smooth surface with a root-mean square (rms) roughness of around 12.8 nm, as shown in Fig. 5-8 (a). After the surface treatment process, the rms roughness of the VLED surface was significantly increased to 398 nm, as shown in Fig. 5-8(b). Current–voltage (I-V) and intensity–current (L-I) characteristics of conventional UV-LED, UV-VLED, and GaN-free UV-VLEDs, with and without a roughened surface, are shown in Fig. 5-9. It was found that the I-V curves were almost identical and similar for these three types of UV-VLEDs, indicating that the fabrication processes would not result in any degradation in the electrical properties of the devices. Besides, the UV-VLEDs presented the lower operating voltage compared to that of conventional UV-LEDs due to the better current spreading property of the vertical conduction chip structure design. According to the corresponding L-I characteristics, the UVVLEDs showed more linear characteristics up to 250 mA, which indicated a better thermal dissipation property of the VLED structure formation. However, the light output power of UV-VLEDs is lower than that of conventional UV-LEDs under smaller current injection, which could be ascribed to the self-absorption effect of the GaN layer. All light generation of the VLED structure emits upward and extracts from the top of the GaN layer. Hence, a large amount of generated light will be absorbed in the GaN layer, resulting in a lower output power. With the increase of injection current, the light output power of the UV-VLED is greater than that of conventional UV-LEDs. The reason for this is the degradation of internal quantum efficiency due to the Joule heating effect of conventional UV-LEDs. Under 250 mA current injection, UV-VLEDs have a relative output power of 0.15, the GaN-free UV-VLEDs have a power of 0.48, and the surface-roughened GaN-free UV-VLEDs have a power of 1.11. That means that the improvement from removing the GaN is 3.2x and the improvement from surface roughening is 2.3x. These results could be attributed to reduction of the self-absorption effect in the GaN layer by the GaN-free UV-VLED structure. Furthermore, the surface-roughened UV-VLED showed the higher output power performance than that of the smooth surface UV-VLED. Light extraction from the LED was definitely enhanced via the roughened surface, which reduces internal light reflection and scatters the light outward. As a result, photos could have a larger probability to emit from the device. The illuminant intensity of surface-roughened GaN-free UV-VLEDs was increased by a factor of 7.8x compared with that of conventional UV-LEDs at a driving current injection of 250 mA. In order to further investigate the influence of the GaN-free UVVLED structure and roughened surface features on the light-output performance of the device, intensity distribution measurements were performed on surface-roughened UV-VLEDs and conventional UVLEDs. Figure 5-10 shows photos of the devices under 100 mA current injections. Each light output intensity distribution is also shown in the same figure. The EL intensities of the UV-VLED are clearly greater than those of conventional UV-LEDs under the same injection current at the top surface area. Such an enhancement could be attributed to the GaN-free structure and the roughened surface that the self-absorption effect reduced, and the photos could have a larger probability to emit from the device. The UV-VLED also presents a better current spreading property than that of conventional UV-LEDs. Light emits evenly from the top surface area, and no current crowding phenomenon is observed, which indicates the lower series resistance of the vertical-injection structure design.

In summary, GaN-free UV-VLEDs with a roughened-surface structure were investigated. The self-absorption effect was decreased by the GaN-free structure design. The formation-roughened surface structure improves not only the surface emission area but the escape probability of photons due to the angular randomization of photos inside the LED structure. In addition, the vertical injection LED structure was demonstrated to achieve high-brightness operation due to its excellent thermal dissipation and lower series resistance.

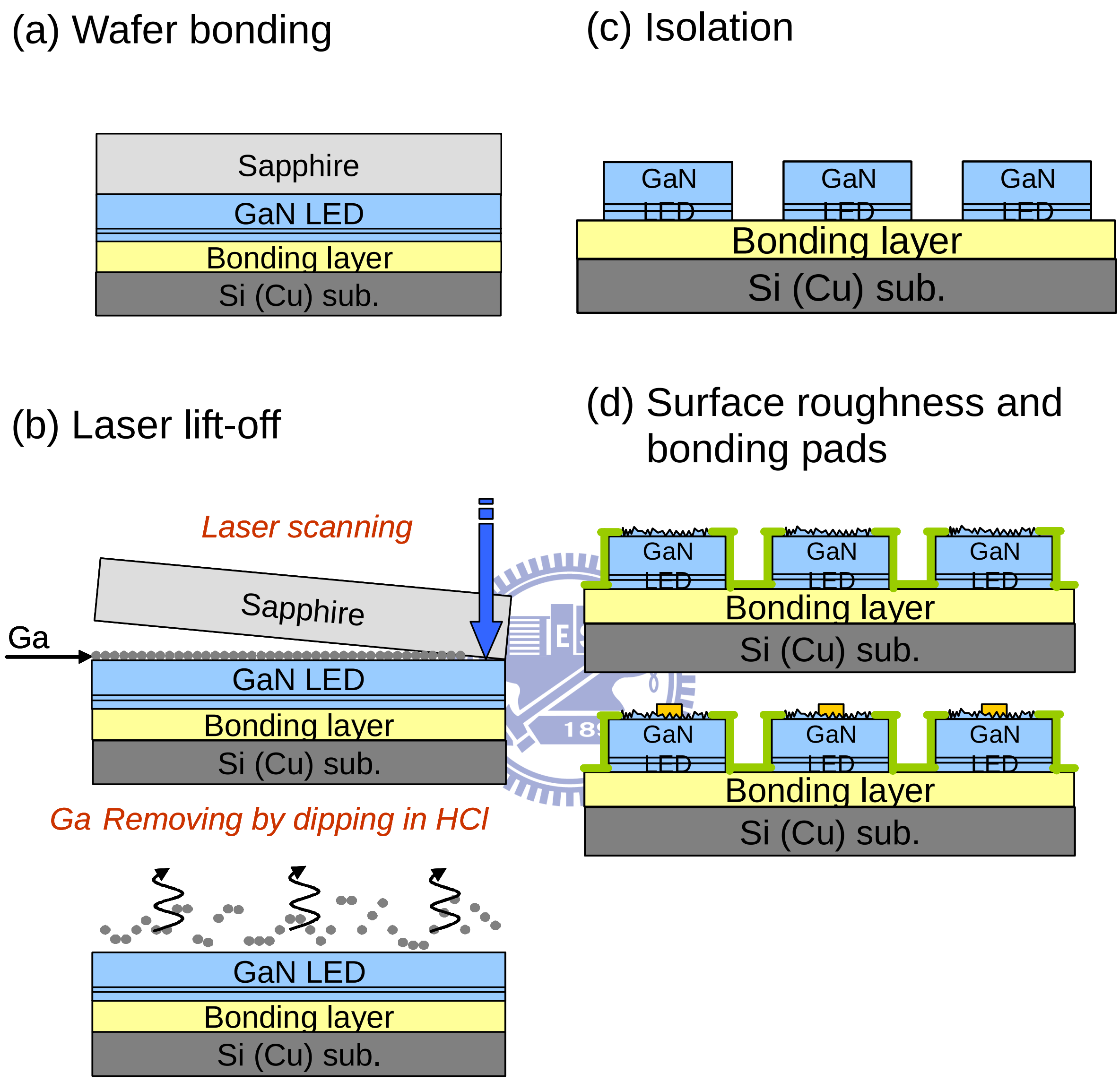

Figure 5-1 Diagrams of fabrication processes for regular VLEDs (a) wafer bonding, (b) laser lift-off, (c) isolation, and (d) surface roughness and bonding pad.

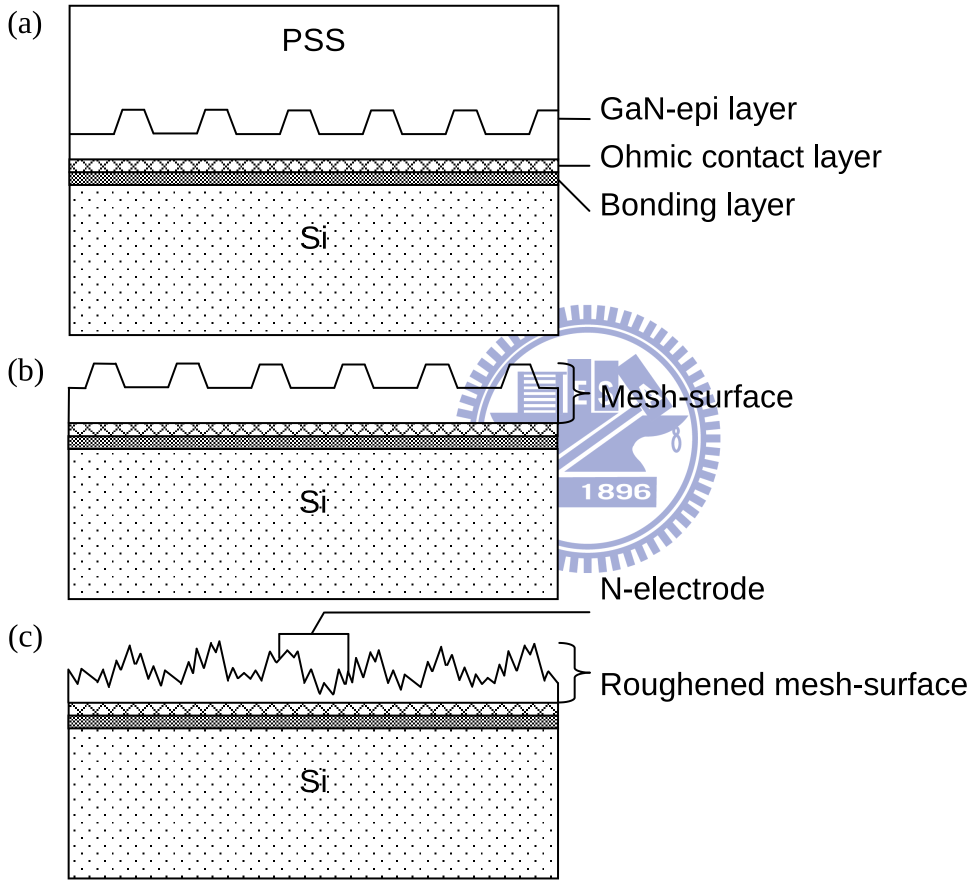

Figure 5-2 Diagrams of fabrication processes for VLEDs with the roughened mesh surface structure (a) wafer bonding, (b) LLO, and (c) chemical wet etching and electrode deposition.

(A)

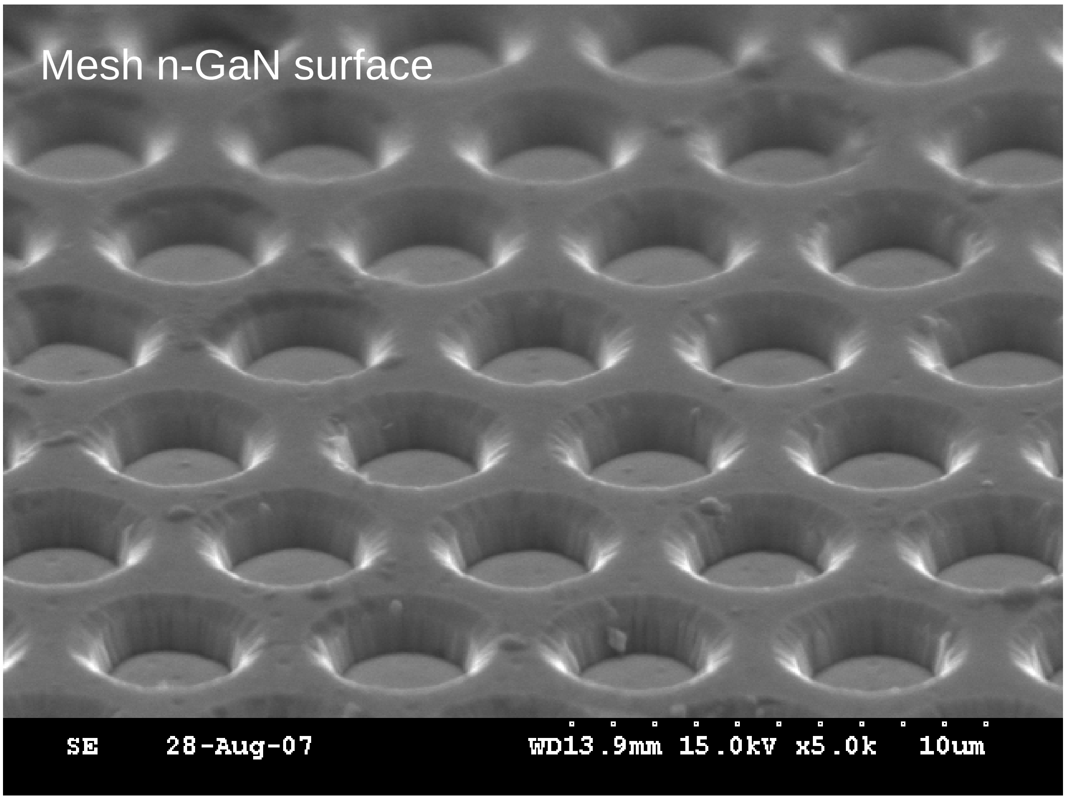

(B)

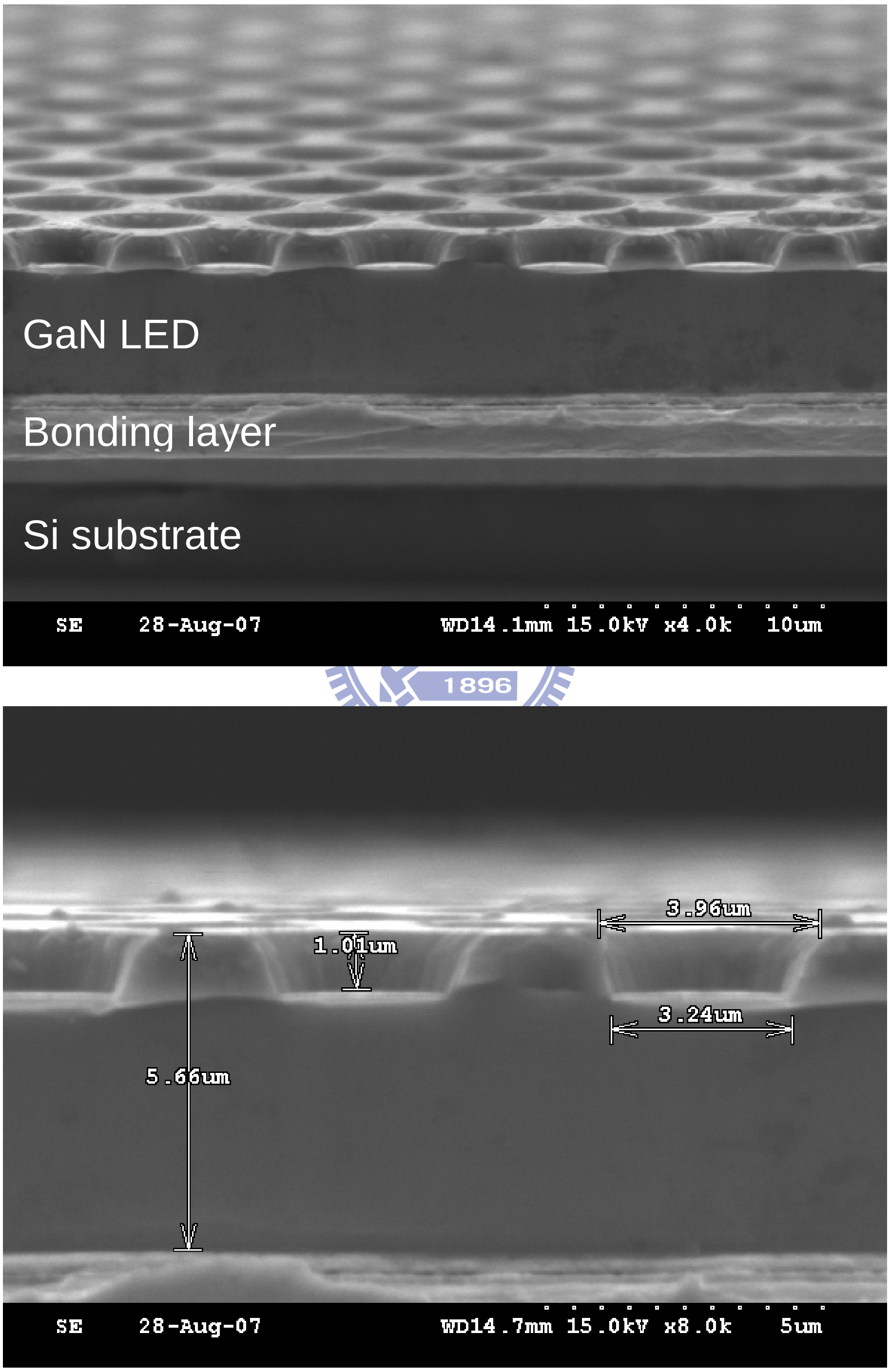

Figure 5-3 SEM images of (a) surface morphology of mesh-surface VLEDs after LLO process, (b) cross sectional view of VLEDs structure

(a) 30 sec.

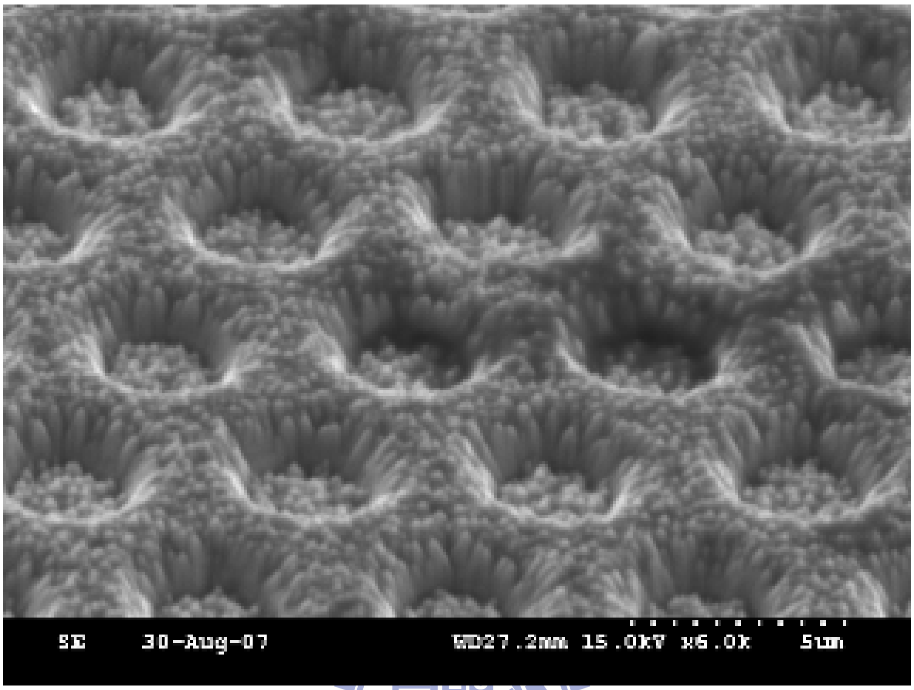

(b) 60 sec.

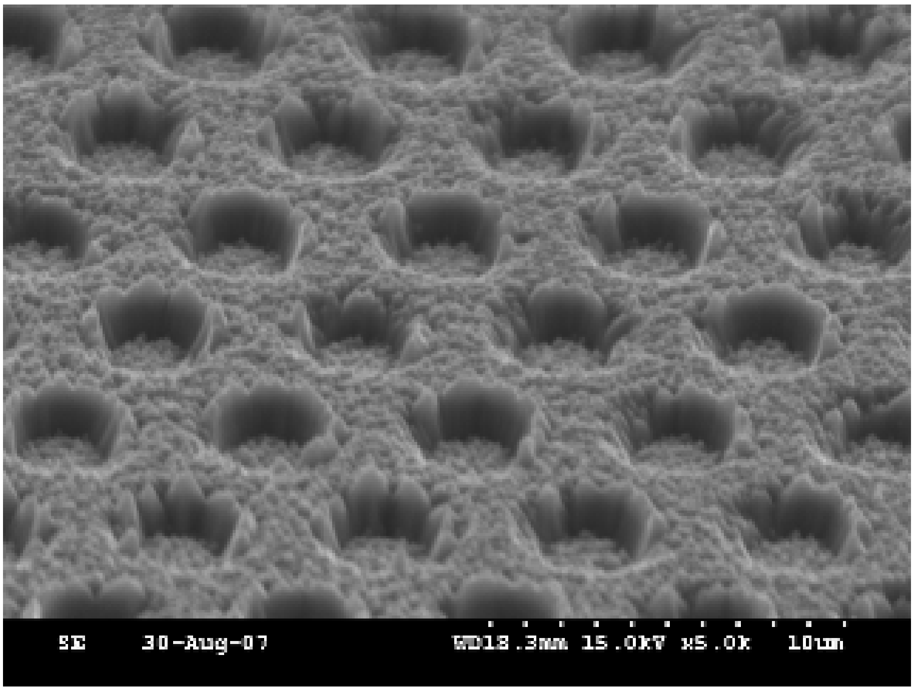

(c) 90 sec.

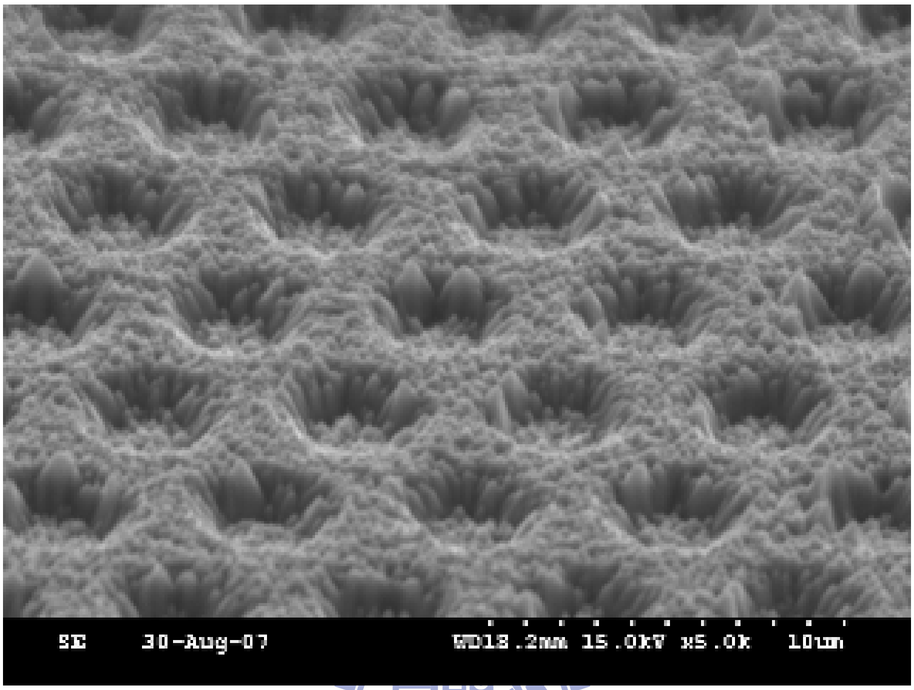

(d) 120 sec.

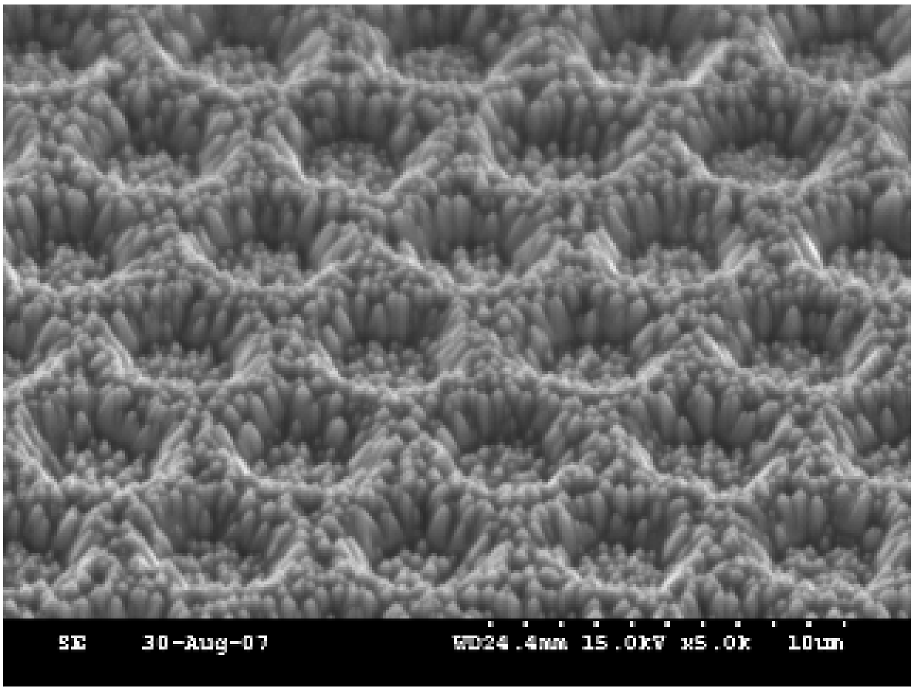

Figure 5-4 SEM images of mesh-surface VLEDs after chemical etching process.

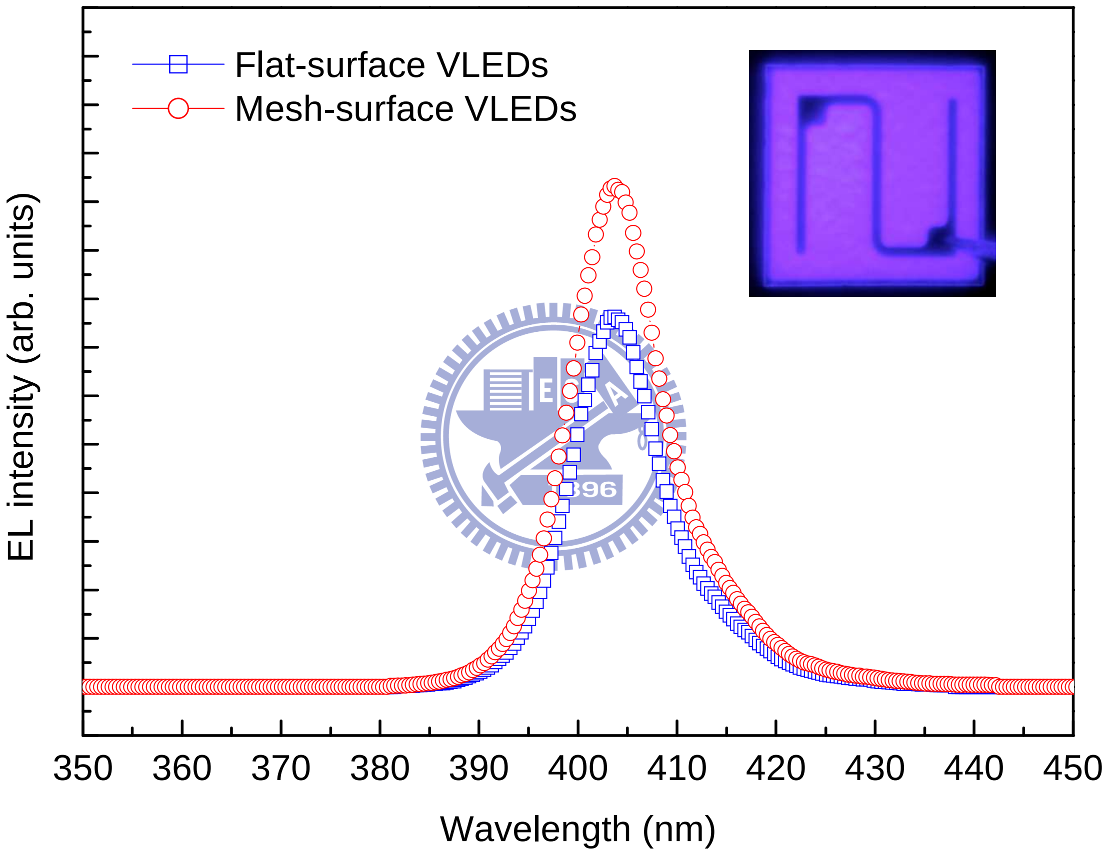

Figure 5-5 Room-temperature EL spectra of flat-surface and mesh-surface VLEDs

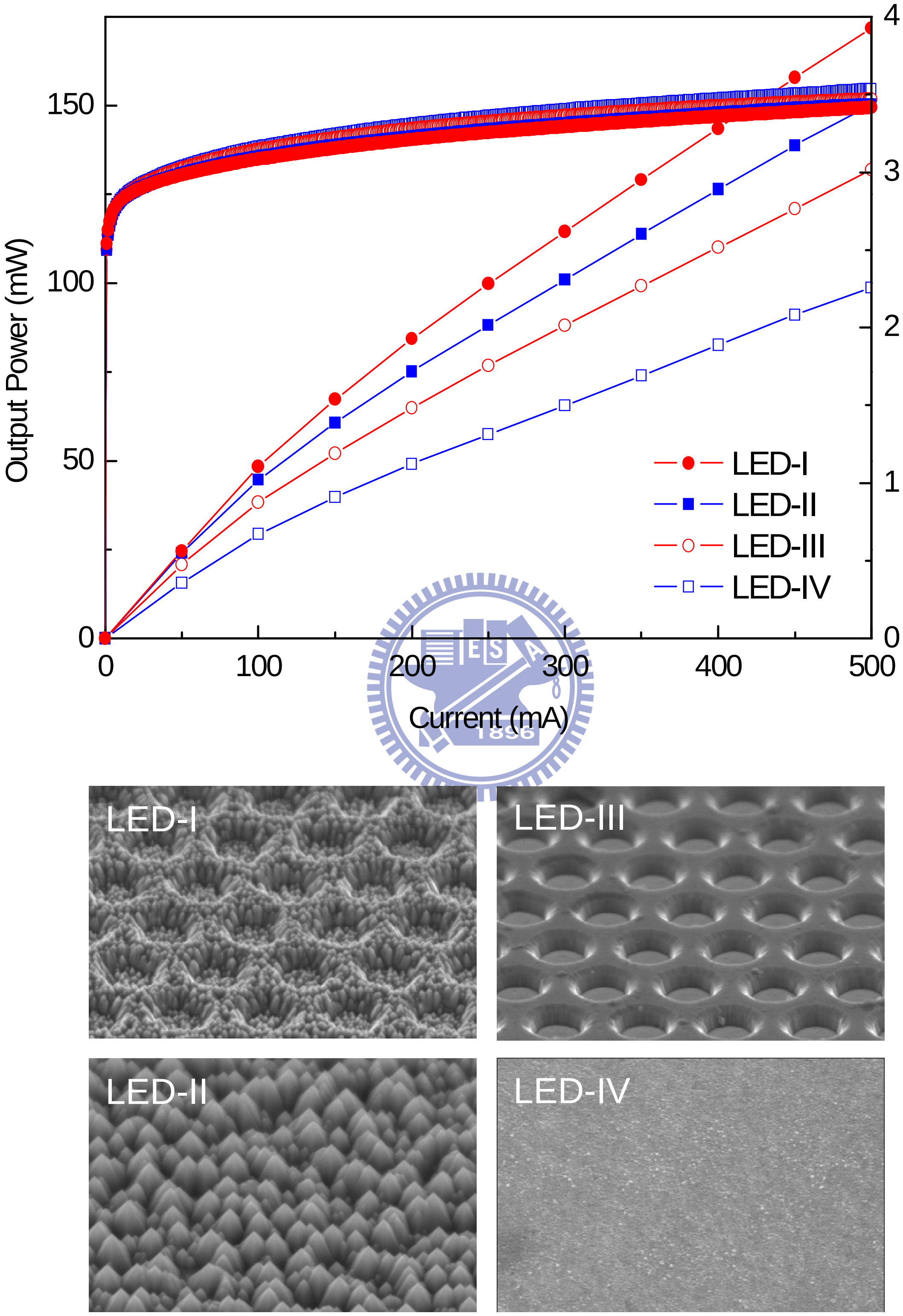

Figure 5-6 L-I-V characteristics of flat- and mesh- surface VLEDs with and without chemical wet etching process.

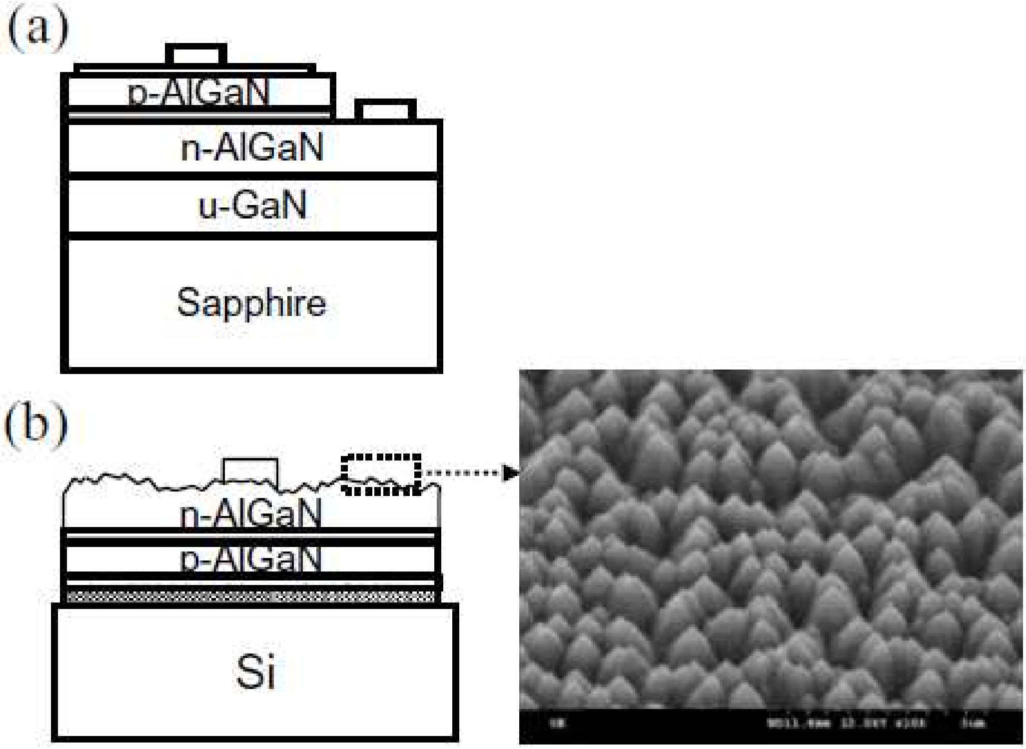

Figure 5-7 Schematic drawings of (a) conventional UV-LED and (b) GaN-free UV-VLED.

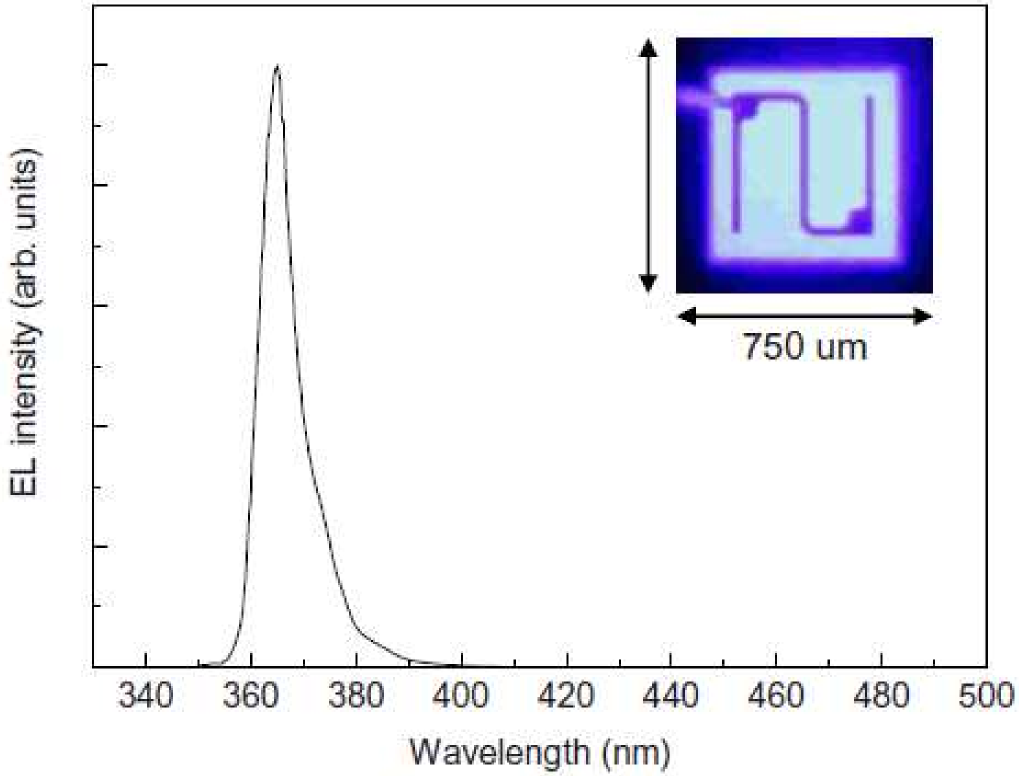

Figure 5-8 Room-temperature EL spectra of the UV-VLEDs.

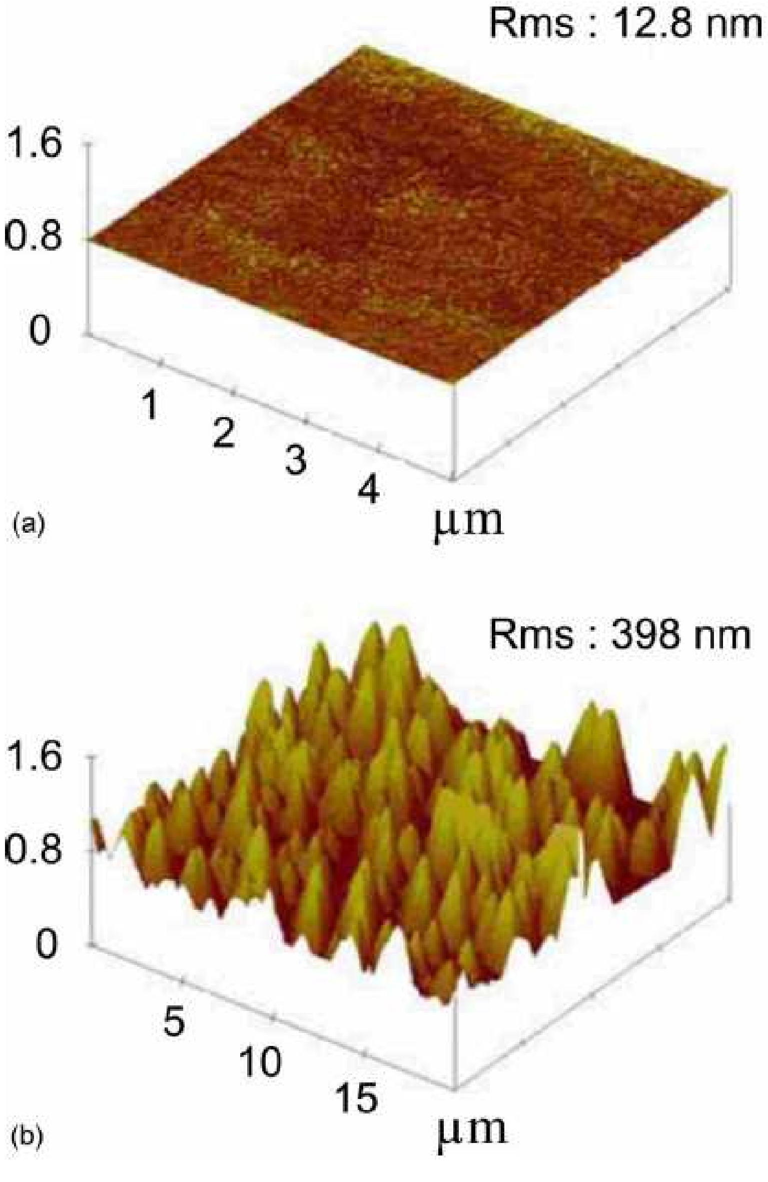

Figure 5-9 (a) AFM image of VLED surface after LLO process and (b) AFM image of VLED surface after surface treatment process.

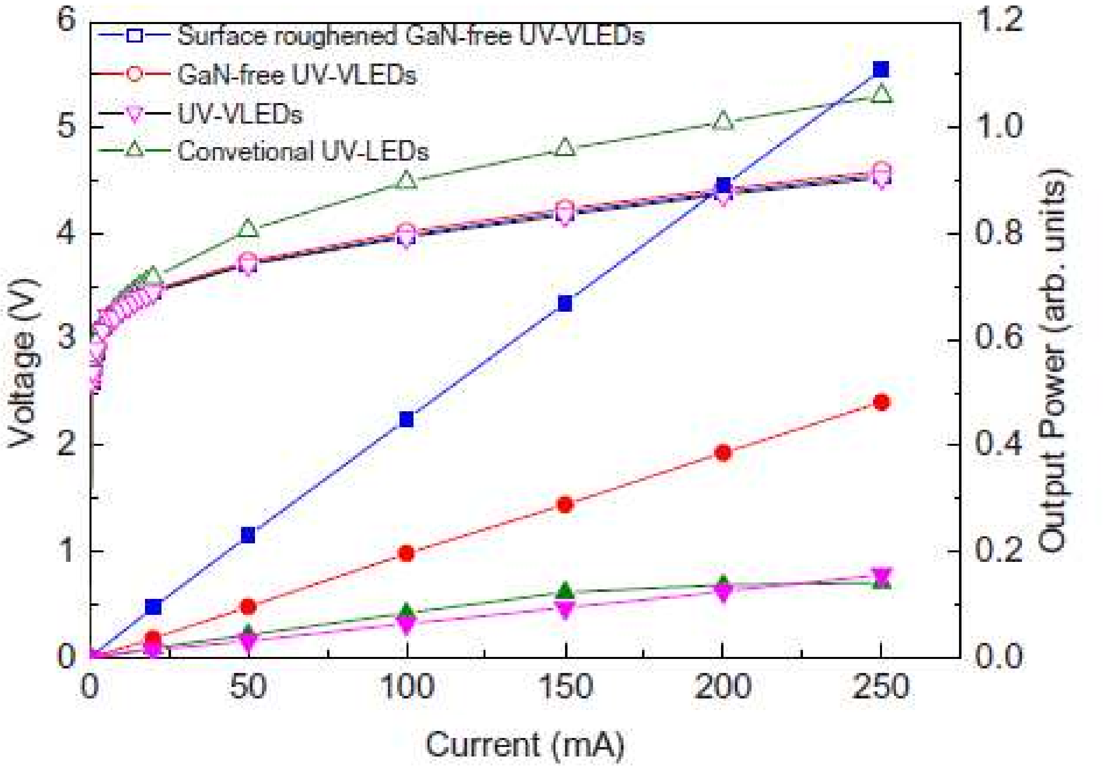

Figure 5-10 L-I-V characteristics of conventional UV-LED, UVVLED, GaN-free UV-LED, and surface roughened GaN-free UV-LED.

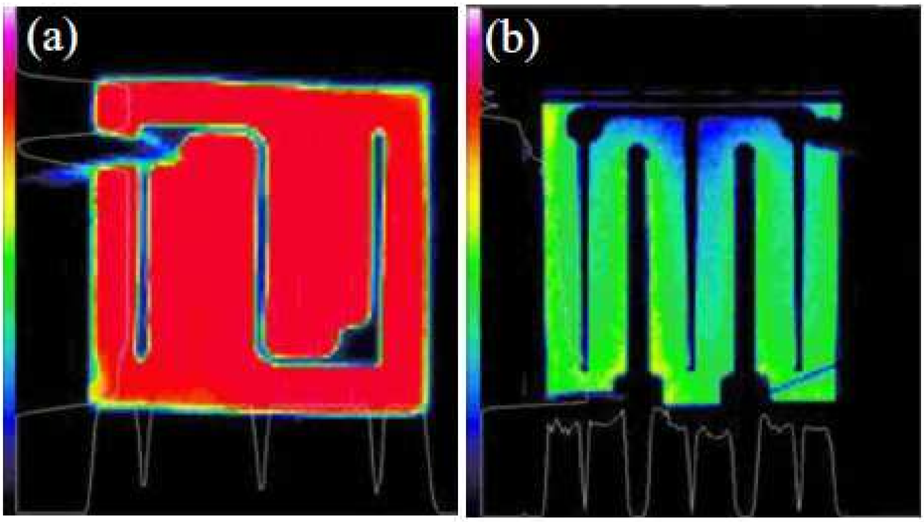

Figure 5-11 Intensity distribution of (a) surface roughened GaN-free UV-VLED and (b) conventional UV-LED at 100 mA current injection.

Chapter 6

Vertical Injection Light Emitting Diodes with Photonic Crystal Surface

6-1 Progress in vertical-injection light-emitting diodes with photonic crystal surface

Recently, tremendous progress has been achieved in GaN-based light emitting diodes (LEDs). High-efficiency white LEDs made with blue LEDs and phosphors have received much interest because the replacement of incandescent, fluorescent, Hg and Xe lamps for general lighting, back lighting in large liquid-crystal displays, vehicle head lamps could be realistic. Although the blue LEDs are commercially available, the performance of LEDs is still limited due to the poor thermal conductivity sapphire substrate and low light extraction efficiency. As a result, the replacement requires that LEDs should be more efficient and high power. At the present time, the VLEDs were demonstrated to be one of high potential light-emitting devices and promise even higher power operation due to its excellent thermal dissipation. Besides, the light extraction efficiency can be further enhanced by adopting a surface random roughening due to the random scattering from the roughened surface. Fujii et al. [58] reported a large enhancement of light–output power for VLEDs using surface roughness formed by photoelectrochemical (PEC) etching. Kim et al. [59] also reported enhancement for light intensity of VLED with “ball” shape roughness fabricated by using dry etching compared to conventional LLO LED. However, the size effect and control of roughening fabricated by dry etching or PEC processes could encounter an additional problem, i.e. uneven surface roughening morphology, which is an important issue for the light output property. It could result in the uneven luminance intensity and decrease the process yield. As a result, in order to increase the light extraction efficiency and more even luminance intensity of VLED, the photonic crystals have been implemented on VLEDs [60]. By employing the unique properties of photonic crystals as the photonic band gap and the high density of leaky modes, the inhibit emission of guided modes or redirect trapped light can be utilized into the radiation modes, resulting in an enhancement in the light extraction from a LED [61]-[63]. Recently, the photonic crystal composed of a PQC lattice has attracted mush interest. Quasicrystals are structures with high-order rotational and line symmetries but without translation symmetries. It was found that PQCs with a higher level of symmetry exhibit unique light scattering [64]-[65]. Thus it is expected that PQCs are promising for various applications on optical devices. In this work, in order to further extract the guided light out of the semiconductor material, a photonic quasicrystal has been utilized to enhance extraction efficiency of VLEDs. Therefore, the LEDs incorporated with PQC on the light-emitting surface are expected to have a significant improvement on the extraction efficiency compared to that of VLEDs without PQC. In this letter, the VLEDs with PQC surface were demonstrated for further enhancement of regular VLEDs by a combination of wafer bonding, LLO, electron-beam lithography. The electrical and optical properties of the VLEDs with PQC surfaces will be reported.

6-2 Fabrication of vertical-injection light-emitting diodes with photonic crystal surface

The GaN-based LED wafers used in this study were grown by low-pressure metal organic chemical vapor deposition onto c-face (0001) 2 in. diameter sapphire substrates. The LED structure comprised a 40-nm-thick GaN nucleation layer, a 1.5 um-thick undoped GaN layer, a 2.5 um-thick Si-doped n-type GaN cladding layer, an unintentionally doped active region of 460-nm emitting wavelength with five periods of InGaN–GaN multiple quantum wells, a 0.2 μm -thick Mg-doped p-type GaN cladding layer and a Si-doped n-InGaN-GaN short period super lattice (SPS) structure. The fabrication process of VLEDs on Si began with the deposition of a highly reflective ohmic contact stack (Ni/Ag), a diffusion barrier (Pt), and bonding metal stack Ti/Pt/Au on the p-side of LED wafer. The metal coated wafer was then flipped and bonded onto a Ti/AuSn-coated p-type conducting Si wafer at 300 ℃ for 30 minutes. The wafer bonded sample was then subjected to the LLO process. A KrF excimer laser at wavelength of 248 nm with a pulse width of 25 ns was used to remove the sapphire substrate. The incident laser was incident from the polished backside of the sapphire substrate onto the sapphire/GaN interface to decompose GaN into Ga and N. After the sapphire substrate removing, the sapphire-removed samples were dipped into HCl solution to remove the residual Ga on the u-GaN. The details of the LLO process are described in [4]. Then the u-GaN was etched away to expose the n-GaN layer by an ICP etcher and another ICP etch is used to define mesa of 1 mm x 1 mm. The PQC patterns were then form on the n-GaN surface. Fabrication of PQC was illustrated as follows: A 50 nm-thick layer of SiO2 was deposited served as the hard mask on the n-GaN by plasma-enhanced chemical vapor deposition. The PQC pattern of circular holes was then defined by electron-beam (e-beam) lithography on the top of the hard mask layer. The lattice constant and air hole diameter of the PQC were chosen to be 520 and 320 nm, respectively. The PQC pattern was then transferred onto the n-GaN surface by dry etching using the main etch gases of chlorine and methane together with a radio-frequency power of 125-W inductively coupled plasma (ICP) and 100-W reactive ion etching. The remaining SiO2 was removed by dipping it in buffered oxide etch solution. Finally, a Ti/Pt/Au electrode was deposited as the n-type contact and the VLEDs with PQC surface were obtained. The schematic drawing of PQC-VLED and scanning electron microscope (SEM) image of PQC surface morphology was shown in Fig. 6-1.

6-3 Characteristics of vertical-injection light-emitting diodes with photonic crystal surface

The SEM micrograph of the PQC-VLEDs surface was shown in fig. 6-2 (a). The 8-folds

PC patterns were observed which consist of 320 nm air hole diameter and 520 lattice constant. Shown in fig. 6-2(b) is a cross-sectional SEM micrograph of PQC patterns on the n-GaN surface. Notice that the depth of air hole is about 300 nm. Current-voltage (I-V) and intensity-current (L-I) characteristics of VLED with PC and chemical wet etching random roughness surfaces were shown in fig. 6-3. It was found that the I-V curve of these devices were almost identical indicating that the VLED and PQC fabrication processes would not result in any degradation in the electrical properties of PQC-VLED. At a driving current of 350 mA, the forward voltages were about 3.19 V. According to the corresponding L-I characteristics, both types of VLED shown more linear characteristics up to 700 mA which indicating a good thermal dissipation management for the VLEDs structure design. It is clearly observed that the light output power of the PQC-VLED was higher than that of regular VLED. This presents the fact that the light extraction from LED was definitely enhanced via the PQC on the top of n-GaN layer. At driving current of 350 mA, the output power of VLED with and without PQC surfaces present 252 and 105 mW respectively. It is noted that PQC-VLED exhibits about 140 % output power enhancement compared to that of VLED without the PQC surface. To further investigate the optical influence of PQC on the light output of VLEDs, the 3D far-field radiation pattern of VLED with and without PQC surfaces were also measured under the same output power condition for beam shape comparison. As shown in fig. 6-4 (a)-(b), the radiation patterns of VLED with and without PQC surface present the regular Lambertian source emission. It is worth noting that the radiation pattern of PQC-VLED is not very highly collimated because the lattice constant of the PQC is large enough to have many diffraction orders in the blue light regime resulting in light leakage along many directions. However, the radiation pattern of PQC-VLED reveals a different beam-shaping effect. From the angular distribution radiation patterns of PQC-VLEDs at a driving current of 350 mA as shown in fig. 6-5(a), most significantly light extraction efficiency into the narrow cones was observed. The phenomena could be ascribed to the lattice symmetry PQC geometry pattern. Since the leakage bands locating above the light cone have different leakage strengths, more light leaks symmetry direction. From the top-view of 3D far-field pattern that the light extraction along many diffraction directions that consistent with our before work, as shown in Fig. 6-5(b).

In order to confirm the experimental results, we simulated the light extraction enhancement of 8-PQC using the three-dimensional (3D) finite difference time domain (FDTD) modeling [66-68]. In simulation, the dipole is located at the center of the MQW position to fit in with PQC thin-film LED structure. The extraction enhancement is defined as the ratio of the fraction of emitted flux through the top surfaces of the PQC to that through top surface of the planar sample without PQC. The calculated extraction enhancement for various lattice constant of PQCs was considered with fixed r/a=0.31 that shown in Fig. 1 (*r* is the hole radius), since the lattice constant is the dominant factor contributing to the light extraction efficiency. We can see that the extraction enhancement about 1.5 in Fig. 6-6 is relatively large at the lattice constant of 550 nm, which we choice the lattice constant in this range fabrication.

In summary, a nitride-based thin-film LED incorporated with a PQC surface structure was investigated. The formation thin-film vertical-injection and PQC surface improves not only thermal dissipation management but the light extraction efficiency due to the lower series-resistance of vertical-injection device structure and leaky modes of PQC structure. By this novel device design, the PQC-VLEDs (@ 350 mA) exhibit about 140 % output power enhancement compared to that of VLED without PQC surface.

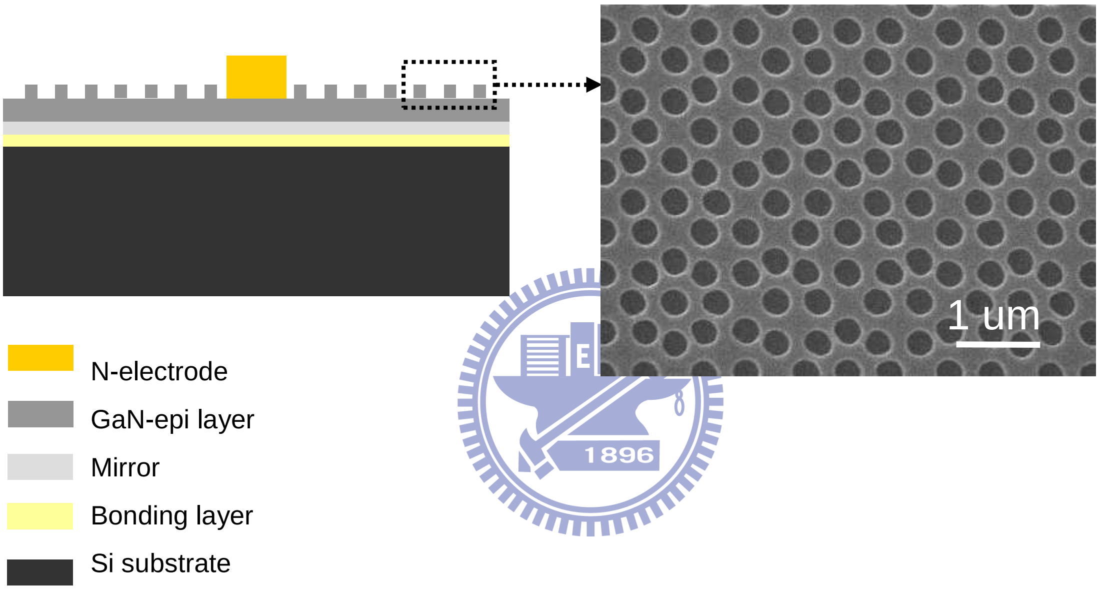

Figure 6-1 Schematic drawings of VLEDs with 2D-PC surface.

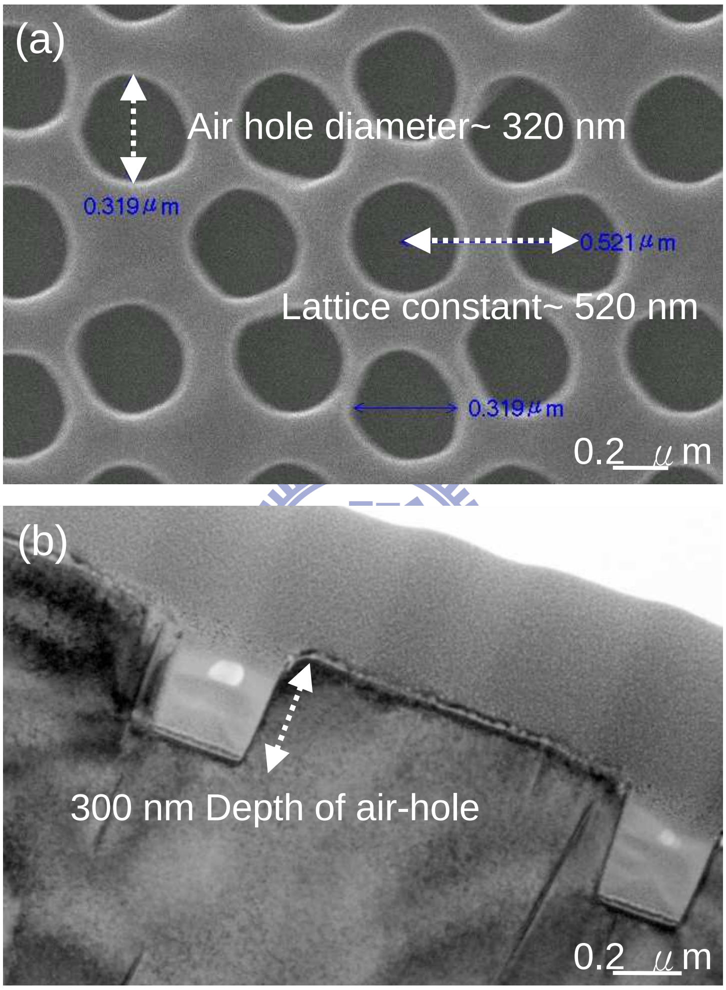

Figure 6-2 SEM images of the etched top n-GaN formed by electron-beam lithography patterns using ICP etch process: (a) top and (b) cross sectional views.

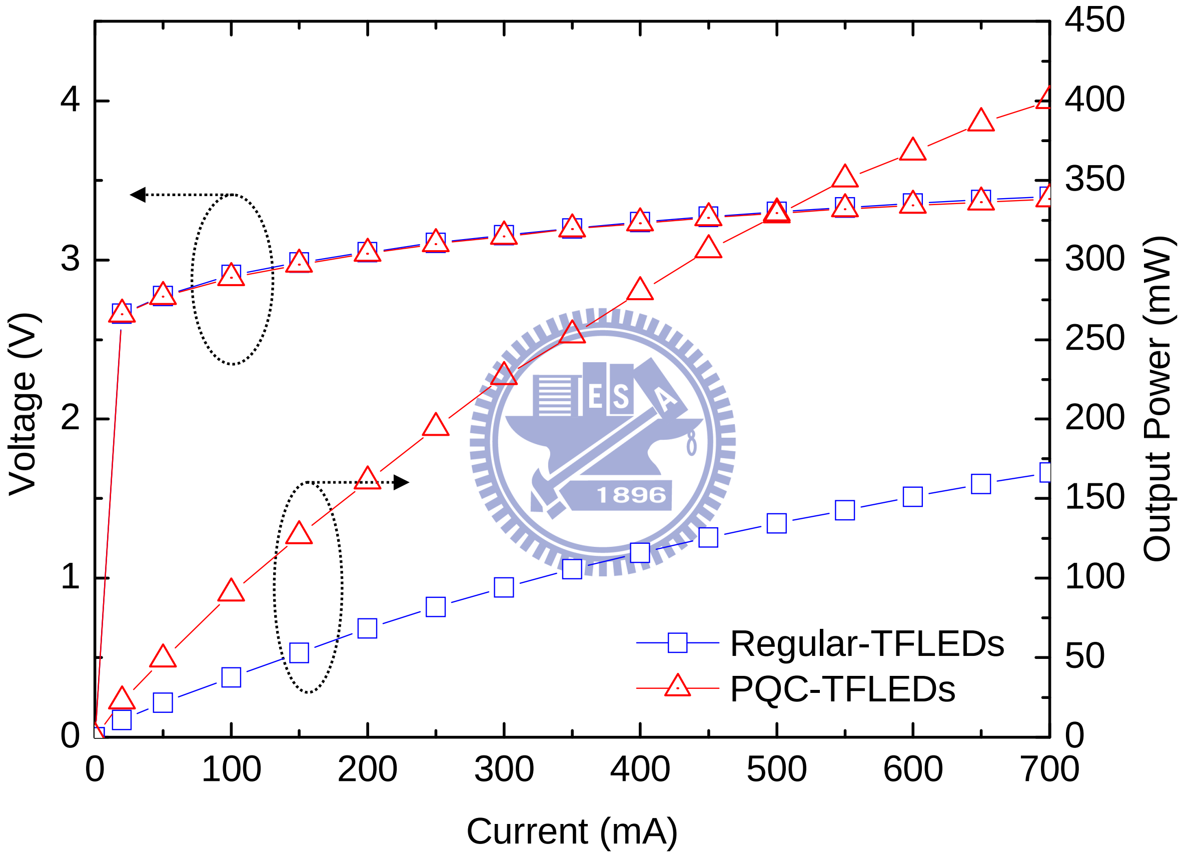

Figure 6-3 L-I-V characteristics of VLEDs with and without PQC surfaces.

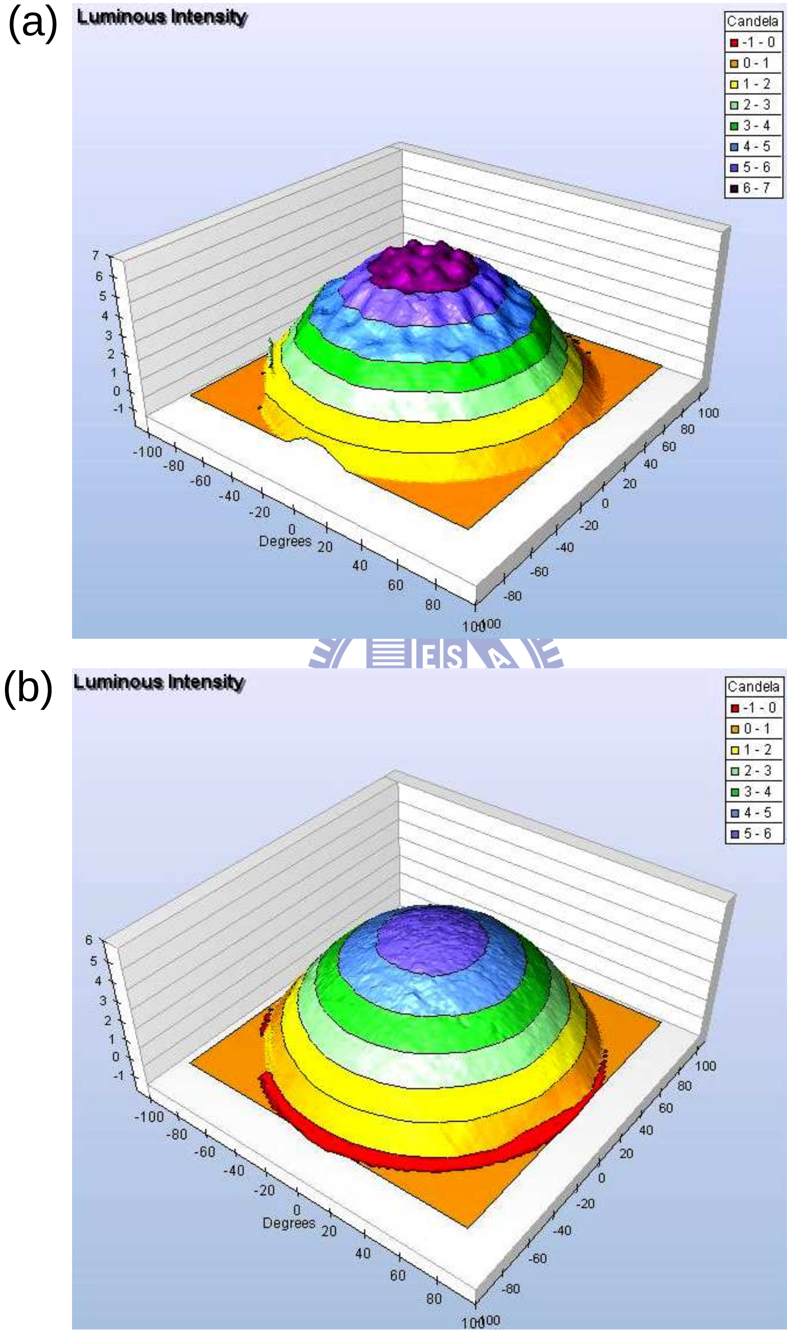

Figure 6-4 3D far-field patterns of (a) PQC-VLED and (b) regular-VLED

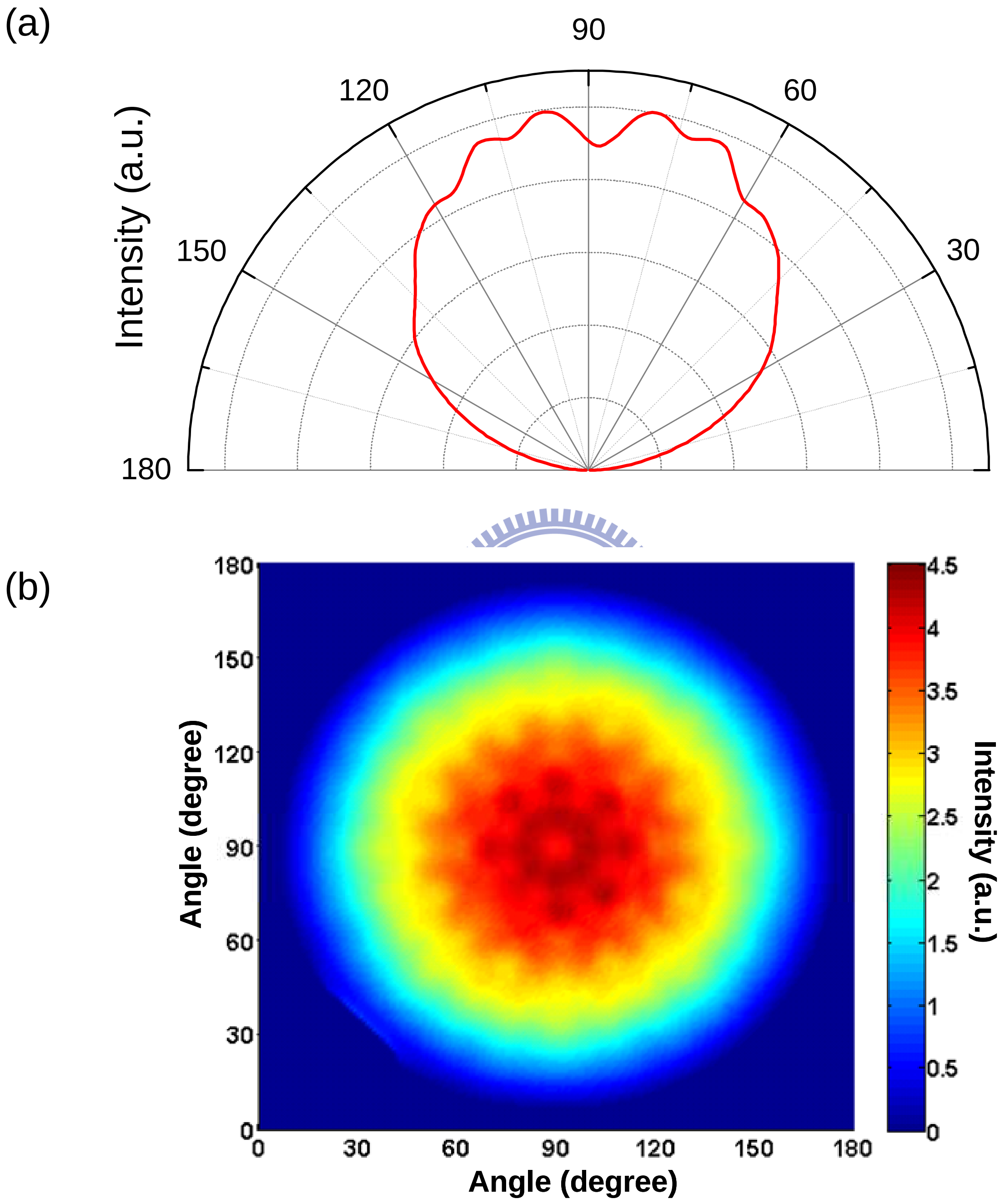

Figure 6-5 (a) Angular distribution radiation pattern and (b) 3D far-field pattern of a PQC-VLED

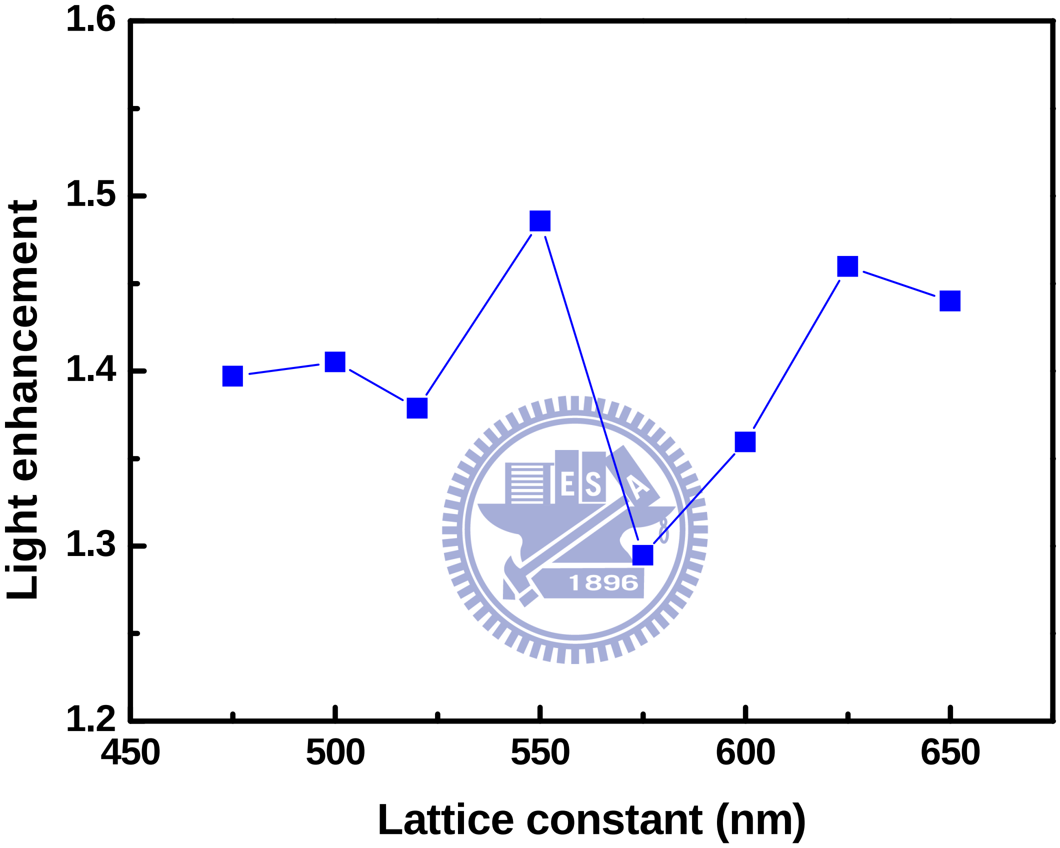

Figure 6-6 The FDTD calculate the various lattice constant with fixed r/a=0.31 in PQC VLED of light enhancement.

Chapter 7

Summary

In summary, in this dissertation we have studied the flip-chip and epilayer-transfer types of GaN-based materials and devices, including their fabrication, electrical and optical phenomena.

Three types of FC-LEDs including FC-LEDs with micro-pillar-array structure, FC-LEDs with oblique sapphire geometric structure, and FC-LEDs with triple light scattering layers are demonstrated. In the case of MPAFC-LEDs, we employ inductively coupled plasma (ICP) to etch micro-pillar-array on the backside surface of sapphire substrate for light extraction enhancement. The light output power of the MPAFC-LEDs was increased by 68 % for a 3.2 μm textured micro-pillar-array on the bottom side of the sapphire substrate. The improved light extraction efficiency can be further supported by simulation data. Such an enhancement can be attributed to the top surface roughness and the fact which photons are more likely to be emitted from the surface-roughed device, resulting in an increase of the light output power of the MPAFC-LED.

In the case of SSFC-LEDs, the FC-LEDs with oblique sapphire geometric structure and greatly thick sapphire window layer were fabricated. The H_2SO_4:H_3PO_4 (3:1) solution is employed to etching backside surface of sapphire substrate. The I-V curve of SSFC-LEDs exhibits a normal p-n diode behavior with a forward voltage (@350mA) of 3.5 V, indicating that high temperature sapphire wet etching process dose not appear to adversely affect I-V characteristics of these devices. The light extraction efficiency enhancement of 100μm SSFC-LEDs has 55% improvement under 350 current injection compared to the CFC-LEDs. The simulated result of 100 μm SSFC-LEDs is similar to experiment performance of 55% and enhancement efficiency gradually converges. The novel FC-LEDs structure could not only reduce the TIR effect but facilitate light emission from the edges of the thicker sapphire windows layer resulting in an increase in the light extraction efficiency of FC-LEDs.

In the case of FC-LEDs with triple light scattering layers structure, the device was fabricated by combination of epi-growth on micrp-pillar array sapphire substrate aand naturally textured surface. The novel FC-LEDs structure could reduce the TIR effect between the interfaces of GaN-air, GaN-sapphrie substrate, and sapphire substrate-air which efficiently facilitate light emission from the top pineapple-like pillar arrays surface and bottom naturally textured p-GaN surface.

The formation rough meshed-surface structure of NUC-VLEDs with rough meshed-surface structure improves not only the surface emission area but the escape probability of photons due to the angular randomization of photos insides the LED structure. In addition, the IQE can be increase by adopting the PSS process. By this novel device design, the output power can be further enhanced up to 20 %. Furthermore, by adopting the method to UV-VLEDs, the self-absorption effect was decreased by the GaN-free structure design. The formation-roughened surface structure improves not only the surface emission area but the escape probability of photons due to the angular randomization of photos inside the LED structure. In addition, the vertical injection LED structure was demonstrated to achieve high-brightness operation due to its excellent thermal dissipation and lower series resistance.

In the case of VLEDs with photonic crystal surface, the VLEDs with a PQC surface were demonstrated for further enhancement of regular VLEDs by a combination of wafer bonding, LLO, and electron-beam lithography. Not only thermal dissipation management but the light extraction efficiency due was improved to the lower series-resistance of the vertical-injection device structure and leaky modes of the PQC structure. By this novel device design, the PQC-VLEDs (at 350 mA) exhibit about 140% output power enhancement compared to that of the VLED without the PQC surface.

References

[1] E. F. Schubert, and J.K. Kim, science, vol. 308, pp. 1274, 2005.

[2] E. F. Schubert, Light-Emitting Diodes. (Cambridge University Press, Cambridge, U.K. 2003).

[3] A. Zukauskas, M. S. Shur, and R. Gaska, Introduction to Solid-State Lighting. (New York: Wiley.)

[4] J. I. Pankove, E. A. Miller, J. E. Berkeyheiser, J. Luminescence, vol. 5, pp. 84, 1992.

[5] H. Amano, N. Sawaki, I. Akasaki, and Y. Toyoda, Appl. Phys. Lett., vol. 48, pp. 353, 1986.

[6] H. Amano, N. Sawaki, I. Akasaki, and Y. Toyoda, Jpn. J. Appl. Phys., vol. 28, pp. L2112, 1989.

[7] S. Nakamura, T. Mukai, M. Senoh, and N. Jwasa, Jpn. J. Appl. Phys., vol. 31, pp. 1258, 1992.

[8] J. H. Lau, “Flip Chip Technologies,” McGraw-Hill, 1995.

[9]徐嘉彬, 劉俊賢, 機械工業雜誌, vol. 258, pp. 218, 2004.

[10] S. Blackstone, Microelectronic Engineering, vol. 48, pp. 313, 1999.

[11] Y. T. Cheng, L. Lin, and K. Najafi, J. Microelectromech. Syst., vol. 9, pp. 3, 2000.

[12] D. Sparks, G. Queen, R. Weston, G. Woodward, M. Putty, L. Jordan, S. Zarabadi, and K. Jayakar, J. Micromech. Microeng., vol. 11, pp. 630, 2001.

[13] Niklaus F, Enoksson P, Kalvesten E and Stemme G, J. Micromech. Microeng., vol. 11, pp. 100, 2001.

[14] F. A. Kish et al., Appl. Phys. Lett., vol. 64, pp. 2839, 1994.

[15] Tan I-H, Vanderwater DA, Huang J-W, Hofler GE, Kish FA, Chen EI, Ostentowski TD, Journal of Electronic Materials, vol. 29, no.2, pp. 188, 2000.

[16] W. C. Peng and Y. S. Wu, Appl. Phys. Lett., vol. 84, pp. 1841, 2004.

[17] R. H. Horng, D. S. Wuu, S. C. Wei, C. Y. Tseng, M. F. Huang, K. H. Chang, P. H. Liu and

K. C. Lin, Appl. Phys. Lett., vol. 75, pp. 3054, 1999.

[18] R. H. Horng, Y. C. Lien, W. C. Peng, D. S. Wuu, C. Y. Tseng, C. H. Seieh, M. F. Huang, S. J. Tsai and J. S. Liu, Jpn. J. Appl. Phys. vol. 40, pp. 2747, 2001.

[19] M. K. Kelly, O. Ambacher, B. Dahlheimer, G. Groos, R. Dimitrov, H. Angerer, and M. Stutzmann, Appl. Phys. Lett., vol. 69, pp. 1749, 1996.

[20] M. K. Kelly, O. Ambacher, R. Dimitrov, R. Handschuh, and M. Stutzmann, Phys. Status Solidi A, vol. 159, R3 , 1997.

[21] W. S. Wong, T. Sands, and N. W. Cheung, Appl. Phys. Lett., vol.72, pp. 599 1998.

[22] W. S. Wong, M. Kneissl, D. P. Bour, P. Mei, L. T. Romano, N. M. Johnson, N. W. Cheung, and T. Sands, Appl. Phys. Lett., vol. 75, pp. 1360, 1999.

[23] E. Yablonovitch, T. Gmitter, J. P. Harbison, and R. Bhat, Appl. Phys. Lett., vol. 51, pp. 2222, 1987.

[24] E. Yablonovitch, T. Sands, D. M. Hwang, I. Schnitzer, T. J. Gmitter, S. K. Shastry, D. S. Hill, and J. C. C. Fan, Appl. Phys. Lett., vol. 59, pp. 3159, 1991.

[25] S. J. Chang, C. S. Chang, Y. K. Su, C. T. Lee, W. S. Chen, C. F. Shen, Y. P. Hsu, S. C. Shei, and H. M. Lo, IEEE Trans. Adv. Packag., vol. 28, no. 2, pp. 273, May 2005.

[26] Hibbard D L, Jung S P, Wang C, Ullery D, Zhao Y S, So W, Liu H and Lee H P, Appl. Phys. Lett. vol. 83, pp. 311–3, 2003.

[27] D. L. Hibbard, S. P. Jung, C. Wang, D. Ullery, Y. S. Zhao, W. So, H. Liu, and H. P. Lee, Appl. Phys. Lett., vol. 83, pp. 311, 2003.

[28] Transl.:Y. Kondoh, S. Wantanabe, Y. Kaneko, S. Nakagawa, N. Yamada, U.S. Patent 6, 194, 743.

[29] T. Fujii, Y. Gao, R. Sharma, E. L. Hu, S. P. DenBaars, and S. Nakamura, Appl. Phys. Lett., vol. 84–86, pp. 855, 2004.

[30] R. Windisch, C. Rooman, S. Meinlschmidt, P. Kiesel, D. Zipperer, G. H. Döhler, B. Dutta, M. Kuijk, G. Borghs, and P. Heremans, Appl. Phys. Lett., vol. 79, pp. 2315, 2001.

[31] H. W. Huang, C. C. Kao, J. T. Chu, H. C. Kuo, S. C. Wang, and C. C. Yu, IEEE Photon. Technol. Lett., vol. 17, no. 5, pp. 983, 2005.

[32] J. K. Kim, T. Gessmann, E. F. Schubert, J. Q. Xi, H. Luo, J. Cho, C. Sone, and Y. Park, Appl. Phys. Lett., vol. 88, pp. 013501, 2006.

[33] T. Gessmann, H. Luo, J.-Q. Xi, K. P. Streubel, and E. F. Schubert, in Proc. SPIE, vol. 5366, pp. 53, 2004.

[34] Y. J. Lee, H. C. Kuo, T. C. Lu, and S. C. Wang, IEEE J. Quantum Electron., vol. 42, no. 12, pp. 1196, 2006.

[35] D. S. Han, J. Y. Kim, S. I. Na, S. H. Kim, K. D. Lee, B. Kim, and S. J. Park, IEEE Photon. Technol. Lett., vol. 18, no. 13, pp. 1406, 2006.

[36] Krames M R et al, Appl. Phys. Lett. vol. 75, pp. 2365–7, 1999.

[37] Eisert D and Harle V, Int. Conf. Numerical Simulation of Semiconductor Optoelectronic Devices, Session 3: Photonic Devices, invited paper, 2002.

[38] Chang C S, Chang S J, Su Y K, Lee C T, Lin Y C, Lai W C, Shei S C, Ke J C and Lo H M, IEEE Photon. Technol. Lett. vol. 16, pp. 750, 2005.

[39] Kao C C, Kuo H C, Huang HW, Chu J T, Peng Y C, Hsieh Y L, Luo C Y, Wang S C, Yu C C and Lin C F, IEEE Photon. Technol. Lett. vol. 17, pp. 19, 2005.

[40] Z. H. Feng and K. M. Lau, IEEE Photon. Technol. Lett., vol. 17, no. 9, pp. 1812, 2005.

[41] D. S. Wuu, W. K. Wang, W. C. Shih, R. H. Horng, C. E. Lee, W. Y. Lin, and J. S. Fang, IEEE Photon. Technol. Lett., vol. 17, no. 2, pp. 288, 2006.

[42] Y. J. Lee, J. M. Hwang, T. C. Hsu, M. H. Hsieh, M. J. Jou, B. J. Lee, T. C. Lu, H. C. Kuo, and S. C. Wang, IEEE Photon. Technol. Lett., vol. 18, no. 10, pp. 1152, 2006.

[43] Y. Narukawa, I. NiKi, K. Izuno, M. Yamada, Y. Murazaki, and T. Mukai, Jpn. J. Appl. Phys., pt. 2 4A, p. L371, 2002.

[44] K. Tadatomo, H. Okagawa, Y. Ohuchi, T. Tsunekawa, Y. Imada, M. Kato, and T. Taguchi, Jpn. J. Appl. Phys., vol. 40, pp. L583, 2001.

[45] M. Yamada, T. Mitani, Y. Narukawa, S. Shioji, I. Niki, S. Sonobe, K. Deguchi, M. Sano, and T. Mukai, Jpn. J. Appl. Phys., vol. 41, pp. L1431, 2002.

[46] D. S. Wuu, W. K. Wang, W. C. Shih, R. H. Horng, C. E. Lee, W. Y. Lin, and J. S. Fang, IEEE Photon. Technol. Lett., vol. 17, no. 2, pp. 288, 2005.

[47] Y. J. Lee, T. C. Hsu, H. C. Kuo, S. C.Wang, Y. L. Yang, S. N. Yen, Y. T. Chu, Y. J. Shen, M. H. Hsieh, M. J. Jou, and B. J. Lee, Mater. Sci. Eng., B, vol. 122, pp. 184, 2005.

[48] C. F. Chu, F. I. Lai, J. T. Chu, C. C. Yu, C. F. Lin, H. C. Kuo, and S. C. Wang, J. Appl. Phys., vol. 95, pp. 3916, 2004.

[49] H.-W. Huang, C. C. Kao, J. T. Chu, H. C. Kuo, S. C. Wang, and C. C. Yu, IEEE Photon. Technol. Lett., vol. 17, no. 5, pp. 983, 2005.

[50] R. Windisch, C. Rooman, S. Meinlschmidt, P. Kiesel, D. Zipperer, G. H. Döhler, B. Dutta, M. Kuijk, G. Borghs, and P. Heremans, Appl. Phys. Lett., vol. 79, pp. 2315, 2001.

[51] D. A. Stocker, E. F. Schubert, and J. M. Redwing, Appl. Phys. Lett., vol. 73, pp. 2654, 1998.

[52] S. Watanabe, N. Yamada, M. Nagashima, Y. Ueki, C. Sasaki, Y. Yamada, K. Tadayomo, H. Okagawa, and H. Kudo, Appl. Phys. Lett., vol. 83, pp. 4606, 1998.

[53] T. Nishida, H. Saito, and N. Kobayashi, Appl. Phys. Lett., vol. 79, pp. 711, 2001.

[54] T. Nishida, H. Saito, and N. Kobayashi, Appl. Phys. Lett., vol. 79, pp. 711, 2001.

[55] M. Kahn, V. Adivarahan, J. P. Zhang, C. Chen, E. Kuokstis, A. Chitnis, M. Shatalov, J. W. Yang, and G. Simin, Jpn. J. Appl. Phys., Part 1, vol. 40, 1308, 2001.

[56] M. Iwaya, S. Terao, T. Sano, S. Takanami, T. Ukai, R. Nakamura, S. Kamiyama, H. Amano, and I. Akasaki, Phys. Status Solidi A, vol. 188, pp. 117, 2001.

[57] T. Nishida, N. Kobayashi, and T. Ban, Appl. Phys. Lett., vol. 82, pp. 1, 2003.

[58] T. Fujii, Y. Gao, R. Sharma, E. L. Hu, S. P. DenBaars, and S. Nakamura, Appl. Phys. Lett., vol. 84, pp. 855, 2004.

[59] D. W. Kim, H. Y. Lee, M. C. Yoo, and G. Y. Yeom, Appl. Phys. Lett., vol. 86, pp. 052108,

2005.

[60] C. H. Lin, H. H.Yen, C. F. Lay, H.W. Huang, C. H. Chao, H. C.Kuo, T. C. Lu, and S. C.Wang, IEEE Photon. Technol. Lett., vol. 20, no. 10, pp. 836, 2008.

[61] C. F. Lai, H. C.Kuo, C. H. Chao, H. T. Hsueh, J. F. T.Wang, W. Y.Yeh, and J. Y. Chi, Appl. Phys. Lett., vol. 91, pp. 123117, 2007.

[62] T. N. Oder, K. H. Kim, J. Y. Lin, and H. X. Jiang, Appl. Phys. Lett., vol. 84, pp. 466, 2004.

[63] J. J.Wierer,M. R. Krames, J. E. Epoer, N. F. Gardner,M. G. Craford, J. R. Wendt, J. A. Simmons, and M. M. Sigalas, Appl. Phys. Lett., vol. 84, pp. 3885, 2004.

[64] K. Nozaki and T. Baba, Appl. Phys. Lett., vol. 84, pp. 4875, 2004.

[65] M. D. B. Charlton, M. E. Zoorob, and T. Lee, in Proc. SPIE, vol. 6486, 64860R1–R10, 2007.

[66] C. F. Lai, H. C. Kuo, C. H. Chao, H. T. Hsueh, J. –F. T. Wang, W. Y. Yeh, and J. Y. Chi, Appl. Phys. Lett., vol. 91, 123117, 2007.

[67] C. F. Lai, J. Y. Chi, H. C. Kuo, C. H. Chao, H. T. Hsueh, J. –F. T. Wang, and W. Y. Yeh, Optics Express, vol. 16, 7285, 2008.

[68] C. H. Chao, S. L. Chuang, and T. L. Wu, Appl. Phys. Lett., vol. 89, 091116, 2006.

Publication List

(A) Journal Papers:

1. C. F. Lai, J. Y. Chi, H. C. Kuo, H. H. Yen, **C. E. Lee**, C. H. Chao, H. T. Hsueh, and W. Y. Yeh" Far-field of GaN film-transferred green light-emitting diodes with two-dimensional photonic crystals," ***Opt. Express***, vol.17, Iss. 11, pp. 8795-8804, 2009

2. C. F. Lai, J. Y. Chi, H. C. Kuo, H. H. Yen, **C. E. Lee**, C. H. Chao, W. Y. Yeh, and T. C. Lu" Far-field and near-field distribution of GaN-based photonic crystal LEDs with guided mode extraction," ***J. Sel. Topics Quantum Electron.***, vol.15, Iss.4, pp. 1234-1241, 2009

3. C. F. Lai, C. H. Chao, H. C. Kuo, H. H. Yen, **C. E. Lee**, and W. Y. Yeh, " Directional light extraction enhancement from GaN-based film-transferred photonic crystal light-emitting diodes," ***Appl. Phys. Lett.***, 94, 123106, 2009

4. **C. E. Lee**, C. F. Lai, H. C. Kuo, T. C. Lu and S. C. Wang," Nitride-based thin-film light –emitting diodes with photonic quasicrystal surface," ***IEEE Photon. Technol. Lett.***, vol.21, no.5, pp. 331-333, 2009

5. **C. E. Lee**, B. S. Cheng, Y. C. Lee, H. C. Kuo, T. C. Lu and S. C. Wang," Output power enhancement of vertical-injection light –emitting diodes by GaN-free and surface roughness structures," ***Electrochem. Solid-State Lett.***, 12 (2), H44-H46, 2009

6. Yea-Chen Lee, Hao-Chung Kuo, **Chia-En Lee**, Tien-Chang Lu, and Shing-Chung Wang, " High-PerformanceAlGaInP-Based Flip-Chip Light-Emitting Diode With a Geometric Sapphire Shaping Structure," ***IEEE Photon. Technol. Lett.***, vol.20, no. 23, pp. 1950-1952, 2008

7. C. H. Chiu, **C. E. Lee**, M.H. Lo, H. W. Huang, T. C. Lu, H. C. Kuo and S. C. Wang, "Metal organic chemical vapor deposition growth of GaN-based LEDs with naturally formed nano-pyraims," ***Jpn. J. Appl. Phy.***, vol. 47, no. 4, pp. 2954-2956, 2008

8. Y. C. Lee, **C. E. Lee**, T. C. Lu, H. C. Kuo and S. C. Wang, "Small GaN-based light-emitting diodes with a single electrode pad fabricated on a sapphire substrate," ***Semicond. Sci. Technol.***, 23, pp. 1-5, 2008

9. **C. E. Lee**, Y. C. Lee, H. C. Kuo, T. C. Lu and S. C. Wang," Further Enhancement of Nitride-Based Near-Ultraviolet Vertical-Injection Light-Emitting Diodes by Adopting a

Roughened Mesh-Surface,” ***IEEE Photon. Technol. Lett.***, vol.20, no.10, pp. 803-805, 2008

10. **C. E. Lee**, Y. C. Lee, H. C. Kuo, T. C. Lu and S. C. Wang,” High Brightness InGaN/GaN Flip-Chip Light-Emitting Diodes with Triple Light Scattering Layers,” ***IEEE Photon. Technol. Lett.***, vol.20, no.8, pp. 659-661, 2008

11. C. H. Chiu, **C. E. Lee**, C. L. Chao, B. S. Cheng, H. W. Huang, H. C. Kuo, T. C. Lu, S. C. Wang, W. L. Kuo, C. S. Hsiao, and S. Y. Chen,” Enhancement of Light Output Intensity by Integrating ZnO Nanorod Arrays on GaN-Based LLO Vertical LEDs,” ***Electrochem. Solid-State Lett.***, 11, H84, 2008

12. Y. C. Lee, **C. E. Lee**, H. C. Kuo, T. C. Lu and S. C. Wang,” Enhancing the light extraction of AlGaInP based LEDs fabricated via geometric sapphire shaping,” ***IEEE Photon. Technol. Lett.***, vol.20, no.5, pp. 369-371, 2008

13. **C. E. Lee**, Y C Lee, H C Kuo, M R Tsai, T C Lu and S C Wang,” High brighness GaN-based flip-chip light emitting diodes by adopting geometric sapphire shaping,” ***Semicond. Sci. Technol.***, **23** no. 2, pp. 1-5, 2008

14. **Chia-En Lee**, Yi-Jiun Lee, Hao-Chung Kuo, Meng-Ru Tsai, Tien-Chang Lu, Shing-Chung Wang, and Chia-Tai Kuo, ”Luminance Enhancement of Flip-Chip Light-Emitting Diodes by adopting a geometric sapphire shaping structure,” ***IEEE Photon. Technol. Lett.***, vol.20, no.3, pp. 184-186, 2008

15. C H Chiu, H C Kuo, **C. E. Lee**, C H Lin, P C Cheng, HW Huang, T C Lu, S C Wang and K M Leung,“Fabrication and characteristics of thin-film InGaN–GaN light-emitting diodes with TiO2/SiO2 omnidirectional reflectors,” ***Semicond. Sci. Technol.***, **22** no. 7, pp. 831-835, 2007

16. Huang, H.W., Kuo, H.C., Lai, C.F., **Lee, C. E.**, Chiu, C.W., Lu, T.C., Wang, S.C., Lin, C.H., Leung, K.M., ”High-Performance GaN-Based Vertical-Injection Light-Emitting Diodes With TiO2–SiO2 Omnidirectional Reflector and n-GaN Roughness,” ***IEEE Photon. Technol. Lett.***, vol 18, no. 8, pp.565-567, 2007

17. **Chia-En Lee**, Yi-Jiun Lee, Hao-Chung Kuo, Meng-Ru Tsai, B. S. Cheng, Tien-Chang Lu, Shing-Chung Wang, and Chia-Tai Kuo,”Enhancement of Flip-Chip Light-Emitting Diodes With Omni-Directional Reflector and Textured Micropillar Arrays,” ***IEEE Photon. Technol. Lett.***, vol.19, no.16, pp. 1200-1202, 2007

18. Lee, Y. C., Kuo, H. C., **Lee, C. E.**, Lu, T. C., Wang, S. C., and Chiou, S. W., ”High-Temperature Stability of 650-nm Resonant-Cavity Light-Emitting Diodes Fabricated Using Wafer-Bonding Technique on Silicon Substrates,” ***IEEE Photon. Technol. Lett.***, vol. 19, no. 14, pp. 1060-1062, 2007

19. Yea-Chen Lee, **Chia-En Lee**, Bo-Siao Cheng, Tien-Chang Lu, Hao-Chung Kuo, Shing-Chung Wang, and Shu-Woei Chiou, “High-Performance 650 nm Resonant-Cavity Light-Emitting Diodes for Plastic Optical-Fiber Application,” ***Jpn. J. Appl. Phy.***, vol. 46, no. 4B, pp. 2450-2453, 2007

20. R. H. Horng, C. C. Yang, J. Y. Wu, S. H. Huang, **C. E. Lee**, and D. S. Wuu, “GaN-based light-emitting diodes with indium tin oxide texturing window layers using natural lithography,” ***Appl. Phys. Lett.***, vol. 86, pp. 221101, May 2005.

21. W. Y. Lin, D. S. Wuu, K. F. Pan, S. H. Huang, **C. E. Lee**, W. K. Wang, S. C. Hsu, Y. Y. Su, S. Y. Huang, and R. H. Horng, “High-Power GaN–Mirror–Cu Light-Emitting Diodes for Vertical Current Injection Using Laser Liftoff and Electroplating Techniques,” ***IEEE Photon. Technol. Lett.***, vol. 17, pp. 1809-1811, Sep. 2005.

22. D. S. Wuu, S. C. Hsu, S. H. Huang, C. C. Wu, **C. E. Lee**, and R. H. Horng, “GaN/Mirror/Si Light-Emitting Diodes for Vertical Current Injection by Laser Lift-off and Wafer Bonding Techniques,” ***Jpn. J. Appl. Phy.***, vol. 43, no. 8A, pp. 5239-5242, Aug. 2004.
23. R. H. Horng, **C. E. Lee**, S. C. Hsu, S. H. Huang, C. C. Wu, C. Y. Kung, and D. S. Wuu, “High-power GaN light-emitting diodes with patterned copper substrates by electroplating,” ***Phys. Stat. Sol. (a)***, 201, pp. 2786-2790, 2004.

24. R. H. Horng, **C. E. Lee**, C. Y. Kung, S. H. Huang, and D. S. Wuu, ‘High-power AlGaInP light-emitting diodes with patterned copper substrates by electroplating’, ***Jpn. J. Appl. Phys.***, vol. 43, no. 4B, pp. L576-578, 2004.

(B) Conference Papers:

1. **Chia-En Lee**, Bo-Siao Cheng, Yea-Chen Lee, Ching-Hua Chiu, Hao-Chung Kuo, Tien-Chang Lu, and Shing-Chung Wang," Enhancement of Nitride-based Near-Ultraviolet Vertical-Injection Light-Emitting Diodes with Roughened Mesh-Surface by Adopting Pattern Sapphire Substrate," **the 2008 International Conference on Solid State Devices and Materials (SSDM)** Tsukuba, Japan, Sep. 23-26, 2008

2. **Chia-En Lee**, Bo-Siao Cheng, Yea-Chen Lee, Ching-Hua Chiu, Hao-Chung Kuo, Tien-Chang Lu, and Shing-Chung Wang," Vertical-Injection Ultraviolet Light-Emitting Diodes with GaN-Free Structures," **the 2008 International Conference on Solid State Devices and Materials (SSDM)** Tsukuba, Japan, Sep. 23-26, 2008

3. Bo-Siao Cheng, **Chia-En Lee**, Hao-Chung Kuo, Tien-Chang Lu, and Shing-Chung Wang," Power Enhancement of GaN-Based Flip-Chip Light-Emitting Diodes with Triple Roughened Surfaces," **the 2008 International Conference on Solid State Devices and Materials (SSDM)** Tsukuba, Japan, Sep. 23-26, 2008

4. C. H. Chiu, H. C. Kuo, **C. E. Lee**, C. H. Lin, H. W. Huang, T. C. Lu, S. C. Wang, and K. M. Leung," Study of the Thin-Film GaN-Based LEDs with TiO2/SiO2 Omnidirectional Reflectors and PEC Roughened Surfaces," **the Wide-Bandgap Semiconductor Materials & Devices** Washington, DC, USA, Oct. 7-12, 2007

5. Y. C. Lee, **C. E. Lee**, S. W. Chiou, H. C. Kuo, T. C. Lu and S. C. Wang, "High performance of 650 nm resonant cavity light emitting diodes for plastic optical fiber applications." **the 2006 International Conference on Solid State Devices and Materials (SSDM)** Yokohama, Japan, Sep. 12-15, 2006.

6. Ray-Hua Horng, **Chia-En Lee**, S. C. Hsu, S. H. Huang, C. C. Wu, C. Y. Kung, and D. S. Wuu. "High-Power GaN Light-Emitting Diodes with Patterned Copper Substrates by Electroplating," **the 5th International Symposium on Blue Laser and Light Emitting Diodes**, Gyeongju, Korea, Mar. 15-19, 2004.

Curriculum Vita

Name: Mr. Chia-En Lee

Place of Birth: Chia-Yi, Taiwan

Date of Birth: Jan 28, 1979

Electronic Mail: lce0143@gmail.com

Education:

Ph.D. 2005-2009, Electro-Optical Engineering, National Chiao Tung University, Taiwan

M.S. 2002-2004, Electrical Engineering, National Chung Hsing University, Taiwan

B. S. 1998-2002, Electrical Engineering, National Chung Hsing University, Taiwan

Areas of Special Interest:

AlGaInP and Nitride based materials and optical devices

Title of M.S. Thesis:

Development of a novel chip structure for high-power light emitting diodes with heat-dissipation mirror substrates

Title of Ph.D. Thesis:

Study of Efficiency Enhancement for GaN-based Light Emitting Diodes by Flip-Chip and Epilayer-Transfer Technology